NTNU – Trondheim
Norwegian University of
Science and Technology

An Experimental and Numerical Study of Polymer Injection in Layered Synthetic Porous Media

Eline Skurtveit Moe

Petroleum Geoscience and Engineering
Submission date: June 2015
Supervisor: Ole Torsæter, IPT
Co-supervisor: Carl Fredrik Berg, Statoil ASA

Norwegian University of Science and Technology
Department of Petroleum Engineering and Applied Geophysics

Acknowledgements

I would like to thank my supervisor, Ole Torsæter, for the feedback and guidance I have received during the writing of my Master thesis. He has also helped with a big part of the organizational work of getting this Master thesis up and running by putting me in contact with people that could help with the experimental work.

I would also like to thank my co-supervisor, Carl Fredrik Berg, working as a Senior Researcher Reservoir Technology in Statoil ASA, for the invaluable help with the development of the concept for this Master thesis. He has helped with the constructing of the numerical simulation models, as well as giving important input for the experimental work. I am thankful for all the time he has spent giving me valuable feedback and guidance.

I would like to thank Roger Overå, Hamid Hosseinzade Khanamiri, and Shidong Li for assistance in the lab. Especially Roger Overå who was always available to teach me what I needed to learn.

Finally, I would like to thank Åge Sivertsen for providing me with the resistivity apparatus, and Iver Espen Pedersen for providing me with the recipe I needed to successfully mix the polymer solution.

Abstract

In this Master thesis there was conducted polymer flooding of two-layered synthetic cores, where the two layers had different permeabilities, representing a stratified reservoir. The main purpose of this thesis was to investigate the crossflow within these layered porous media due to viscosity contrast of the injected fluids. It was tried to distinguish the separable effects of crossflow due to advection and diffusion. In particular it was desirable to find out if there was any significant diffusion of polymer between the two layers. A novel method was used to determine adsorption levels and inaccessible pore volumes within the layers of the cores.

The polymer used for the core floodings was a synthetic polymer named Flopaam 5115 SH. In addition, a tracer was added to the polymer solution. This tracer was an elevated salt content within the injected brine, compared to the saturating brine, so that it could be easily detected by a resistivity apparatus. The polymer production curve was determined by a pressure transducer connected to a coil. To investigate polymer diffusion within the cores they were shut in for two days after being flooded with polymer, allowing time for diffusion to act. They were then flooded with polymer again for a second time. At the beginning of the second polymer flood it should have been possible to see a change in the response of the production curve, if there had been a significant diffusion of polymer between the two layers during the two days the core was shut in. Numerical simulations were also run with different sensitivities, in order to get a better understanding of what had happened during the laboratory core flooding experiments.

The results showed that within the layered cores the high permeability layer was filled up with the injected fluid faster than the low permeability layer. Based on the numerical simulations and the experimental work it can be concluded that there were crossflow of the injected fluid from the high permeability layer to the low permeability layer. The crossflow between the layers of different permeabilities was mostly caused by viscous crossflow, both salt and polymer diffusion was negligible. Based on the sensitivity studies utilizing numerical simulation it seemed to be good fluid conductivity in the area between the two layers within the synthetic cores. Differences in adsorption time between the simulated and experimental cases is probably caused by the adsorption of polymer happening abruptly in the simulator, but during the flooding of the cores in the lab the polymer adsorption happened over time and were thus less concentrated at the flood front. A final concluding remark of this Master thesis is that doing experimental tests on synthetic two-layered cores can give interesting results for evaluation of polymer flooding.

Sammendrag

I denne masteroppgaven har det blitt utført polymerfløming av todelte syntetiske kjerner, hvor begge lag hadde forskjellig permeabilitet for å representere et stratifisert reservoar. Hovedmålet med denne oppgaven var å undersøke kryssflyten inne i de lagdelte porøse mediene, som oppstår på grunn av høyere viskositet på den injiserte væsken. Det ble forsøkt å skille mellom kryssflyt forårsaket av adveksjon og diffusjon. Det var også ønskelig å finne ut om det hadde skjedd en signifikant diffusjon av polymer mellom de to lagene. En relativt ukjent metode ble brukt for å bestemme adsorpsjonsverdiene og det utilgjengelige porevolumet for polymer i de ulike lagene i kjernene.

Det ble brukt en syntetisk polymer, kalt Flopaam 5115 SH, i kjerneflømmingene. En tracer ble også tilsatt polymerløsningen. Traceren var et økt saltinnhold i det injiserte saltvannet, sammenlignet med saltvannet kjernene var saturert med, slik at det skulle være enkelt å påvise for resistivitetsapparatet. Produksjonskurven for polymer ble målt med en trykkonverterer, som var koblet til en kveil. For å undersøke polymerdiffusjon inne i kjernene ble de stengt av i to dager etter å ha blitt fløммet med polymer, slik at diffusjonen fikk tid til å virke. Kjernene ble så fløммet med polymer en andre gang. Ved starten av den andre fløммingen skulle det vært mulig å se en endring i responsen i produksjonskurven hvis det hadde vært noe signifikant diffusjon av polymer i løpet av disse to dagene kjernene var stengt av. Det ble også kjørt noen numeriske simuleringer med ulike sensitiviteter for å få en bedre forståelse av hva som hadde skjedd under den eksperimentelle kjernefløммingen i laben.

Resultatene viste at inne i de todelte kjernene ble det høypermeable laget fylt opp raskere enn det lavpermeable laget. Basert på de numeriske simuleringene og det eksperimentelle arbeidet ble det konkludert med at det var kryssflyt av den injiserte væsken fra det høypermeable laget til det lavpermeable laget. Kryssflyten mellom lagene var hovedsakelig på grunn av strømmen årsaket av viskositetsforskjellene, hvor både diffusjon av salt og polymer ble neglisjerbart. Basert på de numeriske sensitivitetsstudiene virket det som om det var god væskekonduktivitet i området mellom de to lagene inne i de syntetiske kjernene. Forskjell i adsorpsjonstid mellom simuleringene og de eksperimentelle resultatene skyldtes mest sannsynlig at adsorpsjonen skjer momentant i simuleringene. Under fløммingen av kjernene i laben skjedde derimot polymeradsorpsjonen over tid og polymeren var dermed mindre konsentrert ved fronten. En siste konkluderende bemerkning for denne oppgaven er at det kan gi interessante resultater for undersøkelser av polymerfløming ved å utføre eksperimentelle tester på syntetiske todelte kjerner.

Table of Content

List of Figures

List of Tables

1 Introduction

Fossil fuels, like oil, are a big part of the world's energy supply. The world's energy demand is assumed to increase in the future, and it will therefore be important to sustain the production of oil from existing fields for as long as possible. To do this it will be necessary to utilize enhanced oil recovery (EOR). In the beginning of producing an oil field the natural drive mechanisms within the reservoir will be the method of choice to bring up the oil. A typical progression when the natural drive mechanisms start to decline is to implement water and gas injection. EOR is defined as all the methods that can be used to increase oil recovery within a reservoir that does not include natural drive mechanisms and injection of water and gas (Stosur et al., 2003). Such methods can be to add heat into reservoirs with heavy oil, inject chemicals that interact with the oil, or inject microbes into the reservoir. This Master thesis investigates aspects of polymer flooding.

Polymer flooding is when a very small amount of water-soluble polymer is added to the water that will be injected into a reservoir. By adding polymer to the injected fluid the viscosity of the solution will increase. This makes the mobility ratio decrease and the displacement of oil from the reservoir will be more effective. For polymer flooding, adsorption of polymer on the rock's surface and inaccessible pore volume, are important factors for the polymers propagation through the reservoir. Types of polymer used in the oil industry include biopolymers and synthetic polymers. Both types have advantages and disadvantages when being used for polymer flooding in the oil industry. It is a synthetic polymer that will be utilized for the experiments in this Master thesis. Polymer flooding is a valuable recovery technique especially in reservoirs containing heavy oil and in reservoirs that is stratified with layers of different permeabilities.

In this Master thesis there will be conducted polymer flooding of two-layered synthetic cores, where the two layers have different permeabilities, representing a stratified reservoir. The main purpose of this thesis is to investigate the crossflow within these layered porous media due to viscosity contrast of the injected fluids. We will try to distinguish the separable effects of crossflow due to diffusion and advection. Looking at the crossflow caused by diffusion it is desirable to be able to determine if there has been diffusion of both salt and polymer molecules between the two layers. To be able to determine what is causing the different types of flows within the cores, only brine and polymer mixed with brine will be utilized to get a cleaner system. Numerical simulations of the experiments will be conducted to get a better understanding of what has happened during the core floodings in the lab. It will be used a

novel method to determine adsorption levels and inaccessible pore volumes within the different layers of the synthetic cores.

1.1 Structure of this Master thesis

The structure of this Master thesis is organized as followed:

- Chapter 2 provides a general introduction of polymer flooding, introducing different polymer properties as well as some practical aspects of polymer flooding when used in heavy oil reservoirs and stratified reservoirs. This chapter is rounded off by explaining the different types of crossflow.
- Chapter 3 is a presentation of the novel method to be used to find the adsorption levels and inaccessible pore volume for the polymer within the different layers of the synthetic core.
- Chapter 4 explains all the experimental preparations done to the cores and the injected fluids before starting the main flooding experiments.
- Chapter 5 describes the experimental setup for the main experiments, as well as explaining the processing of the experimental data and presenting the final experimental results.
- Chapter 6 presents the numerical simulations and sensitivity studies, as well as a comparison of the experimental results to the numerical results.
- Chapter 7 is the final discussion of everything that has been presented in this Master thesis.
- Chapter 8 presents the conclusions of this thesis and further work.

2 Introduction of polymer flooding

The first two sub sections in this chapter, 2.1 and 2.2, are mostly taken from the author's specialization project "Literature survey of waterflooding theory and practical and theoretical aspects of polymer flooding" (Moe, 2014).

When a very small amount of water-soluble polymer is added to the water that is to be injected into a reservoir, it is called polymer flooding. The polymer increases the waters viscosity, and this increases the oil displacement efficiency. Polymer flooding enhances the water flooding process, and is a valuable technique especially in the reservoirs containing oil with a high viscosity (Pope, 1980).

2.1 Polymer properties

2.1.1 Viscosity

Mobility ratio, *M*, is an important factor, deciding the displacement efficiency within the reservoir, and it is defined as

$$M = \frac{k_w}{k_o}\frac{\mu_o}{\mu_w}\ , \qquad \textbf{Eq. 2.1}$$

where k_w is the water permeability, k_o is the oil permeability, μ_w is the water viscosity, and μ_o is the oil viscosity.

A low mobility ratio gives the most ideal displacement, and by increasing the viscosity of the water with polymer, the mobility ratio decrease, increasing the displacement efficiency.

In Figure 2.1 two fractional flow curves are depicted, where f_w is the water fraction and S_w is the water saturation. The red curve is based on a water flooding case that has a viscosity ratio of 0.1, while the blue curve is based on a polymer flooding case that has a viscosity ratio of 1.0. From Eq. 2.1 it can be concluded that the blue curve is the case with the lowest mobility ratio.

The difference between the two average water saturations behind the flood front is about 0.18. This is the same as the oil recovery factor having increased with 18% at breakthrough, by increasing the viscosity of the displacing fluid (Sheng, 2013).

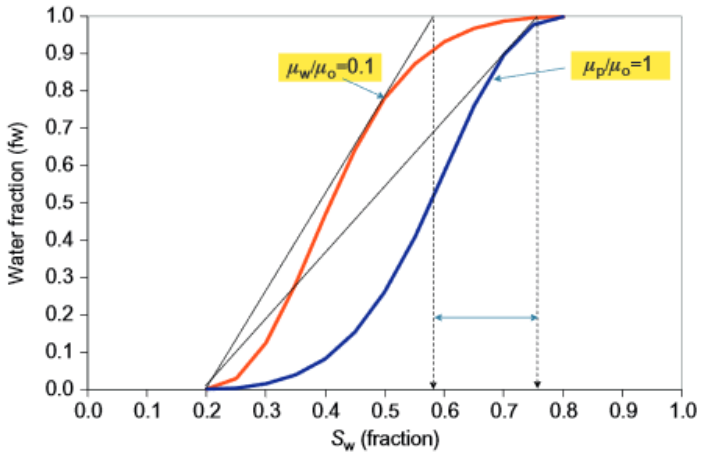

Figure 2.1 Fractional flow curves for two different viscosity ratios (Sheng, 2013).

2.1.2 Permeability reduction

Some polymers can in addition to increasing the water viscosity also decrease the water permeability, k_w, thereby decreasing the mobility ratio even further. The polymers then, directly or indirectly, act as a fluid-flow blocking agent (Petrowiki #1, 2013). The reduction of the oil and/or gas permeability due to polymer takes place at a much smaller extent than for the water permeability (Petrowiki #2, 2013). Therefore, there is no significant change in the relative permeability curves for oil and/or gas due to polymer flooding. This is pictured in Figure 2.2, where it is a clear reduction of the relative permeability curve for water, compared to the oil curve.

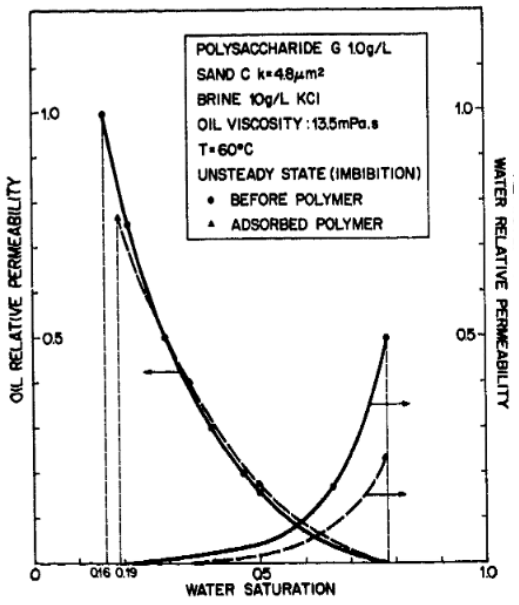

Figure 2.2 Permeability reduction due to polymer flooding (Zaitoun & Kohler, 1988)

The residual resistance factor, R_{rf}, gives a measure of the polymer-induced permeability reduction, and is given by (Petrowiki #3, 2014)

$$R_{rf} = \frac{k_b}{k_a} \quad . \qquad \textbf{Eq. 2.2}$$

k_b is the brine permeability before the flood, while k_a is the brine permeability after the flood.

2.1.3 Polymer transport

During a polymer flood the polymer molecules will interact with the solid surface of the rocks. The polymer molecules will be physically bound to the solid surface and thereby adsorbed (Sheng, 2013). This adsorption will cause some retention for the polymer solution and delay the rate of the polymer propagation. The retention of the polymer varies with polymer type, molecular weight, brine salinity, brine hardness, rock composition, flow rate, and temperature (Lake, 1989).

In a reservoir subject to polymer flooding, some pores will be too small for the polymer molecules to enter. The volume these pores comprise is known as inaccessible pore volume (IPV) (Sheng, 2013). The result of this inaccessible pore volume is that the polymer flow will be accelerated, which is the opposite effect of the adsorption causing retention (Dawson & Lantz, 1972). Composition and other properties of the rock determine which of these factors will be the most significant. Usually the adsorption factor is dominant when injecting polymer into a reservoir for the first time, thus the acceleration due to IPV will not cancel out the retention of the polymer.

When a polymer mixed with water propagates through the flooded reservoir, the average molecular weight of the polymer can be reduced. This process is known as degradation, and the degradation can be either chemical, biological or mechanical. When the molecular weight of the polymer is reduced, the viscosity will drop, and the effect of the polymer flooding will decrease (Levitt et al., 2011).

Chemical degradation involves oxidation/reduction (redox) reactions involving free radicals, and hydrolysis. The most serious source of degradation is usually considered to be the free radical chemical reactions. To prevent or retard these reactions, oxygen scavengers and antioxidants are often added to the polymer solution (Lake, 1989). It has been found that C_4-C_5 aliphatic alcohols and thiourea (a sulfur compound) are good antioxidants that works as free radical inhibitors (Wellington, 1983). Hydrolysis is when the polymer molecular weight

is reduced due to reactions when the pH within the reservoir is either high or low (basic or acid) (Petrowiki #3, 2014).

Biological degradation is affected by the type of bacteria in the brine, temperature, pressure, salinity, and chemicals present in the reservoir. It is highly recommended to use biocide in the solution as a preventive measure, which is also used in waterflooding (Lake, 1989).

Mechanical degradation takes place if the polymer solution is subjected to a sufficiently high velocity. The form of mechanical degradation that is of most concern for polymers is shear degradation. The high velocity share rates usually occurs in the surface-injection equipment, such as valves, pumps, orifices, and tubing, or in the perforations and screens downhole, or at the formation face of the injection well (Petrowiki #3, 2014). Most polymer injections are therefore conducted through open-hole or gravel-pack completions. Within the reservoir, except by the injector, the fluid velocity is lower, and there will be little mechanical degradation within the reservoir itself (Lake, 1989).

2.1.4 The polymers

Polymers are molecules that are the result of many monomers being joined together chemically. Monomers are small and repeating molecular entities. The chemical process where the monomers are joined to make a polymer, is referred to as the polymerization reaction process (Petrowiki #4, 2013). The polymers used in the oil industry are polymers that can be dissolved in an aqueous solution and increases the viscosity of this solution. The two different types of polymers that have been used in polymer floods are biopolymers and man-made synthetic polymers. Typical biopolymers are xanthan and scleroglucan, while typical man-made synthetic polymers are polyacrylamides (PAM) (Sohn et al., 1990). Many polyacrylamides are partially hydrolyzed and are called hydrolyzed polyacrylamide (HPAM). See Figure 2.3 for the molecular structures of a biopolymer and a partially hydrolyzed polyacrylamide.

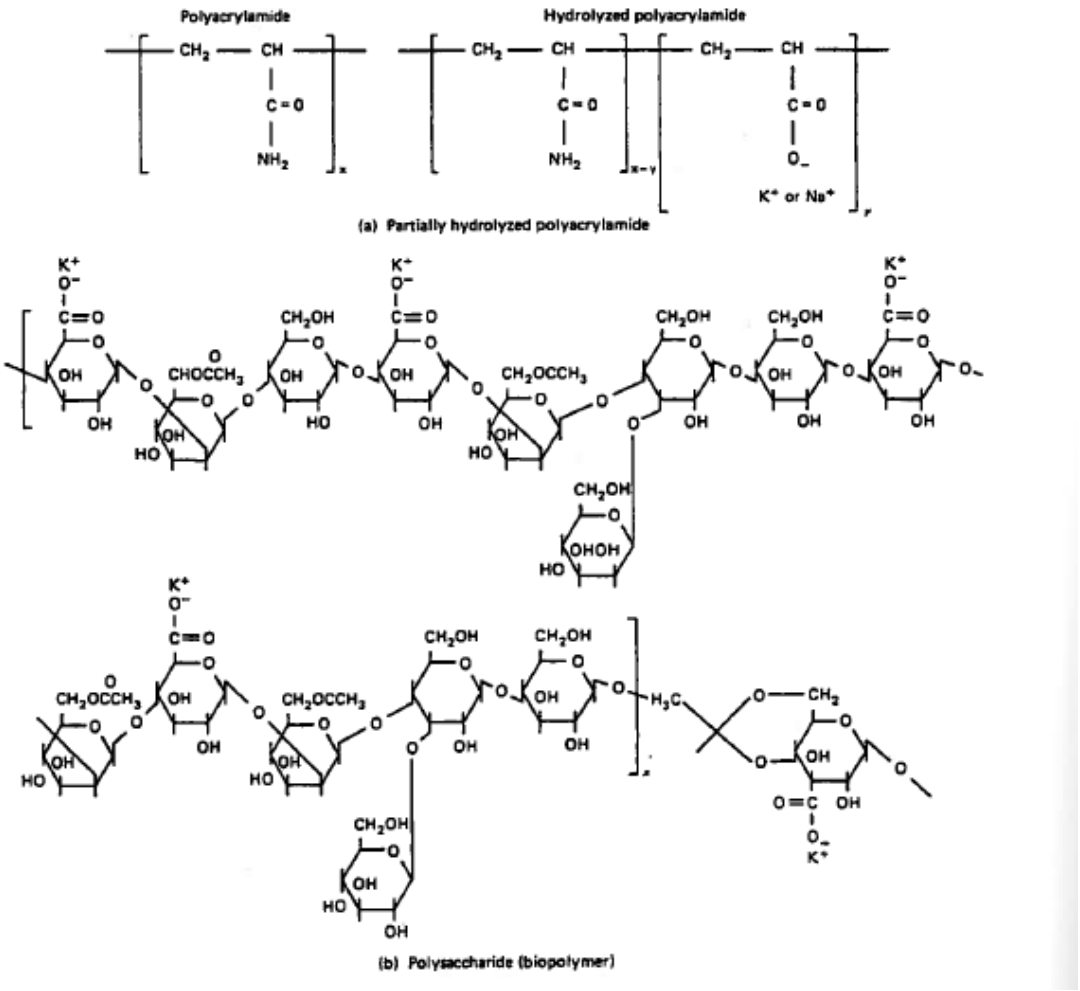

Figure 2.3 Molecular structures of a biopolymer and polyacrylamides (Lake, 1989).

Hydrolysis is when anionic carboxyl groups (-COO^-) is broken of the polyacrylamides and replaced by oxygen from water. For polyacrylamides the degree of hydrolysis makes properties like solubility, viscosity, and retention, more optimal (Lake, 1989). Still, these partially hydrolyzed polyacrylamides are known to be sensitive to high temperature and divalent ions. The polymers contain amide groups that can increase the previously optimal amount of hydrolysis, dependent on the temperature and pH in the reservoir. This may cause precipitation in hard brines, and causes the polymer to lose most of its important viscosity effects (Moradi-Aragi & Doe, 1987). HPAM is also sensitive to the salinity of the brine within the reservoir it is injected into. The carboxylate groups of the HPAM molecules have an electrostatic charge. In a low salinity brine, these charges repulse each other on the polymer's backbone, and cause the polymer to assume a distended form. In a high salinity brine, the electrostatic field from the carboxylate groups shrink substantially, and allows the HPAM molecule to assume a more balled-up form (Petrowiki #4, 2013). See Figure 2.4 for an illustration of the form of the HPAM molecules in low and high salinity brines.

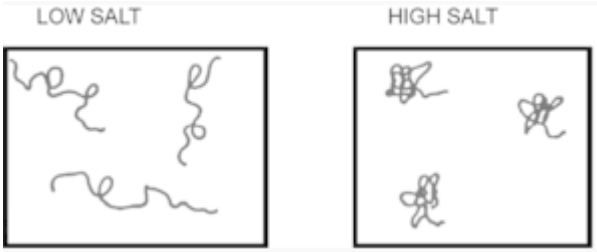

Figure 2.4 Effect of salinity on the form of the HPAM molecules (Petrowiki #4, 2013).

The balled-up form of the HPAM molecules in high salinity brines will cause the viscosity of the polymer solution to decrease. This reduces the important viscosity effect of the polymer flooding. Therefore, when a reservoir with high salinity brine is to be polymer flooded, it is normal to precondition the reservoir first. This is done by flushing the reservoir with a sufficiently large quantity of fresh water (Sohn et al., 1990), called a preflush.

Biopolymers are also known as polysaccharides, and are formed by a bacterial fermentation process that polymerize the saccharide molecules. The fermentation process leaves debris in the polymer product that needs to be removed before the polymer is injected (Lake, 1989). If not all the debris is removed, this can cause injectability issues. When the polymer is injected into the reservoir, the biopolymers are also susceptible to bacterial attacks. Despite these disadvantages, the biopolymers have several advantages compared to the polyacrylamides. These advantages are the ability of resistance to degradation by shear, low adsorption, and relative insensitivity to temperature and water salinity (Carter et al., 1980). When using biopolymers, the important viscosity effect of polymer injection will therefore not be significantly affected. Scleroglucan is known to have the best potential of the biopolymers (Rivenq et al., 1992).

Despite biopolymers having many ideal properties, hydrolyzed polyacrylamides are used more widely than the biopolymers due to advantages in price and large-scale production (Sheng, 2013). At high salinities, the cost of polyacrylamides and biopolymers will be close enough due to the viscosity loss of the polyacrylamides, so the preferred polymer for a given application will be site specific (Lake, 1989).

2.2 Practical aspects of polymer flooding

2.2.1 Heavy oil reservoirs

Polymer flooding is a very valuable recovery technique, especially in reservoirs containing high viscosity oil. In a normal water flood, if the oil's viscosity is higher than the water viscosity the mobility ratio will be high, and this results in an unfavorable displacement

efficiency and an unstable displacement, as water is more mobile than the oil. The water will not push all the movable oil towards the production well, but will move through the heavy oil with viscous fingering, displacing some of the oil towards the well, but leave a lot behind. This leads to early water breakthrough and low recoveries. If a polymer solution of higher viscosity had been used in this reservoir instead, the mobility ratio would have decreased to a smaller and more favorable value. The viscous fingering would be decreased, and the polymer solution would be able to push most of the oil towards the production well. The displacement front will be more stabilized and the recoveries will improve remarkably (Buchgraber et al., 2011).

2.2.2 Crossflow

If a reservoir is stratified and show a lot of heterogeneity between layers in for example permeability, a high recovery in the low permeability layers can be difficult with a water flood. The water will choose the least resistance to flow, which causes the water to mostly displace oil in the high permeability layers. In such stratified reservoirs, slugs of polymer solutions are often injected to improve the vertical sweep efficiency (Clifford, 1988). In the areas of the reservoir that have been flooded by the water, the oil recovery may not be very efficient, and in these zones the polymer may recover very little oil. However, injecting polymer might be very beneficial due to the fluid diversion the polymer produces. Due to the permeability reduction and viscosity increase caused by polymer, the resistance to flow will increase. This resistance will make the injected polymer solution to divert into unswept or poorly swept areas. In reservoirs with high water-oil ratios, this diversion will be much more significant than mobility ratio or fractional flow effects (Needham & Doe, 1987).

2.3 Crossflow at a pore scale

As polymer is injected into a stratified reservoir there will be crossflow as explained in sub-section 2.2.2. Looking at this crossflow on a pore scale within a stratified reservoir, crossflow is a fluid flowing in a direction which is perpendicular to the bulk flow. This type of crossflow might happen due to four different driving mechanisms: viscous forces, capillarity, gravity, and diffusion (Zapata & Lake, 1981). The first three driving mechanisms together represent what is called advective crossflow. The experiments to be conducted in this Master thesis will be on cores where only brine and polymer is utilized as fluids in the system. Therefore crossflow due to capillarity and gravity will not be relevant as there is no oil in the system causing capillary forces, and the density difference between brine and polymer mixed

with brine is negligible. When advective crossflow is mentioned in the rest of this Master thesis, it is basically viscous crossflow that is being discussed.

Crossflow due to viscous forces is caused by the viscosity difference between the displacing and the displaced fluids. The direction of the viscous crossflow will be determined by the mobility ratio. If the displacing fluid has the higher viscosity, the mobility ratio will be less than one. This gives the most favorable displacement within a reservoir. Injecting polymer into a reservoir containing just brine, or brine and oil, will provide a mobility ratio less than one. Looking at a two-layered stratified reservoir of different permeabilities, the pressure distribution, when a fluid of higher viscosity is injected, will be as in Figure 2.5.

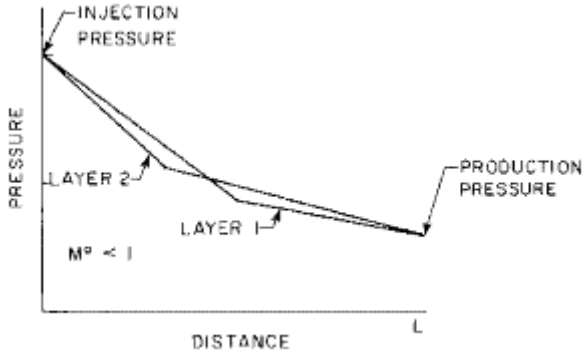

Figure 2.5 Pressure distribution in a two-layered reservoir as high viscosity fluid is injected (Zapata & Lake, 1981).

Layer 1 represents the high permeability layer, which will have the highest velocity, and layer 2 represents the low permeability layer with the lowest velocity. At the leading front of the injected fluid, closest to the producer, the high permeability layer has the lowest pressure. This causes the crossflow to go from the low permeability layer to the high permeability layer in the front. At the trailing flood front, the low permeability layer will have the lowest pressure, and here the crossflow will then go from the high permeability layer to the low permeability layer. See Figure 2.6 for an illustration of the crossflow directions at the two different flood fronts.

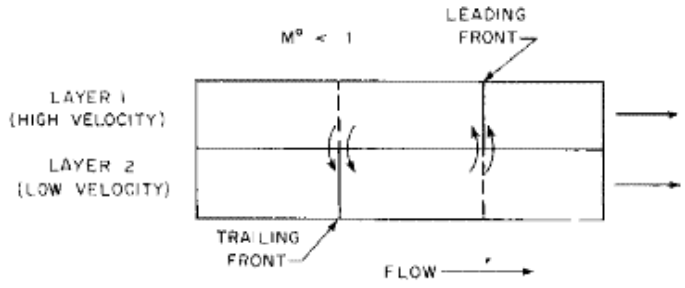

Figure 2.6 Crossflow directions in a two –layered reservoir as high viscosity fluid is injected (Zapata & Lake, 1981).

Crossflow due to diffusion takes place when two miscible fluids are in contact, and in the interface of the contact area the fluids will diffuse into each other (Perkins & Johnston, 1963). Diffusion is possible due to the random motion of molecules.

In this Master thesis the main purpose is to do polymer flooding of two-layered cores of different permeabilities and investigate the crossflow between the two layers. The goal is to try to distinguish the separable effects of crossflow due to diffusion and advection. The cores will be saturated in brine, and the injected fluid will be polymer mixed with a brine of a different salt content than the saturating brine. The increased salt content in the brine mixed with polymer will be used as a tracer. As brine and polymer mixed with brine are miscible fluids, crossflow due to diffusion can take place. Between the leading front and the trailing front the polymer solution is in contact with brine of a lower salt content. Both tracer and polymer can diffuse into the saturating brine in this area, contributing to a higher tracer and polymer concentration in the layer with the lowest permeability.

An important note on diffusion is that diffusion coefficients that is found in literature usually are based on bulk diffusion, which is a substance's ability to diffuse in a large volume of fluid. With flow within a porous media the effective diffusion coefficients will be lower. From calculations in Berg (2012) the fraction between effective porous media diffusion and bulk diffusion is approximately 0.1.

To be able to fully investigate the crossflow within the two-layered cores, it is necessary to find the adsorption value and the inaccessible pore volume for the polymer in each layer.

3 Procedure for finding adsorption and IPV in a core

One of the tasks of this Master thesis is to find the amount of adsorption that is happening within some of the cores, as well as finding how much of the pore volume of these cores that is inaccessible for the polymer (IPV). There does not exist some set experimental apparatus or method to determine these values for a core sample representing a reservoir. However, Lötsch et al. (1985) describe in their paper *The Effect of Inaccessible Pore Volume on Polymer Coreflood Experiments* a way of back-calculating adsorption and IPV if one does a polymer flooding followed by a water flooding. A tracer needs to be added to the polymer solution in order to get one polymer production curve and one tracer production curve as outputs for the core flooding.

During a first time polymer flooding, the retention of the polymer due to adsorption is usually more dominant than the acceleration of the polymer due to IPV. This will cause a delay of the polymer compared to the rest of the solution that was injected with the polymer, as this brine does not become adsorbed on the rock's surface as the polymer. By adding a tracer to the brine mixed with polymer, the delay of the polymer can clearly be seen in the difference between the tracer production curve and the polymer production curve. As water is injected after the polymer flood, displacing the polymer and tracer from the core, the polymer will exit the core quicker than the tracer due to the IPV. The brine with the tracer needs to be displaced from all the pores, but polymer is only displaced from the pores it can enter, which is the entire pore volume minus the IPV.

If a second polymer flood is initiated after the water has displaced all the tracer and movable polymer, the order of the production curves will change. In the first polymer flood, all the polymer that can be adsorbed onto the rock's surface has already been adsorbed. For the second polymer flood, no adsorption will happen, and the acceleration of polymer due to the IPV will dominate. As the tracer enters all pores, the tracer production curve is delayed compared to the polymer production curve. If water is injected after the polymer flood, the production curves will be exactly the same as when water was injected after the first polymer flood, due to IPV being the only factor. Then the tracer exits the core at a later time than the polymer.

By using the production curves, one can find the adsorption and IPV by calculating the integrals between the tracer curve and the polymer curve. The adsorption is found by taking the integral between the tracer curve and the polymer curve during the first polymer flood,

since the delay of the polymer here is caused only by the adsorption of polymer. The IPV can be found by taking the integral between the polymer curve and the tracer curve during the second polymer flood, as the early arrival of polymer is due to the IPV. Another way of calculating IPV is taking the integral between the tracer curve and the polymer curve during the water flood after the first polymer flood, as the early exit of the polymer is due to the IPV (Holt, 2015). One could also find the IPV by using the water flood after the second polymer flood, as this curve will be identical to the first one. By using the production curves from the first water flood, time could be saved in the lab, as it is then only needed to do one polymer flood and one water flood in order to get both the values of adsorption and IPV. This is the way it has been done in this Master thesis.

In order to be able to take the integral between the production curves, the concentrations needs to be normalized, as the maximum concentration of the polymer in solution in g/cm^3 is not the same as the maximum concentration of the tracer in solution in g/cm^3. This way the curves can be compared correctly to each other. One can normalize the polymer concentration, C_{pol}, by using the equation

$$C_{pol,norm} = \frac{C_{pol} - C_{pol,min}}{C_{pol,max} - C_{pol,min}}, \quad \textbf{Eq. 3.1}$$

where $C_{pol,min}$ is the minimum polymer concentration, $C_{pol,max}$ is the maximum concentration, and $C_{pol,norm}$ is the resulting normalized polymer concentration.

For the tracer concentration, C_{tra}, the normalization can be done using the equation

$$C_{tra,norm} = \frac{C_{tra} - C_{tra,min}}{C_{tra,max} - C_{tra,min}}, \quad \textbf{Eq. 3.2}$$

where $C_{tra,min}$ is the minimum tracer concentration, $C_{tra,max}$ is the maximum concentration, and $C_{tra,norm}$ is the resulting normalized tracer concentration.

The equation giving the IPV is

$$IPV = \sum[(C_{tra,norm} - C_{pol,norm}) * \Delta PV], \quad \textbf{Eq. 3.3}$$

where ΔPV is the incremental change in pore volume.

The equation giving the adsorption is

$$Adsorption = \{\sum[(C_{tra,norm} - C_{pol,norm}) * \Delta PV] + IPV\} * \frac{PV * C_{pol,max}}{W_{rock}}, \quad \text{Eq. 3.4}$$

where PV is the pore volume of the rock, and W_{rock} is the weight of the rock.

To verify this method, a simulation was done using Eclipse with defined input values for adsorption and IPV. From the resulting production curves for the polymer and tracer, the adsorption and IPV was back calculated using Eq. 3.3 and Eq. 3.4 to check if this gave the same values as the input.

The core in the simulation was rectangular, measuring 10 cm in the x-direction, 4.5 cm in the y-direction, and 2.25 cm in the z-direction. The porosity was put to 25 %, and the permeability was put to 50 mD. The adsorption within the core was defined as $70*10^{-6}$ g/g, while the IPV was defined as 0.2 (20 %). The maximum concentration of polymer was 1000 ppm, having a viscosity of 20 cP at this concentration. The brine used for water flooding contained 3 wt% of salt. Salt content was used as the tracer, so the brine injected with the polymer contained 3.5 wt% of salt, so that it would be a clear difference between the brine used for water flooding and the brine used for polymer flooding.

In this simulation it was flooded with polymer and water twice, even though it strictly was not necessary, just to be able to see the difference between the production curves from the first polymer flood to the other. See Figure 3.1 for the production curves that were the result of the simulation.

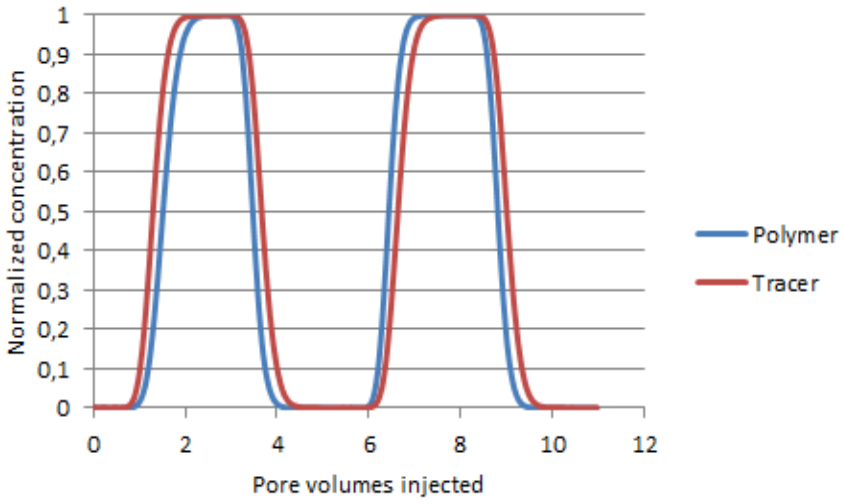

Figure 3.1 Production curves based on test simulation.

The production curves from Figure 3.1 clearly show the delay of the polymer curve during the first polymer flooding. They also show the acceleration of the polymer curve during the second polymer flooding. The early exit of the polymer compared to the tracer is clearly shown during both the first and second water flooding, where the curves are identical.

By using Eq. 3.3 on the curves of the first water flood, and Eq. 3.4 on the curves of the first polymer flood, the calculated values for IPV and adsorption were as shown in Table 3.1.

IPV	0.2004	
PV	25.31	cm^3
Total vol	101.25	cm^3
Porosity	0.25	
Rock vol	75.94	cm^3
Weight rock	151.87	g
Ads. integral + IPV	0.4197	
Max conc pol	0.001	g/cm^3
Polymer adsorbed	0.01062	g
Adsorption	6.996E-05	g/g

Table 3.1 Calculated values for IPV and adsorption for simulated test case.

From this we concluded that the method, described above, using the production curves and taking the integrals of the area between them, works. The IPV value was calculated to be 0.2004, compared to the original of 0.2, and the adsorption value was calculated to be $69.96*10^{-6}$ g/g, compared to the original of $70*10^{-6}$ g/g.

During an experiment it will not be possible to be certain that the accuracy is as good as it was for this simulation, as there are a lot of sources of possible errors that can affect the production curves and the results.

The data file for the simulation can be found in Appendix C.

4 Experimental preparations

4.1 The cores

The cores to be used for experiments in this Master thesis are synthetic cores of sandstone, made at the Northeast Petroleum University, in Daqing China. Each core consists of two layers with different permeabilities. There were two types of cores, one type called A, and one type called B. The cores are rectangular with dimensions of 4.5 cm * 4.5 cm * 30 cm. The A-type core was supposed to have one layer with a permeability of 50 mD, and the second layer a permeability of 2000 mD. The B-type core was supposed to have layers with permeabilities of 200 mD and 1000 mD. The cores should have a clay content of 5 – 10 %, and be slightly oil wet.

There is no type of glue holding the two parts of the core together. We believe the cores were made by first casting one layer in a squared shape, and then waiting until this layer has set, before casting the second layer on top of the first one. See Figure 4.1 for a picture of one of the cores.

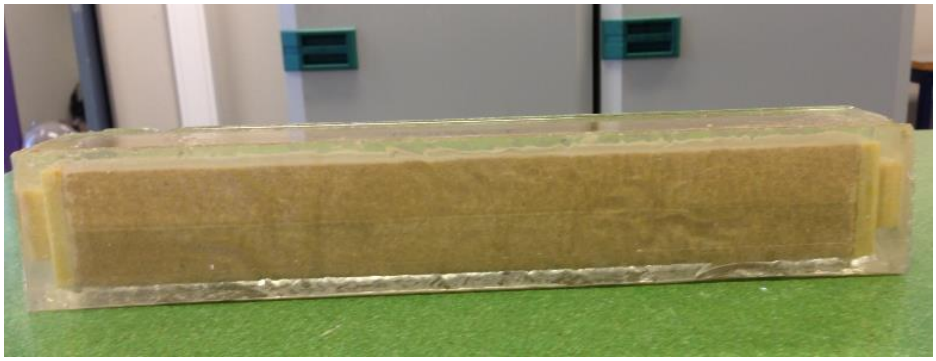

Figure 4.1 Picture of one of the cores.

Since the cores have an unorthodox shape, a core holder would have had to be made in order to be able to conduct a core flooding with them. To avoid this task, some of the cores came incorporated in epoxy, with possibilities for connections with 1/8 inch tubes. I received two cores embodied in epoxy, and two plain ones. There were both an A and B version in epoxy and without epoxy.

The A- and B-type cores in epoxy were the ones being used for the main core flooding experiments. Since we did not know all the information about the cores, it was necessary to do preliminary experiments to determine porosity, permeability, IPV, and adsorption. This was not possible on the cores in epoxy, as cutting in the core and breaking the epoxy, both would have made a following core flooding impossible. Therefore, our only choice was to use

the A and B cores without epoxy to find this information. The two A, and the two B cores, were made in pairs in the same batch, and thereafter cut into cores of 4.5 cm * 4.5 cm * 30 cm. The assumption that was made was that these cores would be so similar to each other, that the results from one core would be transferable to the same type of core in epoxy, being used in the main core flooding.

To be able to do the preliminary experiments in orthodox core holders and apparatus, the cores not embodied in epoxy were cut into circular core plugs of 1.5 inch diamater. The length of the layered core enabled for six core plugs to be made from each layer of each core. The length of the core plugs were made as long as possible, with each layer originally being in average 2.25 cm.

4.2 Preparation of the homogeneous core plugs

4.2.1 Cleaning the core plugs

Even though the cores we received were dry and unused, it was still necessary to clean the core plugs, so that we could be certain that the measurements that were to come would be as accurate as possible. The cleaning was done by Soxhlet extraction.

In Figure 4.2 a schematic diagram of the Soxlet apparatus is depicted. To start a Soxhlet extraction, toluene or methanol is set to a boil in a Pyrex flask. In our case we used methanol since there were no need for toluene, as the cores did not contain oil. The core plugs are located in the thimble, and the vapor from the boiling methanol will move upwards into the thimble. The condenser contains circulating cold water, and this will make the vapor in contact with the condenser into a liquid form, that then falls down and soaks the core plugs. This will dissolve and remove any dust or impurities that may be inside the pores. As the liquid level within the thimble rises to the top of the siphon tube arrangement, the liquid will be emptied by a siphon effect, and go back to the flask containing methanol. The methanol can then be reused to continue the cleaning process (Torsæter & Abtahi, 2000).

When the core plugs were done being cleaned in the Soxhlet extractor, they needed to be dried in a heating cabinet overnight.

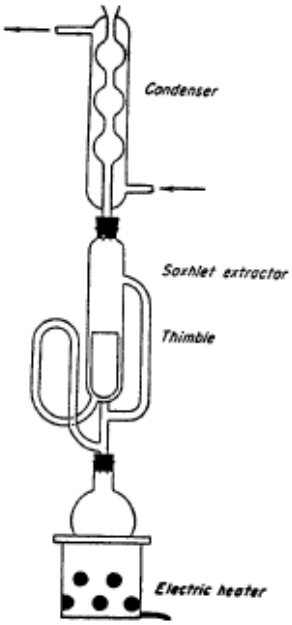

Figure 4.2 The Soxhlet apparatus (Torsæter & Abtahi, 2000).

4.2.2 Core plug data

After the core plugs were cleaned and dried, the next step was to measure each core plug's dry weight, length, and diameter. This data is listed in Table 4.1. Cores named AL are the low permeability core plugs of type A, and the ones named AH are the high permeability core plugs of type A. For the type B core plugs, the low permeability plugs are named BL, and the high permeability plugs are named BH.

4.2.3 Porosity

The porosity of the core plugs were determined by the helium porosimeter method. Helium is a gas that has small molecules, and can thereby penetrate small pores. It is an inert, ideal gas for the pressures and temperatures used in the experiment. Helium will not adsorb onto the surface of the rock, as well as having a high diffusivity ideal to determine porosity even in rocks with low permeability (Torsæter & Abtahi, 2000). This makes the helium technique one of the most used techniques in determining porosity. The technique is based on Boyle's law (for isothermal expansion)

$$p_1V_1 + p_2V_2 = p(V_1 + V_2)\,. \qquad \textbf{Eq. 4.1}$$

A schematic diagram of the helium porosimeter apparatus is shown in Figure 4.3. The reference cell has a volume V_1, and a pressure p_1, while the sample chamber contains the core plug with an unknown volume V_2, and an initial pressure of p_2. p is the pressure read directly from the gauge.

Core plug	Weight	Length	Diameter
	[g]	[mm]	[mm]
AL1	42.22	21.46	37.76
AL2	42.59	21.94	37.77
AL3	41.82	21.58	37.77
AL4	41.98	21.74	37.7
AL5	42.38	21.72	37.73
AL6	42.8	21.94	37.83
AH7	38.52	19.82	37.88
AH8	38.27	20.14	37.89
AH9	38.29	20.2	37.85
AH10	38.95	20.48	37.84
AH11	38.2	20.28	37.83
AH12	38.54	20.28	37.81
BL1	40.47	21.32	37.78
BL2	40.6	21.66	37.89
BL3	40.94	21.44	37.73
BL4	39.97	21.54	37.69
BL5	40.75	21.41	37.78
BL6	40.86	21.28	37.82
BH7	38.45	20.34	37.76
BH8	39.18	20.35	37.78
BH9	38.16	20.05	37.83
BH10	39.98	21.01	37.87
BH11	39.36	20.34	37.78
BH12	37.74	20.07	37.82

Table 4.1 Core plug data.

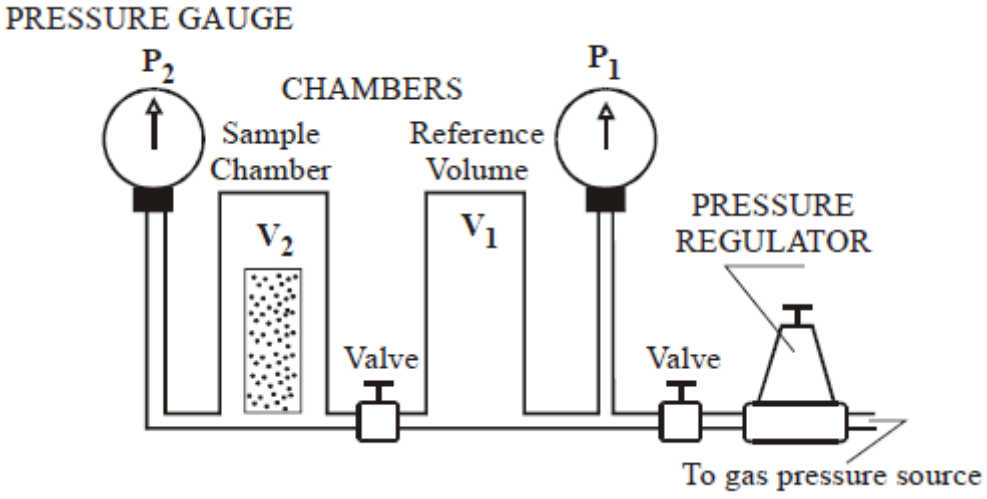

Figure 4.3 The helium porosimeter apparatus (Torsæter &Abtahi. 2000).

When the valve between the reference cell and the sample chamber is opened, the helium gas enters the sample chamber, and V_2 can be read directly of a panel integrated in the helium porosimeter. Had a panel like this not existed on the apparatus, V_2 could have been found by rearranging Eq. 4.1. If the bulk volume, V_b, of the core plug has been measured, the porosity can be calculated. The volume of the core plug without the pore volume, V_K, is given by

$$V_K = V_1 - V_2 \,. \qquad \textbf{Eq. 4.2}$$

The pore volume of the core plug, V_p, is then expressed as

$$V_p = V_b - V_K \,. \qquad \textbf{Eq. 4.3}$$

Finally, the porosity, φ, is given by the ratio

$$\varphi = \frac{V_p}{V_B} \,. \qquad \textbf{Eq. 4.4}$$

The porosity for each core is listed in Table 4.2.

Core plug	V1	V2	Vk	Vb	Vp	Porosity
	[cm^3]	[cm^3]	[cm^3]	[cm^3]	[cm^3]	[-]
AL1	50	31.3	18.7	24.0	5.3	0.222
AL2	50	31.3	18.7	24.6	5.9	0.239
AL3	50	31.6	18.4	24.2	5.8	0.239
AL4	50	31.6	18.4	24.3	5.9	0.242
AL5	50	31.4	18.6	24.3	5.7	0.234
AL6	50	31.0	19.0	24.7	5.7	0.230
AH7	50	33.8	16.2	22.3	6.1	0.275
AH8	50	34.0	16.0	22.7	6.7	0.295
AH9	50	34.0	16.0	22.7	6.7	0.296
AH10	50	33.9	16.1	23.0	6.9	0.301
AH11	50	34.0	16.0	22.8	6.8	0.298
AH12	50	33.9	16.1	22.8	6.7	0.293
BL1	50	32.8	17.2	23.9	6.7	0.280
BL2	50	32.7	17.3	24.4	7.1	0.292
BL3	50	32.4	17.6	24.0	6.4	0.266
BL4	50	33.0	17.0	24.0	7.0	0.293
BL5	50	32.6	17.4	24.0	6.6	0.275
BL6	50	32.5	17.5	23.9	6.4	0.268
BH7	50	33.7	16.3	22.8	6.5	0.284
BH8	50	33.2	16.8	22.8	6.0	0.264
BH9	50	33.8	16.2	22.5	6.3	0.281
BH10	50	33.1	16.9	23.7	6.8	0.286
BH11	50	33.2	16.8	22.8	6.0	0.263
BH12	50	33.8	16.2	22.5	6.3	0.281

Table 4.2 Core plug porosity.

See Figure 4.4 and Figure 4.5 for plots of the porosities for each core type compared to each other.

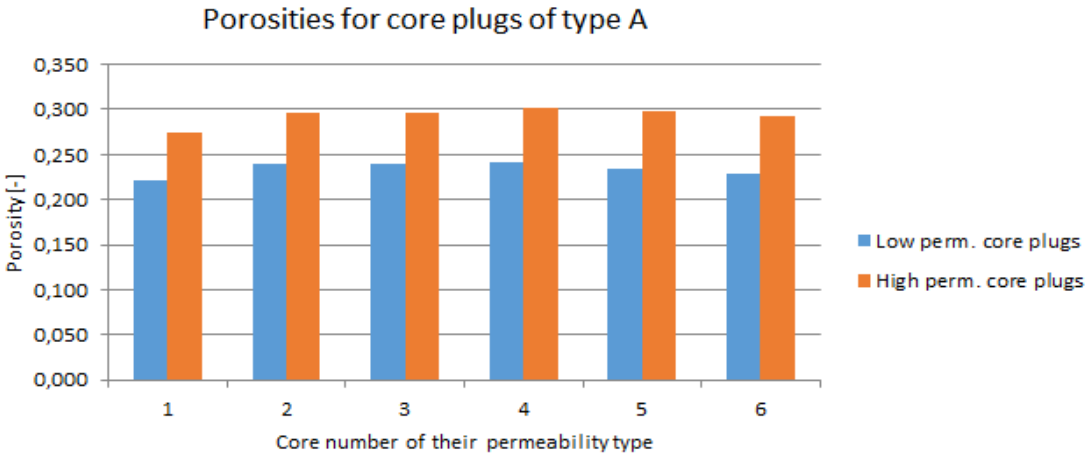

Figure 4.4 Comparison of porosities for the type A core plugs.

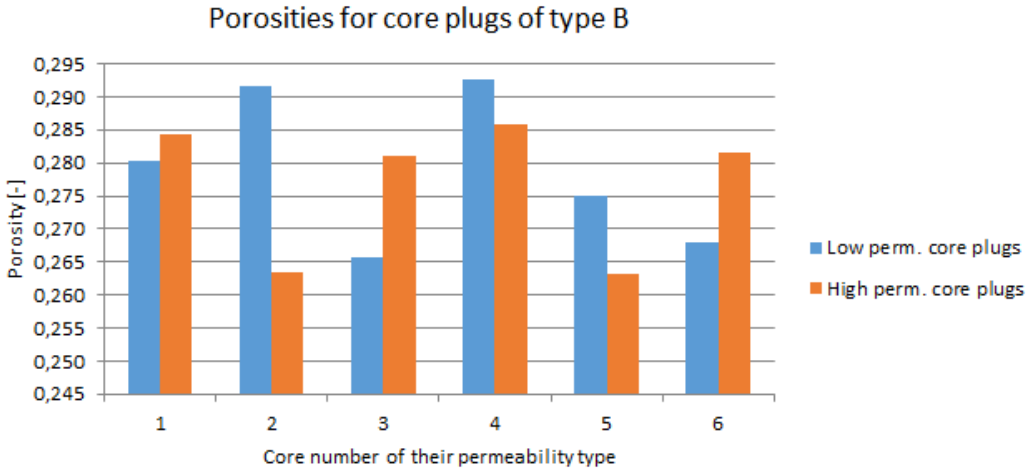

Figure 4.5 Comparison of porosities for the type B core plugs.

The porosities for core A are quite even, and the difference between the porosities of the high and low permeability core plugs is clearly seen. For core B, the porosities within the same layer vary a lot more, and there is no clear difference between the high- and low permeability core plugs.

4.2.4 Saturating the core plugs

After all the measurements for a dry core were done, the core plugs needed to be saturated with the brine to be used in the upcoming water flooding. This water contained 3 wt% of sodium chloride (NaCl). The saturation was done by a vacuum pump, see Figure 4.6.

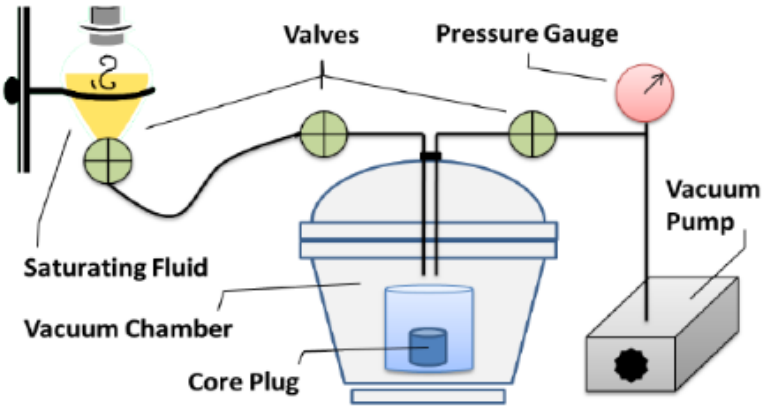

Figure 4.6 Sketch of vacuum pump setup (Dahle, 2014).

The cores were placed inside the vacuum chamber. The vacuum is created by the pump, providing a pressure of about 100 mbar. The saturating fluid is placed in a flask above the vacuum chamber, and when all the air is sucked out of the pores of the core plugs and the chamber that contains them, the valves underneath the flask, containing the brine, are opened. The brine will drip down onto the core plugs and fully saturate them. One hour within the vacuum chamber was enough for the cores to be saturated. If the saturation had been done without vacuum, one risk air getting trapped within the pores. After the saturation it is important to keep the core plugs in containers with the same brine as they were saturated in.

4.2.5 Permeability

The given permeabilities for the two layers in core type A, were 50 mD and 2000 mD. For the core type B, the permeabilities given were 200 mD and 1000 mD. As it is difficult to make cores of an exact permeability, it was necessary to check what the true permeability of each layer really was.

First, we tried to measure the air permeability of the dry core plugs, but since the core plugs were short, the results fluctuated a lot. For the high permeability core plugs it was impossible to get any usable data.

The next step was then to measure the absolute permeability of the core by conducting a standard water flooding of the core plugs, measuring the upstream and downstream pressures by manometers on both sides of the core. The absolute permeability, k_{abs}, can then be calculated using the rearranged Darcy's equation

$$k_{abs} = \frac{\mu_w * L * Q}{\Delta P * A}, \qquad \textbf{Eq. 4.5}$$

where μ_w is the water viscosity, L is the length of the core, Q is the flow rate, ΔP is the pressure drop over the core, and A is the cross-sectional area of the core. For the low permeability core plugs, a flow rate of 10 ml/min was used, and for the high permeability core plugs, a flow rate of 15 ml/min was used. Figure 4.7 shows a schematic of an apparatus used for permeability measurements (originally used as sketch for measuring air permeability).

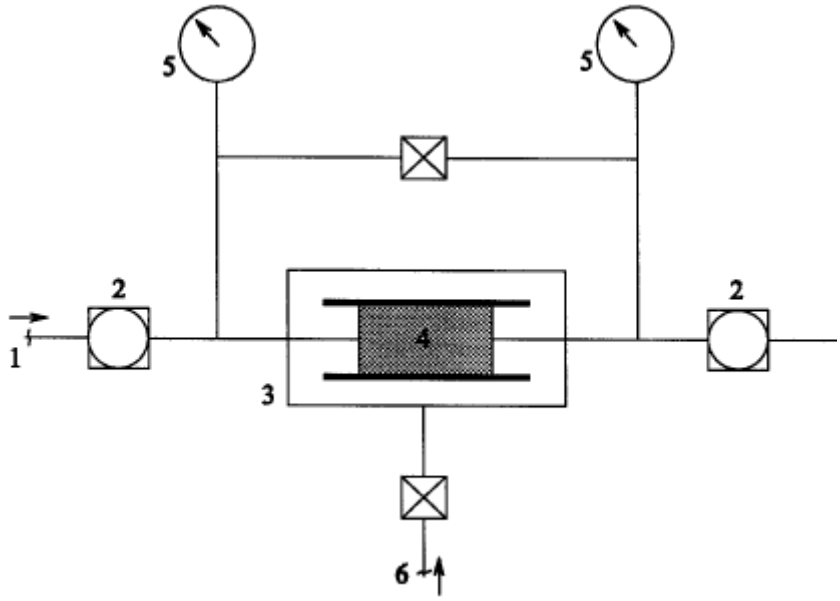

Figure 4.7 Diagram of permeameter (Torsæter & Abtahi, 2000).

1) Water supply	**4) core plug**
2) Reduction valves	**5) Pressure manometers**
3) Core holder	**6) Sleeve pressure for core holder**

The core holder for this experiment was a Hassler cell. Then the core is placed within a flexible rubber tube (Torsæter & Abtahi, 2000). High air pressure (sleeve pressure) is connected to the core holder pushing the rubber tube against the core, making the space around the core tight. Then the fluid entering the core holder may only go through the core, and not around it. A schematic of a Hassler core holder is shown in Figure 4.8.

Since the air permeability measurements gave us difficulties due to short core plugs, the permeability measurements using water were conducted a bit differently. 3 core plugs from each layer (12 in total) were used, and two different measurements for each type of core plug were done. The first measurement was done with only one core plug in the core holder, and the second with the remaining two core plugs together, in order to get a longer core plug. The results of the permeability measurements are shown in Table 4.3.

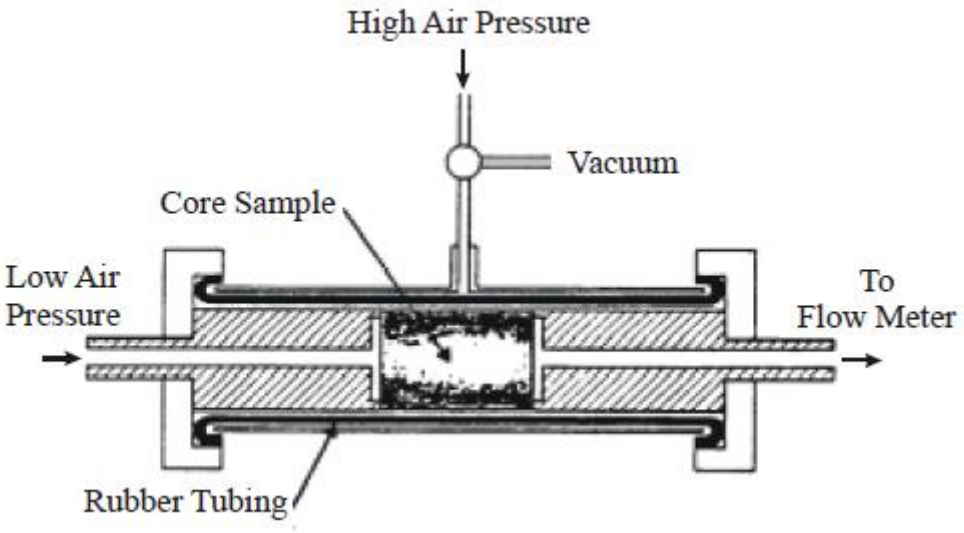

Figure 4.8 Hassler core holder (Torsæter &Abtahi, 2000).

Core plugs	Length [cm]	Diameter [cm]	Radius [cm]	Delta P [bar] (atm)	Q [cm^3/s]	kabs [cm^2]	kabs [mD]
BL1	2.1	3.8	1.9	0.16	0.17	2.0E-09	201
BL2+BL3	4.3	3.8	1.9	0.38	0.17	1.7E-09	171
BH8	3.9	3.8	1.9	0.03	0.25	2.9E-08	2959
BH9+BH11	4.0	3.8	1.9	0.10	0.17	6.0E-09	609
AL1	2.1	3.8	1.9	0.32	0.17	1.0E-09	101
AL2+AL3	4.4	3.8	1.9	0.60	0.17	1.1E-09	110
AH7+AH8	4.0	3.8	1.9	0.03	0.17	2.0E-08	2001
AH9	2.0	3.8	1.9	0.01	0.25	4.5E-08	4560

Table 4.3 Core plug permeabilities.

From these permeability measurements one can also see that the single core plugs of higher permeability causes problems due to their short length. The single core plugs of lower permeability are close to the double core plugs in value, but it is believed that the doubled core plugs give the most realistic information about each layers permeability. The four permeability values for the doubled core plugs are not far from the originally stated permeabilities, with the high permeability B as an exception. Therefore, it is reasonable to conclude that the absolute permeability of core type A is about 100 mD for the low permeability layer, which is slightly higher than the value of 50 mD given by the manufacturer, and 2000 mD for the high permeability layer, as was specified by the manufacturer. The absolute permeability of core type B is concluded to be a bit less than 200 mD for the low permeability layer, which was the value specified by the manufacturer, and about 600 mD for the higher permeability layer, which is less than the value of 1000 mD given by the manufacturer.

4.3 The experimental fluids

4.3.1 The brine

The brine used for the experiments had a concentration of 3 wt% NaCl. The water that was used to make the brine was distilled and purified water, where impurities that exist in tap water has been removed. When the salt had been mixed into the water with a magnetic stirrer, the brine was filtered using a 0.45 µm filter.

4.3.2 The Polymer

The polymer used for the experiments was a synthetic HPAM polymer with the name Flopaam 5115 SH. It was received in a dry state, where one was to mix the polymer with water yourself. See Figure 4.9. The brine that was used to mix with the dry polymer, had a 3.5 wt% of Nacl, and were made and filtered in the same way as the brine in chapter 4.3.1. To make the polymer solution, the dry polymer needed to be added evenly into the brine, while using a magnetic stirrer. At first the brine and polymer will not mix, but when the solution has been stirring overnight, the polymer and the brine are completely mixed.

Figure 4.9 The polymer in a dry state

In the experiments, the concentration of polymer in the brine was 1000 ppm, 1.0 g of dry polymer per 999.0 g of water. As the polymer that was received had a dry ratio of 89.18 %, and the rest water, it was necessary to mix 1.121 g of polymer to get 1 L of a 1000 ppm polymer solution.

4.3.3 Polymer density

The determination of the density of the polymer solution was done by using a pycnometer. Density, ρ, is defined as

$$\rho = \frac{m}{V}, \qquad \textbf{Eq. 4.6}$$

where m is mass, and V is volume. The pycnometer is a flask with an accurately measured volume. See Figure 4.10 for a picture of a pycnometer. The flask is filled with the liquid which is having its density determined, and the weight of the flask containing the liquid is measured. Subtracting this weight from the weight of the empty flask gives the weight/mass of the liquid. Using Eq. 4.6, the density of the liquid can then be determined.

Figure 4.10 Pycnometer.

The polymer that was used in the experiments had a density of **1.02** g/cm^3. For our later flow simulations the density difference to water is insignificant.

4.3.4 Polymer viscosity

Polymer is a non-Newtonian fluid. This means that the viscosity of the polymer will change if the shear rate changes, and shear rate changes are related to flow rate changes. It is therefore difficult to measure a polymer viscosity in an apparatus that uses a predetermined speed to do so. A method of measuring a fluid viscosity, and avoid this problem, is to use a capillary type of viscometer (see Figure 4.11).

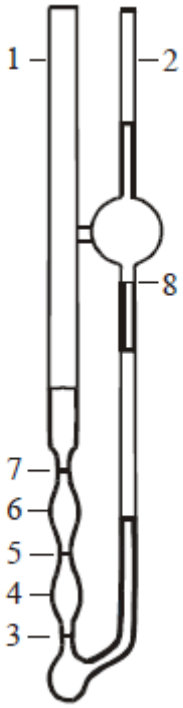

Figure 4.11 A capillary type of viscometer (Torsæter & Abtahi, 2000).

To use this type of viscometer, one fill up with polymer in tube 2 until it reaches the mark at 8. Wait until the polymer reaches mark 3, and time the number of seconds the polymer uses until it reaches mark 5. Repeat the same procedure between mark 5 and mark 7 (Torsæter & Abtahi, 2000). By doing it twice, one double checks the result from the first measurement.

Each capillary type of viscometer have their own calibration constants, K_1 and K_2. With the measured flow times, t_1 and t_2, the kinematic viscosity, ν, of the polymer can be calculated by

$$\nu_1 = K_1 * (t_1 - \vartheta_1)\,, \qquad \textbf{Eq. 4.7}$$

and

$$\nu_2 = K_2 * (t_2 - \vartheta_2)\,, \qquad \textbf{Eq. 4.8}$$

where ϑ is the Hagenbach correction factor. ϑ is 0 when t < 400 sec.

When the kinematic viscosity is calculated, and one knows the density of the fluid, the dynamic viscosity, μ, can be found by

$$\mu_1 = \rho * \nu_1\,, \qquad \textbf{Eq. 4.9}$$

and

$$\mu_2 = \rho * \nu_2\,. \qquad \textbf{Eq. 4.10}$$

A fluid like a polymer solution does not follow a linear correlation between viscosity and the concentration of polymer in the solution, as Newtonian fluids do. The concentration of the polymer used for the experiments will be known, but the concentration of polymer that will be produced from the cores will not be known. Therefore it was necessary to make a correlation curve for polymer concentration versus viscosity. There were done 3-4 viscosity measurements on 4 different polymer concentrations of 500 ppm, 1000 ppm, 1500 ppm, and 2000 ppm. The results of these measurements can be seen in Table 4.4.

Concentration [ppm]	Viscosity [cP]
500	2.61
500	2.65
500	2.44
500	2.50
1000	4.52
1000	4.84
1000	4.24
1000	4.56
1500	6.18
1500	7.00
1500	6.29
1500	6.91
2000	11.42
2000	10.00
2000	11.34

Table 4.4 Viscosity data.

Non-newtonian fluids usually follow an exponential function for correlation between concentration and viscosity. In Figure 4.12 the data from Table 4.4 is plotted.

An exponential curve gave the best fit for the data points, and the correlation curve for the polymer then follows the function

$$y = 1{,}6436 * 1.0009^{x} . \qquad \textbf{Eq. 4.11}$$

With this correlation curve, one can by measuring the viscosity of the polymer being produced, also get the true concentration.

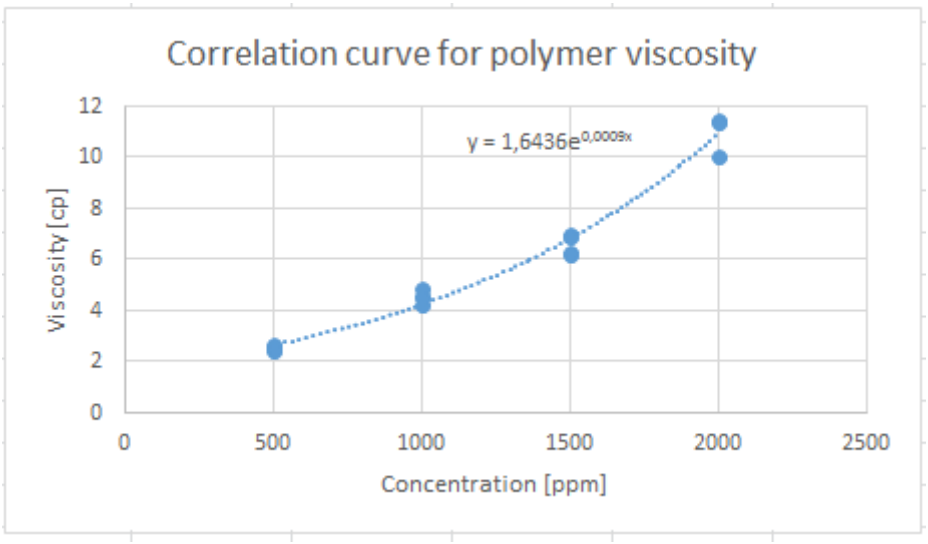

Figure 4.12 Correlation curve for polymer viscosity

The Flopaam polymer will lose some viscosity over time if it has been exposed to oxygen at any point, during mixing, when poured into a new container and so on. Since there were no air tight space to mix polymer in the student lab at NTNU, exposure to some oxygen was inevitable. The viscosity measurements that has been presented here was therefore done on polymer that had enough time to completely react with the oxygen, which took less than two weeks. In this way the viscosity is stable over time, even though it is a bit lower than when freshly mixed. For the experiments conducted in this Master thesis the viscosity of the polymer is not the critical element, as we are not looking at oil recovery, but adsorption and crossflow with brine.

5 Main flooding experiments

5.1 Experimental Setup

As the preparations with the homogeneous core plugs were done, it was time to put together the main experiment of flooding all the cores with brine and polymer. A diagram of the experimental setup is shown in Figure 5.1.

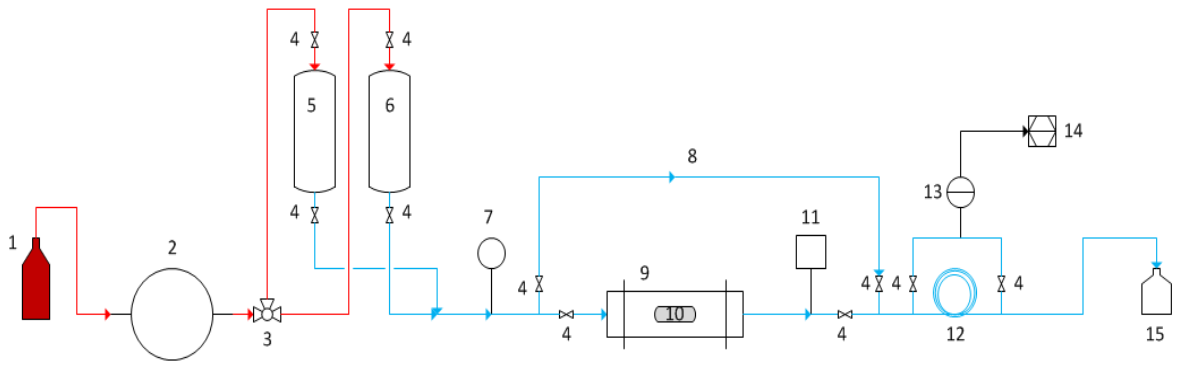

Figure 5.1 Experimental setup of main core flooding experiment.

1) **Flask with Exxsol D-60**
2) **Pump**
3) **Three-way valve**
4) **Two-way valve**
5) **Reservoir for polymer solution**
6) **Reservoir for brine**
7) **Pressure manometer**
8) **Bypass**
9) **Core holder**
10) **Core**
11) **Resistivity apparatus**
12) **Coil**
13) **Pressure transducer**
14) **Computer**
15) **Flask**

There are two reservoirs, one containing brine with 3 wt% salt for water flooding, and one containing the polymer solution, polymer mixed with brine of 3.5 wt% salt for the polymer flooding. The pump was set to provide a constant rate of 0.33 ml/min, which is 19.8 ml/hr. The rate was picked so that it should be close to a fluid velocity of 1m/day for the big cores, which is a normal rate of propagation within a reservoir. The pump is connected to a flask of the oil Exxsol D-60 at the inlet, which is pumped out the outlet and into the top of the two reservoirs. Exxsol D-60 does not mix with water or with polymer in a water solution, and provides the pressure needed to pump the fluid out of the reservoir in use, and into the flooding system.

By the outlet of the core holder, a resistivity apparatus is connected to the flow. This apparatus measures the resistivity of the fluid passing by, and it shows a clear difference if the water contains 3 wt% of salt or 3.5 wt% of salt. Then it is easy to see when the brine

containing polymer exits the core. This provides the tracer curve explained in sub section 3, which is needed to find the adsorption and IPV for the homogenous core plugs.

The second curve needed to find adsorption and IPV is the polymer production curve. This curve is produced from the pressure drop caused by polymer flowing through the coil. The pressure transducer is connected to a computer, and will record the pressure drop over the coil at a predetermined interval. From the pressure drop, the viscosity, and the concentration of the polymer, can be found.

The bypass over the core was installed to be able to double check the viscosity through the coil, when the polymer did not go through the core. In this way, one could know for sure if the polymer were destroyed, or lost its viscosity, while propagating through the core.

The pressure that is created from the coil, while polymer solution or brine is propagating through it, will provide a sort of outlet pressure for the core. The pressure manometer before the inlet to the core therefore measures the pressure drop over both the core and coil, assuming ambient pressure at the outlet. As the pressure manometer before the core holder is supposed to measure the pressure drop over the core, the pressure over the coil needs to be deducted from the number shown at the display of the manometer. Then one gets the real pressure drop over the core. After the fluids exits the coil, it is led out into a flask at atmospheric pressure.

All the pipes used in this experiment had an outer diameter of 1/8 inch, and an inner diameter of 1.5 mm, except the coil who had an outer diameter of 1/16 inch, and an inner diameter of 0.5 mm. The coil needed this smaller inner diameter in order to get a pressure drop in the right range for the pressure transducer.

The experimental setup that has been explained in this chapter is the same for both the flooding of the homogeneous core plugs and for the layered cores. For the homogeneous core plugs the core holder is a Hassler cell, explained in chapter 4.2.5. Within the core holder, two core plugs are put together in order to make one core plug of about 4 cm in length. For the layered cores the core holder is the epoxy with connections for 1/8 inch tubes.

It is from the homogeneous core plugs one can find the adsorption and IPV of each layer within the two different cores. To get the data needed for this, it was necessary to first flood with brine, then switch to flooding with polymer solution, and then brine again. In this way one get the production curves of the polymer and tracer as the polymer displaces the brine,

used for calculating the adsorption, and when the brine displaces the polymer, used for calculating the IPV. See Figure 5.2 and Figure 5.3 for pictures of the experimental setup in the lab.

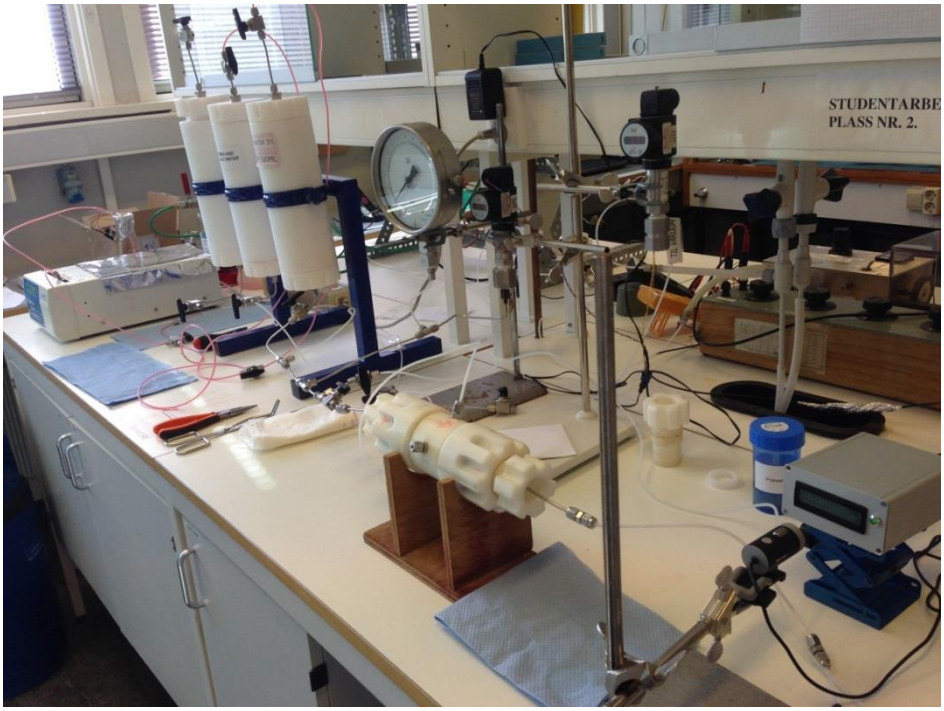

Figure 5.2 Experimental setup in lab.
Showing pump, reservoirs, pressure transducer, core holder, and resistivity apparatus.

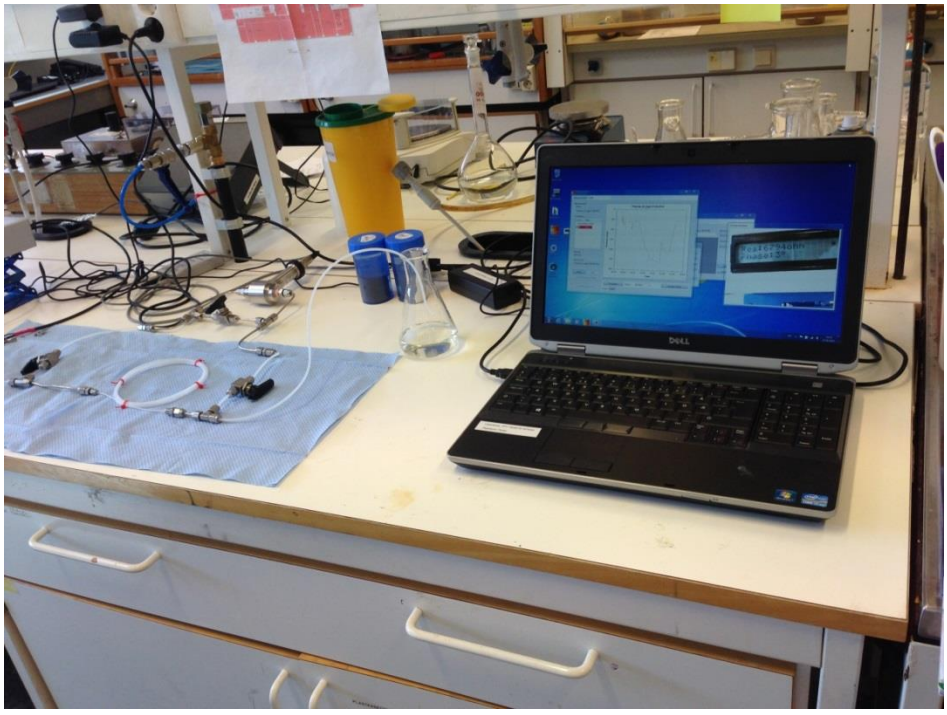

Figure 5.3 Experimental setup in lab.
Showing coil, digital pressure apparatus, connection to computer, and flask at outlet.

The goal of flooding the layered cores was not to find adsorption and IPV, as these values would at that time already be known. It was therefore only necessary to do a water flood and then a polymer flood. One of the main goals of this Master thesis is to find out if there has been any polymer diffusion from the high permeability layer to the low permeability layer, therefore it was decided to leave the core for two days and then flood with polymer a second time. This shut-in period will give time for diffusion. When flooding with polymer the second time it should be possible to see a change in the response of the production curve, if there has been a significant diffusion of polymer into the low permeable layer during the two days the core was shut in.

As it was not possible to saturate the layered cores in the same way as with the homogeneous core plugs, due to the core being incorporated in epoxy at arrival, the saturation needed to happen during the water flooding. This is not a perfect way to saturate a core, as air might get trapped inside the pores if the injection rate is not low enough. As the pore volume of the cores was quite big, 160 ml for core type A and 168 ml for core type B, there was no time to flood the core with a rate of about 0.01 ml/min. Instead, the cores were flooded in a vertical position with the normal injection rate of 0.33 ml/min, see Figure 5.4. By having the cores in a vertical position the air will be helped by gravity and the difference in density between air and brine, to rise towards the top of the core as brine is injected. This should ensure that less air will be trapped inside the porous medium.

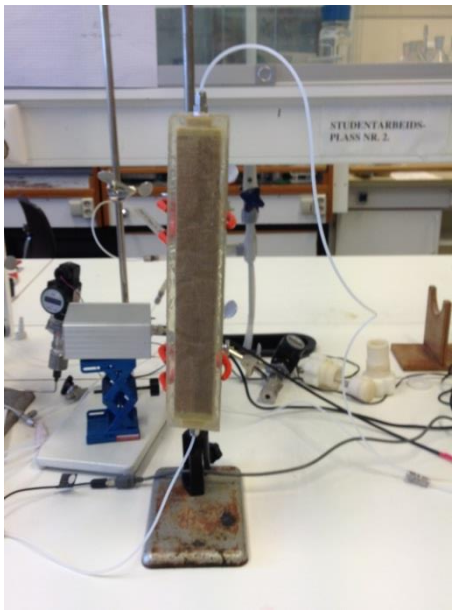

Figure 5.4 Saturation of core in vertical position.

For the homogeneous core plugs, it takes about 35-40 minutes to flood 1 PV with a rate of 0.33 ml/min, but for the layered cores it takes about 8 hours to flood 1 PV. How often the

computer is going to measure and save the pressure drop over the coil can be varied. Therefore it was taken measurements every minute for the core plugs, and every 5 minutes for the layered cores, in order to get enough data points for further calculations and plotting.

The program used for the recording of the pressure measurements was ControlCenterSeries30. Since there was no connection from the resistivity apparatus to a computer, a web camera was put in front of the display. By using the program Dorgem210 at the computer, one could set an interval for the camera to take a still photo. This interval was set to the same as for the pressure transducer over the coil. To get this data into Excel, the values were manually read in from the images of the resistivity apparatus.

5.2 Processing of the experimental data for the homogeneous core plugs

As the experimental setup contains a lot of pipeline both before and after the core holder, the time it takes to get the full response in the resistivity apparatus, and over the coil, will be delayed. Even though a pore volume only takes 35-40 minutes, dependent on which of the 4 core plugs is flooded, it took longer until the pressure over the coil stabilized at a base value. Therefore, in these core plug experiments it was not switched from brine to polymer solution, and then brine again, until the curve stabilized for each flood. In this way, one can be certain that the curves that was to be used to calculate adsorption and IPV was complete. To get these curves it was necessary to inject around 10-12 pore volumes.

The direct results that came out of the experiments were the pressure drop over the coil, as well as the resistivity of the fluids getting produced from the core. As mentioned before, these measurements came every minute, and provided enough data points for further processing. The goal was to produce the normalized production curve of polymer and tracer versus the amount of pore volumes injected.

5.2.1 The polymer curve

To get from the curve of pressure drop over the coil to the normalized polymer concentration, which was the end result, a few more calculations were necessary. By using the Hagen-Poiseuille equation for pressure drop for flow through a cylindrical pipe, the viscosity could be estimated. The equation solved for pressure drop, ΔP, is

$$\Delta P = \frac{8\mu LQ}{\pi r^4}. \qquad \textbf{Eq. 5.1}$$

By rearranging this equation, knowing the pressure drop, the viscosity, μ, can be found instead, by

$$\mu = \frac{\Delta P \pi r^4}{8LQ}. \qquad \textbf{Eq. 5.2}$$

Here, r is the radius of the pipe, in this case the coil, L is the length of the pipe, and Q the flow rate. In this experiment the radius of the coil was 0.25 mm, the length of the coil was 4 m, and the flow rate 0.33 ml/min. The pressure drop under the experiments was in the range between 0 - 1000 mbar (0 - 1 bar).

The Hagen-Poiseuille equation holds for Newtonian fluids, while the polymer solution is a non-Newtonian fluid. This introduces uncertainty. However, as we are only interested in normalized values, we assume that the Hagen-Poiseuille equation gives a fair approximation.

For the coil of an inner diameter of 0.5 mm, and with a flow rate of 0.33 ml/min, the shear rate for the polymer solution will be 112 s^{-1}. This makes the polymer molecules uncoil, and the viscosity decreases. Furthermore, at such high shear rates the relation between polymer concentration and pressure drop is assumed to be linear. By knowing the pressure drop when there is only brine in the system (concentration of polymer is zero), and the pressure drop as it stabilizes at the maximum value when the polymer is led through the bypass (concentration of polymer is 1000 ppm), one gets a correlation curve between pressure and concentration. For the polymer used for the flooding of the four core plugs, the correlation curve was as seen in Figure 5.5.

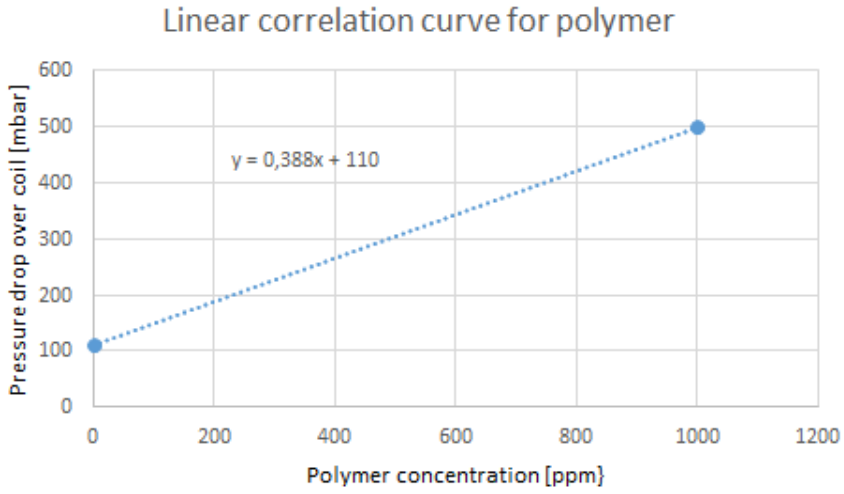

Figure 5.5 Linear correlation curve for core plugs.

The function to find the polymer concentration in µg/cm^3, was then

$$x = \frac{y}{0.388} - \frac{110}{0.388}. \qquad \textbf{Eq. 5.3}$$

To get the polymer concentration to g/cm^3, the concentration in µg/cm^3 was divided by 10^6.

To compare, the concentrations that were calculated if one used the correlation curve for viscosity versus concentration of polymer in solution, from sub section 4.3.4, would never reach the maximum polymer concentration of 1000 ppm. One of the reasons for this is that the shear rate of the polymer in movement has not been taken into consideration. This correlation curve should only be used if the polymer is not in movement, or if it is subjected to very low shear rates. By using the bypass that provides a polymer concentration of 1000 ppm through the coil, the polymer concentration based on the viscosity calculation and this correlation curve would be 930 ppm.

There were a few anomalies during the water flood where the polymer concentration became negative when there was just water in the system. These values were put to zero.

After calculating the polymer concentrations, they were normalized by using Eq. 3.1.

It was also necessary to compensate for the time lag between the resistivity measurements and until the same response was seen in the pressure measurements over the coil. The pipelines between the resistivity apparatus and the coil gave a time difference of 17 minutes. Therefore, the values of the normalized polymer concentration needed to be transferred 17 minutes forward in time to correlate to the correct tracer concentrations.

5.2.2 The tracer curve

To get from the resistivity output to the normalized tracer concentration, resistivity needed to be transformed into conductivity. Conductivity, σ, is the reciprocal of resistivity, ρ_r, giving the equation

$$\sigma = \frac{1}{\rho_r}. \qquad \textbf{Eq. 5.4}$$

From the conductivity of the fluid, one can find the tracer concentration, as conductivity is known to have a linear correlation with the concentration of NaCl in the solution. The minimum tracer concentration is known to be 0.03 g/cm^3, and the maximum tracer concentration is known to be 0.035 g/cm^3, correlating to 3 wt% of salt in the saturating brine and 3.5 wt% salt in the polymer solution. By picking the minimum and maximum conductivity, a correlation curve of tracer concentration versus conductivity can be made. An

example of such a correlation curve for the core plug of the high permeability layer in core type A, is seen in Figure 5.6.

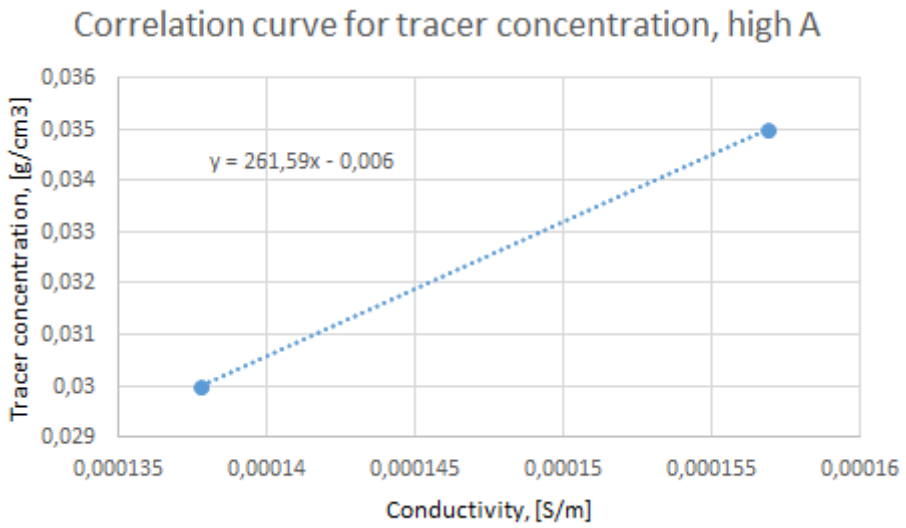

Figure 5.6 Correlation curve for tracer concentration for high permeability layer, type A core.

The tracer concentrations for the high permeability core plug type A is then found using the equation

$$y = 261.59x - 0.006\,. \qquad \textbf{Eq. 5.5}$$

As the resistivity apparatus was quite sensitive, there were some fluctuations in the stable areas of the tracer curve, as well as a few spikes of extra high and low values. Therefore, it became necessary to pick the "correct" minimum and maximum values of the conductivity curve. In Figure 5.7, the conductivity plot for the high permeability core plug type A, can be seen.

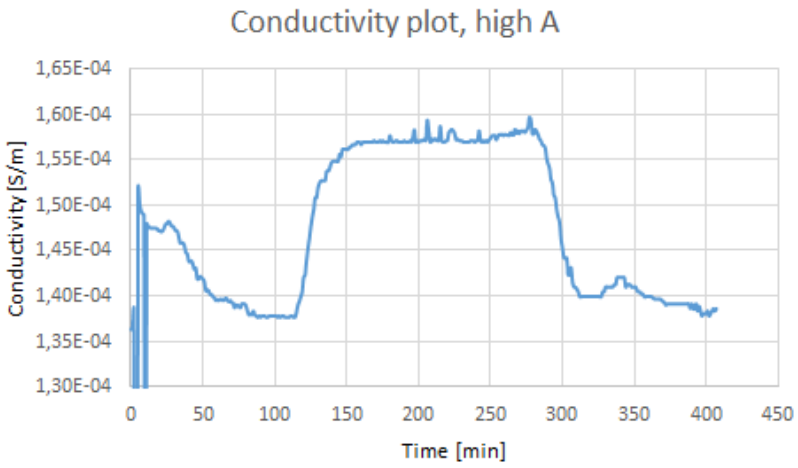

Figure 5.7 Conductivity plot for high permeability layer, type A core.

From Figure 5.7 one can clearly see how it would give the wrong tracer concentrations to blindly choose the minimum and maximum conductivity to make the correlation curve for the tracer concentration. For this core plug it was correct to pick the minimum conductivity at about 100 min, representing a stable value of the water flooding, and the maximum conductivity at about 170 min, representing a stable value of when the tracer production is at 100 %.

The correlation curves for the tracer concentration and the conductivity plots for the three other types of core plugs can be found in Appendix A.

Tracer concentrations below the minimum tracer concentration were put to 0.03 g/cm^3, and those above the maximum tracer concentration were put to 0.035 g/cm^3. In this way, some of the worst spikes were removed.

When the tracer concentrations had been calculated, they were normalized using Eq. 3.2.

5.2.3 Adjustments on the raw normalized concentration curves

For the raw normalized polymer concentration curve, it was still necessary to do some adjustments, to get an overall smooth production curve that could be used to calculate adsorption and IPV by integrals.

On all of the four core plugs, the normalized polymer production curves had a lot of volatility during the water flooding, until it stabilized and reached the concentration of zero it was supposed to have. These values were put to zero.

When the polymer flood had stabilized in the pressure curve over the coil, it was switched to brine again. This action, of closing the valve underneath the polymer reservoir and opening the valve underneath the brine reservoir, even for just 2 seconds in total, gave a pressure response in the coil. This pressure response can be seen as a sharp drop in pressure on the polymer curve. The pressure starts to build up gradually, but does not reach the maximum polymer value before the production curve for polymer has started declining again, due to water displacing polymer within the core. For this missing area of the real polymer curve, it was necessary to adjust the curve by finding a trend line for the downward going curve to fill in the lost values. The trend line that gave the best fit to the following data points were either a polynomial function, or a logarithmic function.

On three out of four core plugs, the end of the polymer curve did not go all the way down to a concentration of zero. To calculate the most likely IPV of the core plug, the polymer curve,

from the area it started to deflect, was fitted to follow the function of the rest of the downward going curve. The best fit was either a polynomial, logarithmic or linear function.

For the high permeability core plug, type B, there was an anomaly in the end of the upward going polymer curve. This area was fitted to follow the same trend as the previous part of the curve and the curves of the other core plugs. To do this it was necessary to extrapolate by hand to find the correct shape, and then find a best fit function to calculate all the data points of this area. A polynomial function gave the best fit in this case.

For the raw normalized tracer concentration curve, it was also necessary to do adjustments to get a smooth production curve that could be used to calculate adsorption and IPV by integrals.

The volatility in the data at the beginning of the water flood from the polymer curve was also found in the tracer curve, and these data points were therefore also put to zero.

As for the polymer curve, the end of the tracer curves did not go all the way down to a concentration of zero. To calculate the most likely IPV of the core plugs, the deflected end area of the curve was fitted to follow the function of the rest of the downward going curve. The best fit for these curves were either a polynomial or logarithmic function.

For the low permeability core plug, type B, there were more fluctuations in the tracer concentration, during the polymer flood, than for the other three core plugs. Even though the shape of the curve was the same as for the other three, it was necessary to smooth it out to get the most correct adsorption integral. This was done using a logarithmic trend line.

As the tracer curve was based on the resistivity measurements, the pressure drop in the transition from polymer flooding to water flooding did not affect the tracer curve.

All the plots of the trend lines, with accompanying functions, can be found in Appendix B.

5.3 Results for the homogeneous core plugs

5.3.1 High permeability core plug, core type A

The plot of the raw normalized concentration curves, described in 5.2.1 and 5.2.2, can be seen in Figure 5.8.

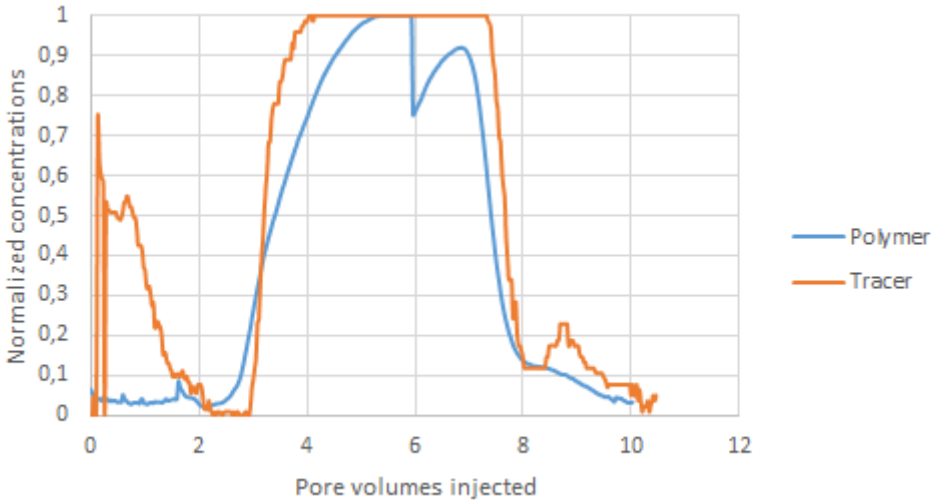

Figure 5.8 Raw normalized concentration curves for high permeability core type A.

The plot of the adjusted normalized concentration curves, described in 5.2.3, can be seen in Figure 5.9.

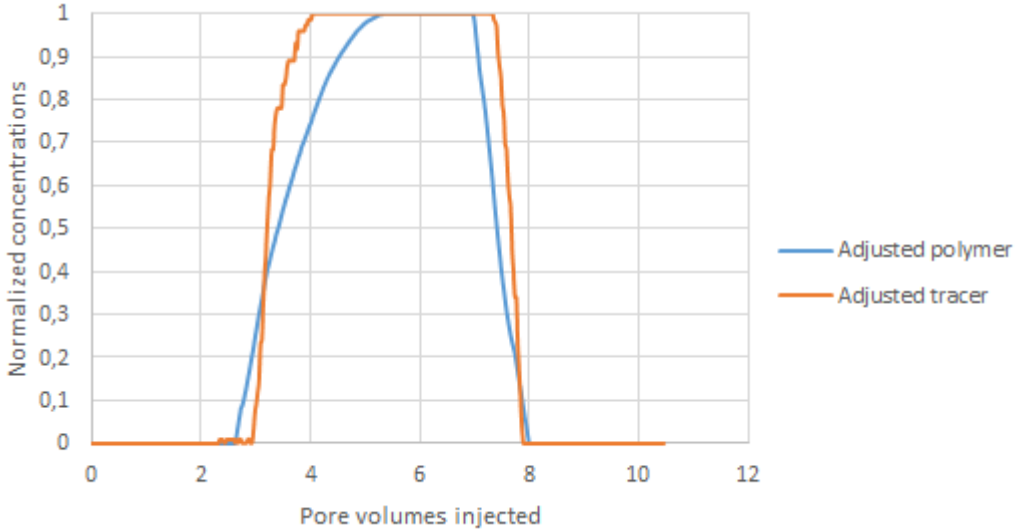

Figure 5.9 Adjusted normalized concentration curves for high permeability core type A.

A plot comparing the raw normalized concentration curves to the adjusted normalized concentration curves, is found in Figure 5.10.

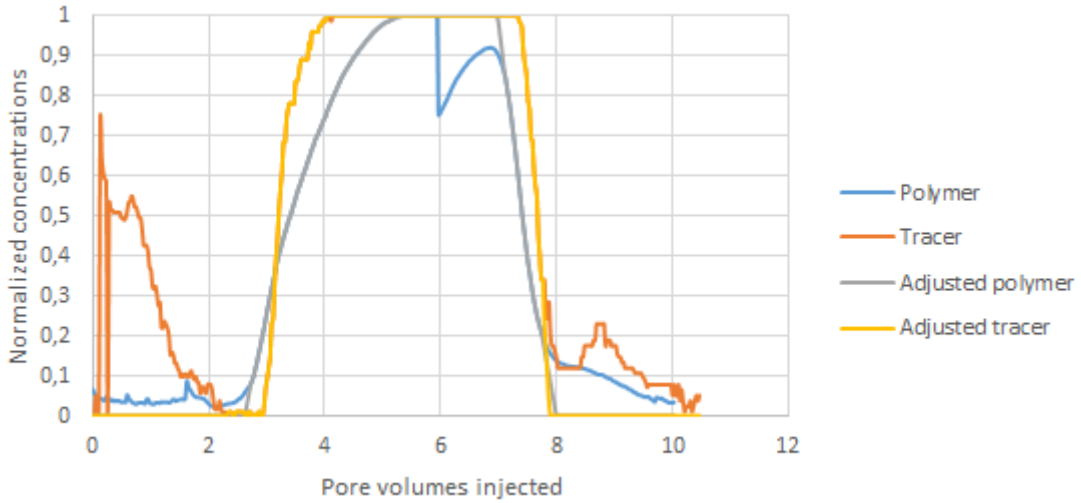

Figure 5.10 Comparing raw and adjusted normalized concentration curves for high permeability core type A.

The resulting values of the adsorption and IPV for the high permeability core plug type A, calculated with Eq. 3.3 and Eq. 3.4, for the adjusted concentration curves, are shown in Table 5.1.

IPV	0.2140	
PV	12.84	cm^3
Total vol	45.05	cm^3
Porosity	0.2851	
Rock vol	32.20	cm^3
Weight rock	76.79	g
Ads. integral + IPV	0.4834	
Max conc pol	0.001121	g/^cm3
Polymer adsorbed	0.006959	g
Adsorption	9.063E-05	g/g

Table 5.1 Adsorption and IPV results for high permeability core type A.

5.3.2 Low permeability core plug, core type A

The plot of the raw normalized concentration curves, described in 5.2.1 and 5.2.2, can be seen in Figure 5.11.

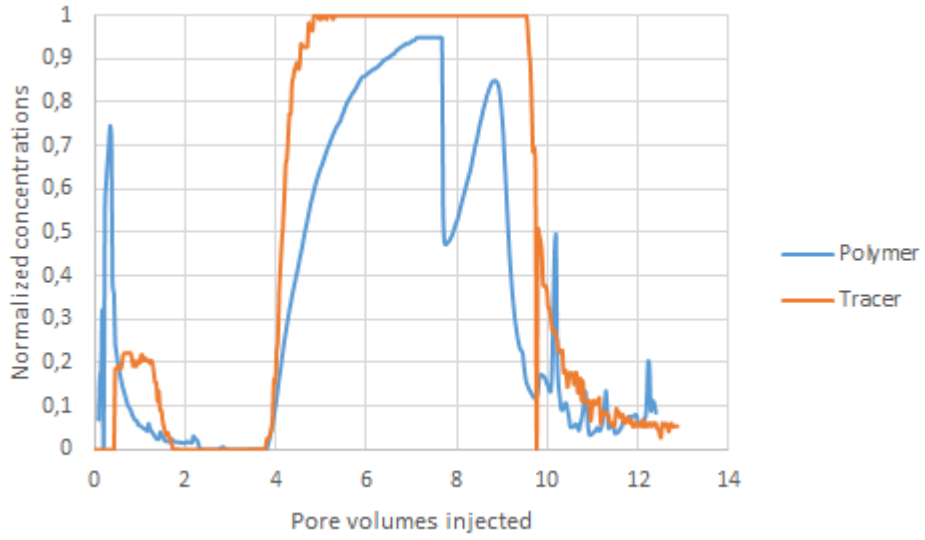

Figure 5.11 Raw normalized concentration curves for low permeability core type A.

The plot of the adjusted normalized concentration curves, described in 5.2.3, can be seen in Figure 5.12.

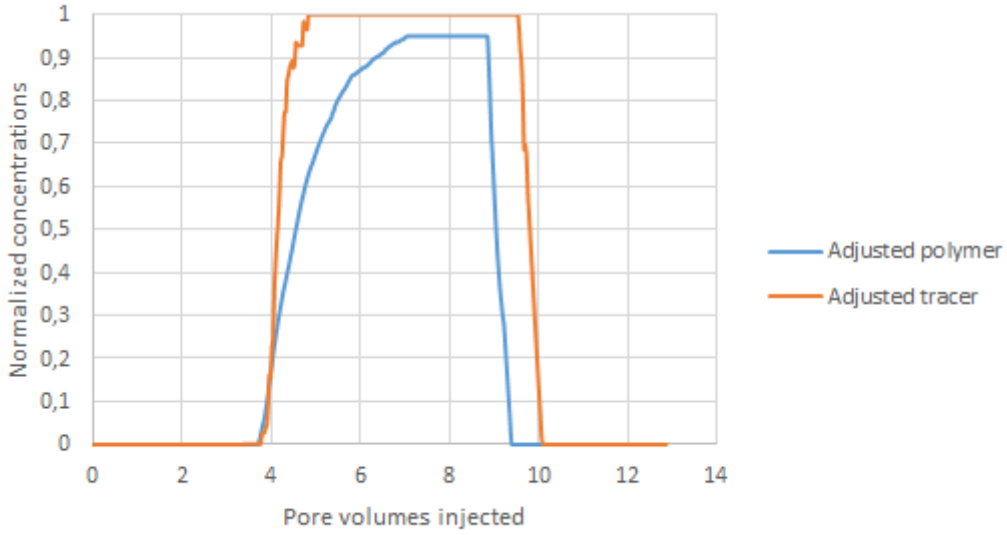

Figure 5.12 Adjusted normalized concentration curves for low permeability core type A.

A plot comparing the raw normalized concentration curves to the adjusted normalized concentration curves, is found in Figure 5.13.

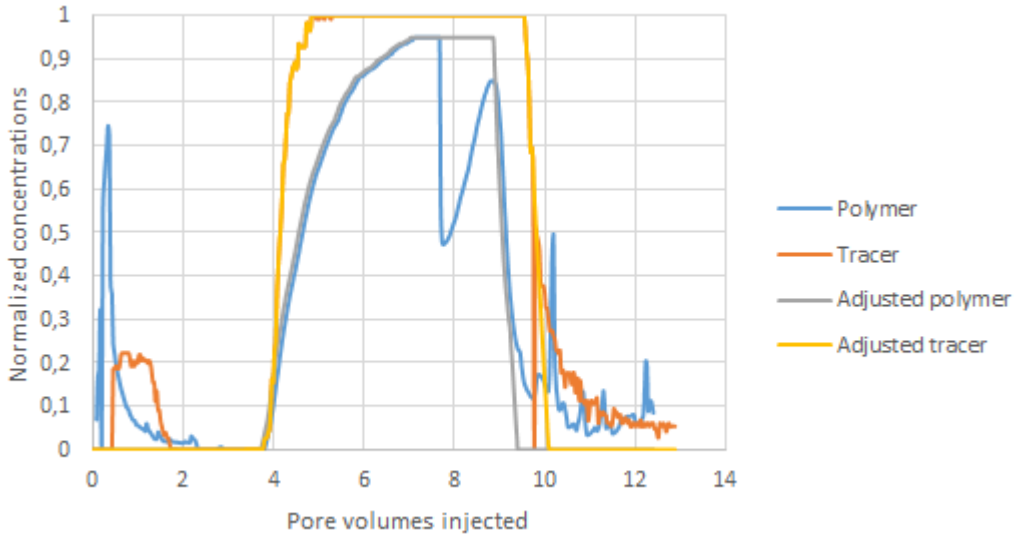

Figure 5.13 Comparing raw and adjusted normalized concentration curves for low permeability core type A.

The resulting values of the adsorption and IPV for the low permeability core plug type A, calculated with Eq. 3.3 and Eq. 3.4, for the adjusted concentration curves, are shown in Table 5.2.

IPV	0.7275	
PV	11.66	cm^3
Total vol	48.76	cm^3
Porosity	0.2391	
Rock vol	37.10	cm^3
Weight rock	84.41	g
Ads. integral + IPV	1.36	
Max conc pol	0.001121	g/cm^3
Polymer adsorbed	0.01780	g
Adsorption	0.0002109	g/g

Table 5.2 Adsorption and IPV results for low permeability core type A.

5.3.3 High permeability core plug, core type B

The plot of the raw normalized concentration curves, described in 5.2.1 and 5.2.2, can be seen in Figure 5.14.

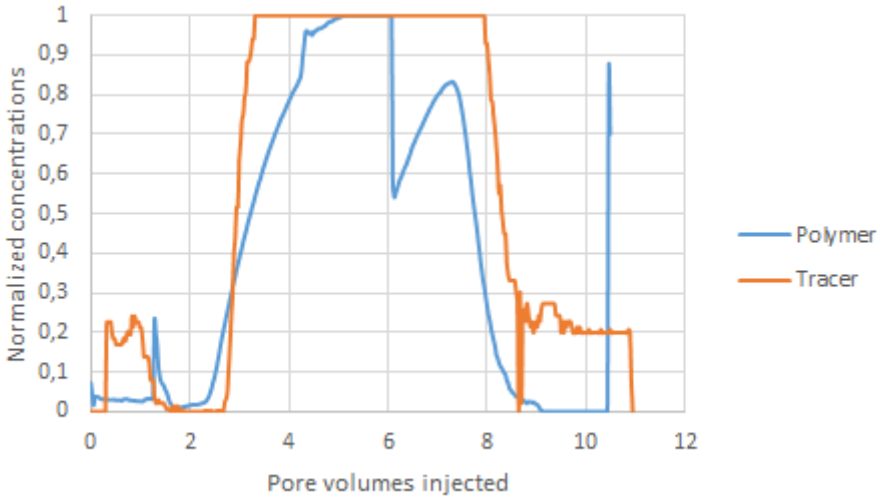

Figure 5.14 Raw normalized concentration curves for high permeability core type B.

The plot of the adjusted normalized concentration curves, described in 5.2.3, can be seen in Figure 5.15.

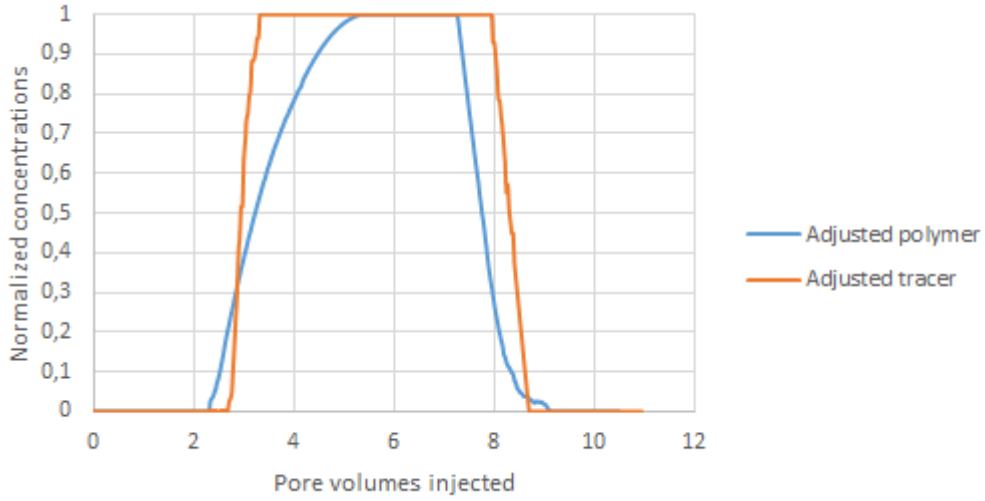

Figure 5.15 Adjusted normalized concentration curves for high permeability core type B.

A plot comparing the raw normalized concentration curves to the adjusted normalized concentration curves, is found in Figure 5.16.

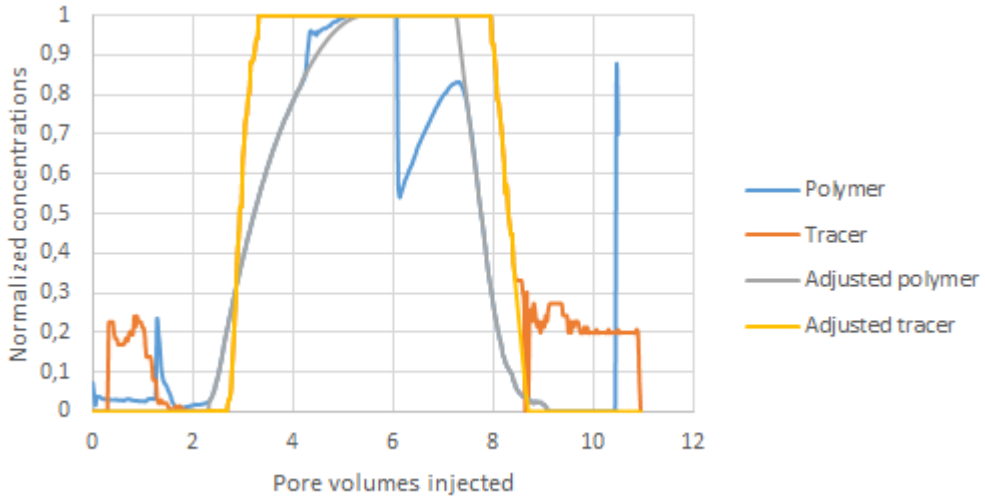

Figure 5.16 Comparing raw and adjusted normalized concentration curves for high permeability core type B.

The resulting values of the adsorption and IPV for the high permeability core plug type B, calculated with Eq. 3.3 and Eq. 3.4, for the adjusted concentration curves, are shown in Table 5.3.

IPV	0.5026	
PV	12.34	cm^3
Total vol	45.34	cm^3
Porosity	0.2722	
Rock vol	33.00	cm^3
Weight rock	77.52	g
Ads. integral + IPV	0.9004	
Max conc pol	0.001121	g/cm^3
Polymer adsorbed	0.01246	g
Adsorption	0.0001607	g/g

Table 5.3 Adsorption and IPV results for high permeability core type B.

5.3.4 Low permeability core plug, core type B

The plot of the raw normalized concentration curves, described in 5.2.1 and 5.2.2, can be seen in Figure 5.17.

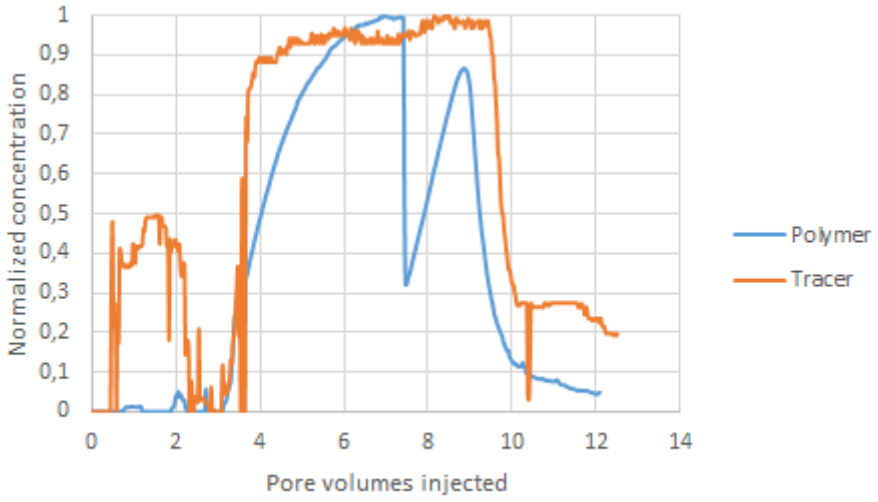

Figure 5.17 Raw normalized concentration curves for low permeability core type B.

The plot of the adjusted normalized concentration curves, described in 5.2.3, can be seen in Figure 5.18.

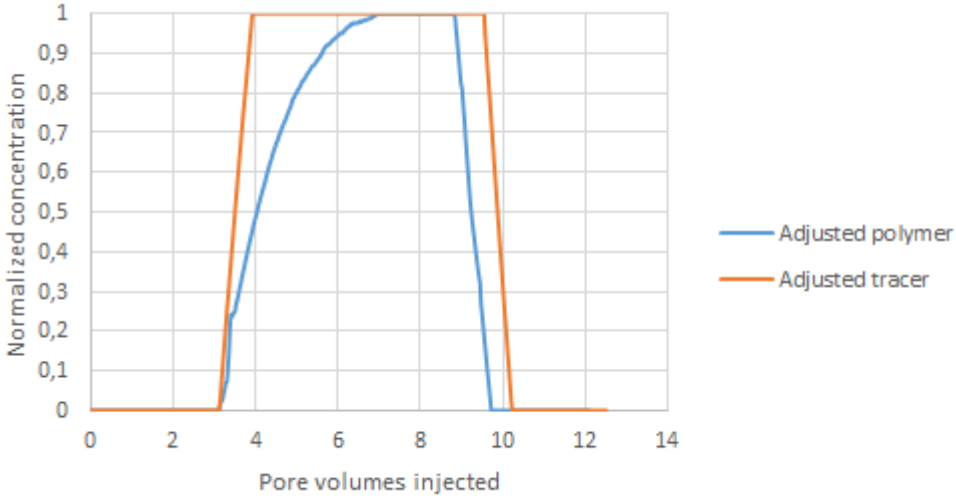

Figure 5.18 Adjusted normalized concentration curves for low permeability core type B.

A plot comparing the raw normalized concentration curves to the adjusted normalized concentration curves, is found in Figure 5.19.

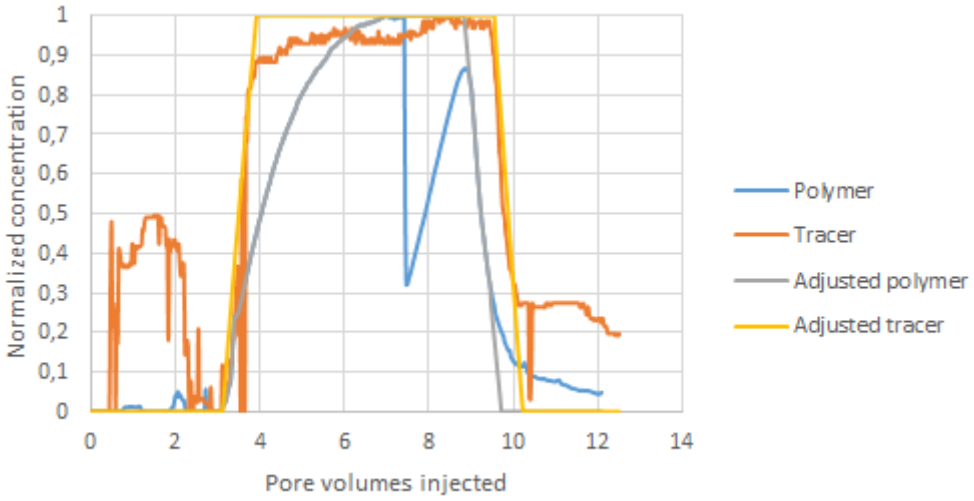

Figure 5.19 Comparing raw and adjusted normalized concentration curves for low permeability core type B.

The resulting values of the adsorption and IPV for the low permeability core plug type B, calculated with Eq. 3.3 and Eq. 3.4, for the adjusted concentration curves, are shown in Table 5.4.

IPV	0.6112	
PV	13.49	cm^3
Total vol	48.39	cm^3
Porosity	0.2787	
Rock vol	34.90	cm^3
Weight rock	81.54	g
Ads. integral + IPV	1.352	
Max conc pol	0.001121	g/cm^3
Polymer adsorbed	0.02044	g
Adsorption	0.0002506	g/g

Table 5.4 Adsorption and IPV results for low permeability core type B.

5.4 Processing of the experimental data for the layered cores

As the pore volume of the layered cores was between 160-168 ml, the volume of the reservoirs of 500 ml only made it possible to flood for about 20 hours (ca. 400 ml, as the rate was still 0.33 ml/min). This was the margin that seemed safe, to prevent the reservoir from becoming empty of brine or polymer solution, and Exxsol D-60 from entering the flooding system. If any Exxsol D-60 had entered the core, it would be ruined. Flooding for 20 hours means injecting between 2-2.5 pore volumes into the cores.

The experimental setup for the layered cores was the same as for the homogeneous core plugs, with the exception of the core holder. This means that the experimental output, the

pressure drop over the coil and the resistivity of the fluid getting produced from the core, also was the same. As a flooding of 20 hours needed to go over night, the web camera put up to take still pictures of the resistivity data were moved so that it also could take pictures of the pressure manometer before the core. For these two-layered core floodings, it could provide important extra information knowing the pressure drop over the core, at the same time interval of 5 minutes, as for the other two outputs. This pressure drop information was not as important for the core plugs, where the main goal was to find adsorption and IPV, so then it was sufficient to write down the pressure drop by hand.

The goal of flooding the layered cores was not to make normalized production curves, but rather getting the production curve of polymer and tracer over time. In this way, the behavior of the polymer within a two layered core could be studied. From the flooding of the small core plugs, the adsorption and IPV of each layer has been found. Knowing these values makes us more capable to study the production curves from the two-layered cores, and say something about the probability of there being any diffusion from the high permeability layer to the low permeability layer.

5.4.1 The polymer curve

To get from the pressure response over the coil to the production curve of polymer concentration, the same procedure as for the core plugs could be followed, but it was necessary to make new correlation curves for pressure drop over the coil versus polymer concentration. The reason for this was that the first stable batch of polymer was used on the flooding of the core plugs. It was not known by the author at the time that the polymers reaction to oxygen was not instant, but rather making the viscosity decline over a couple of weeks until it became stable. The polymer used on core A and core B was therefore a few days old, but not 2 weeks old and stabilized. As one batch was made as 1 liter at a time, and the consumption of polymer for two polymer floodings of the same core was 1 liter, one batch was used for core A, and another for core B. Therefore it was necessary to make two new correlation curves. The correlation curve for the polymer used for core A is seen in Figure 5.20.

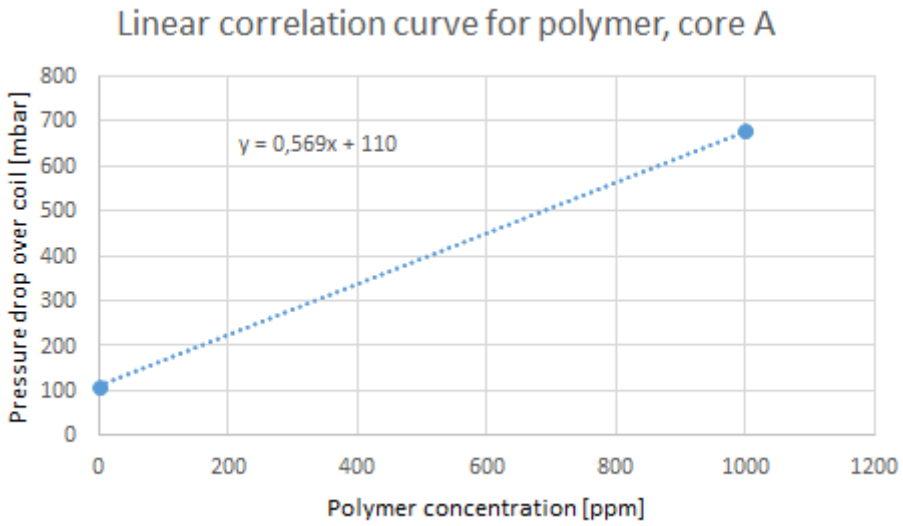

Figure 5.20 Correlation curve for the polymer used for core A.

The correlation curve for the polymer used for core B is seen in Figure 5.21.

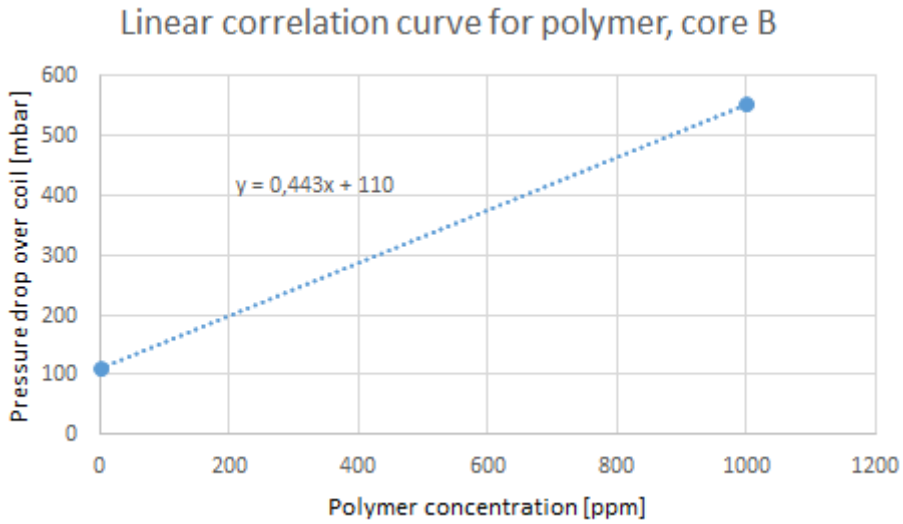

Figure 5.21 Correlation curve for the polymer used for core B.

The function to find the polymer concentration for flooding core A, in µg/cm^3, was then

$$x = \frac{y}{0.569} - \frac{110}{0.569}, \qquad \textbf{Eq. 5.6}$$

and the function to find the polymer concentration for flooding core B, in µg/cm^3, was

$$x = \frac{y}{0.443} - \frac{110}{0.443}. \qquad \textbf{Eq. 5.7}$$

To get the polymer concentrations to g/cm^3, the concentration in µg/cm^3 was divided by 10^6.

As for the core plugs, there were a few anomalies during the water flood where the polymer concentration became negative, when there were just water in the system. These values were put to zero.

The polymer curve's time lag of 17 minutes compared to the tracer curve, due to the pipelines between the resistivity apparatus and the coil, are compensated for by moving the polymer concentrations 17 minutes forward in time.

The viscosity of the polymer propagating through the coil can still be found by using the rearranged Hagen-Poiseuille equation, Eq. 5.2.

For core B, the viscosity of the polymer at the stabilized area of the end of the first polymer flooding was higher than the viscosity at the stabilized area of the second polymer flooding. This indicates that the polymer used for the flooding of core B has lost some viscosity during the two days the core was shut in between the two polymer floods. The concentration at the end of the first polymer flood seems therefore higher than the concentration at the end of the second polymer flood. As both curves are stable at the end values, the polymer concentration should be at its maximum value, and they should be the same. Therefore it was necessary to adjust the concentration of the first polymer curve down to the maximum concentration of the second polymer curve.

5.4.2 The tracer curve

As for the homogeneous core plugs, the tracer curve was made by converting resistivity into conductivity, and finding the tracer concentration by using the correlation curve of tracer concentration versus conductivity. As the brine used for the water flooding and the polymer solution were made new for the experiments on core A and core B, also new correlation curves for tracer concentration had to be made. These do not deflect considerably from the conductivity values used for the small core plugs, but since the resistivity apparatus is sensitive, there will be small variations. The tracer correlation curve for core A can be seen in Figure 5.22.

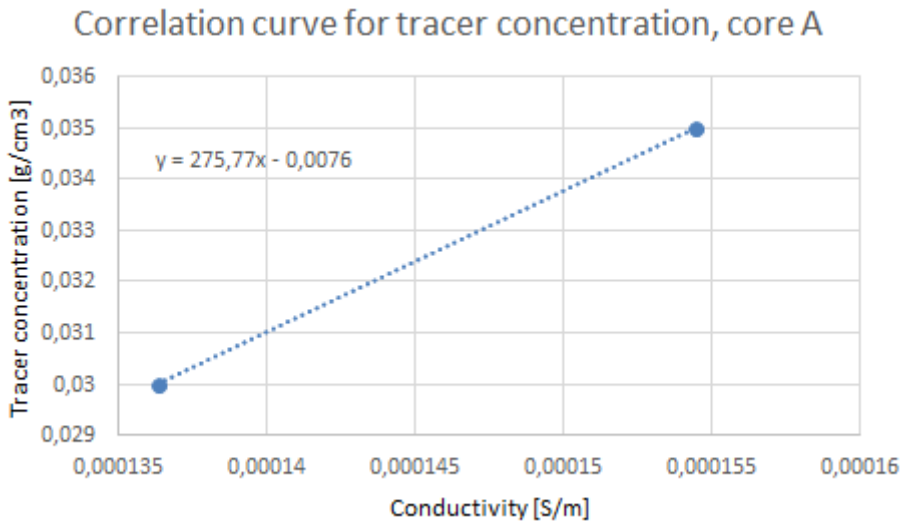

Figure 5.22 Correlation curve for tracer concentration for core A.

The tracer concentrations for core A is then found using the equation

$$y = 275.77x - 0.0076. \qquad \textbf{Eq. 5.8}$$

The minimum and maximum values picked from the conductivity plot for core A, see Figure 5.23, is the conductivity at about 200 min, representing a stable value of the water flooding, and the conductivity at about 800 min, which is the highest area of the conductivity plot.

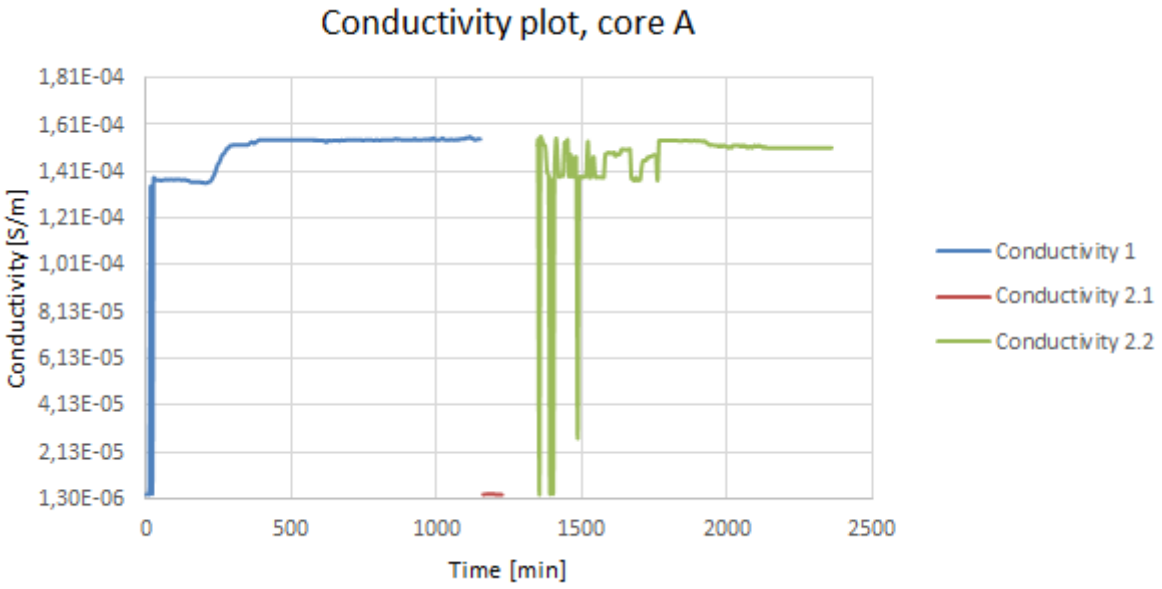

Figure 5.23 Conductivity plot for core A.

For core B, the tracer correlation curve can be seen in Figure 5.24.

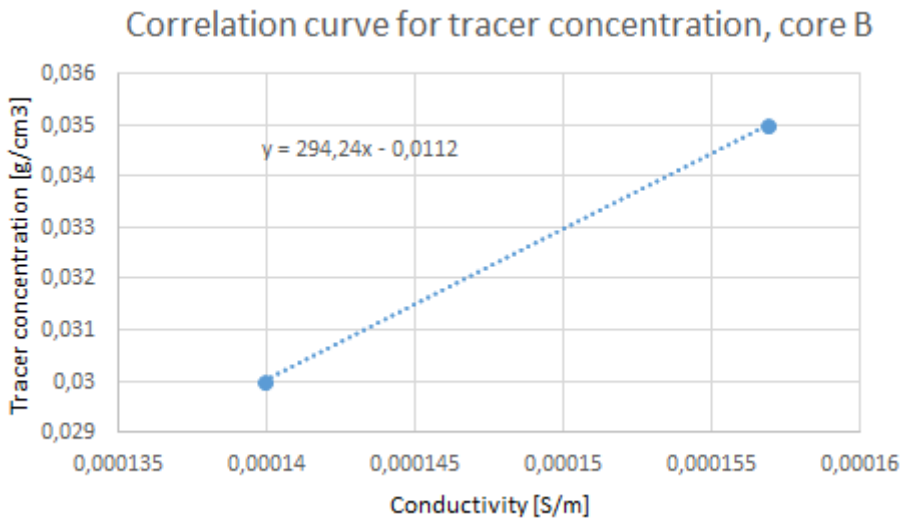

Figure 5.24 Correlation curve for tracer concentration for core B.

The tracer concentrations for core B is then found using the equation

$$y = 294.24x - 0.0112\,. \qquad \textbf{Eq. 5.9}$$

The minimum and maximum values picked from the conductivity plot for core B, see Figure 5.25, are the conductivities at about 150 min and 1900 min. The reason why the highest conductivity value at about 1500 min is not chosen as the maximum conductivity, is that the conductivity curve 1.2 (to be explained in chapter 5.4.3) also represents a stable area of maximum tracer concentration, and this is the same as the conductivities around 1900 min. The resistivity values of conductivity curve 1.2 and around 1900 min is also closer to the maximum resistivity of the tracer used during flooding of core A.

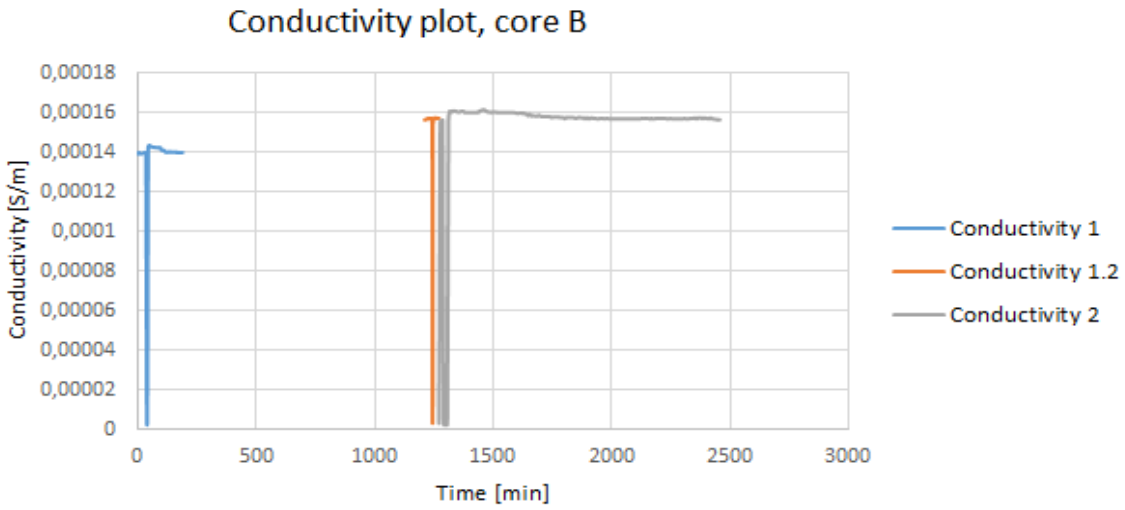

Figure 5.25 Conductivity plot for core B.

To keep the tracer curve as close to the original values as possible, only tracer concentrations below the minimum tracer concentration were changed and put to 0.03 g/cm^3, as this is the lowest physical value the brine should have.

5.4.3 Missing areas of the curves

There were a few events during the flooding of core A and core B leading to some areas of the production curves with missing data.

For core A, the pressure transducer stopped working one hour into the second polymer flooding. As the flooding of the layered cores needed to go over night due to their length, it was not possible to check the experiment very often. That is the reason why there is a two hour gap with missing data, until the pressure transducer was switched with a new one. For the plots of the experiments in chapter 5.4.2 and 5.5 the first polymer flood curve is called polymer 1, the first part of the second polymer flood curve (the first hour) is called polymer 2.1, and the second part of the second polymer flood curve is called polymer 2.2. The same applies to the tracer curves.

The pressure data from the pressure manometer in front of the core was still recording during the two hours of missing pressure data over the coil. By taking the pressure measured here, minus the pressure over the coil, the pressure drop over the core is given. For the other experiments the pressure drop over the core has increased at a steady pace as polymer is injected. Looking at the plot of the pressure drop over the core (pressure manometer minus the pressure over the coil) in Figure 5.26, one can see that this is also the case for most of the flooding of core A, but there is something abnormal happening just before the data is missing. The pressure suddenly drops and starts increasing. After the two hours the pressure drop over the curve has been very high and is on its way down again to the normal state.

During the two hours of missing data for core A it seems like the pressure drop over the coil increased rapidly to a value a lot higher than the value corresponding to the maximum polymer concentration. After the rapid increase it started to decline again until it reached the value corresponding to the maximum polymer concentration. This shape can be verified by looking at the data from the pressure manometer in the two hour gap, which follows the pressure events in the system in the same way as the pressure transducer, and can thereby be directly correlated to the shape of the polymer concentration curve. The plot of the polymer concentrations together with the pressure manometer data, including the data from the two missing hours, is found in Figure 5.28.

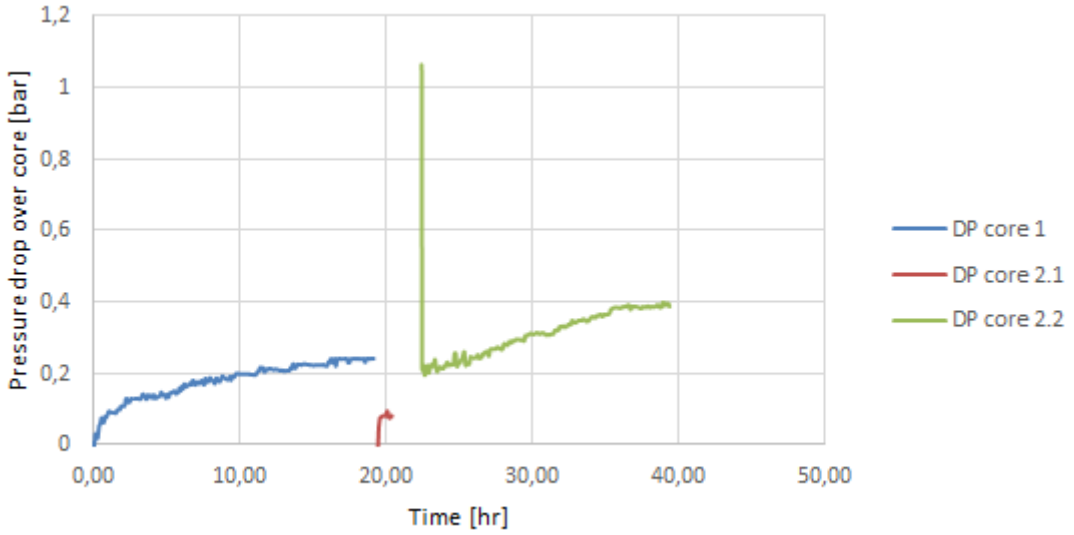

Figure 5.26 Pressure drop over core A.

For core B, there was an even bigger misfortune, causing a larger area of missing data than two hours. During the first polymer flooding overnight, the computer that received the data from the pressure transducer, as well as the still pictures of the resistivity apparatus from the web camera, switched itself off after automatically installing new updates. This happened around 17.15, when students no longer have access to the lab. Therefore, this was not discovered until the next morning, and no data were recorded in these hours. There was enough polymer solution left in the reservoir to flood another hour, so that the concentration of the polymer, when it had stabilized on its maximum value, could be found. For the plots of the experiments in chapter 5.4.2 and 5.5 the first part of the first polymer flood curve is called polymer 1.1, the second part of the first polymer flood curve (the last hour) is called polymer 1.2, and the second polymer flood curve is called polymer 2. The same applies to the tracer curves.

5.5 Results for the layered cores

5.5.1 Core A

The production curves from flooding core A with polymer and tracer for two rounds, described in 5.4.1 and 5.4.2, can be seen in Figure 5.27.

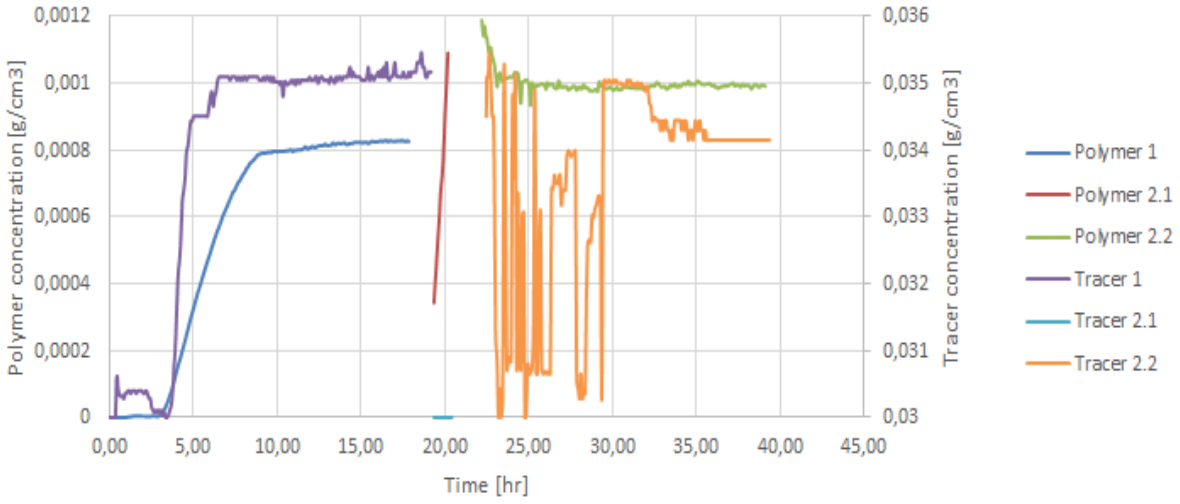

Figure 5.27 Production curves for core A.

The plot of the polymer concentrations together with the pressure manometer data, described in 5.4.3, including the data from the two missing hours, is found in Figure 5.28.

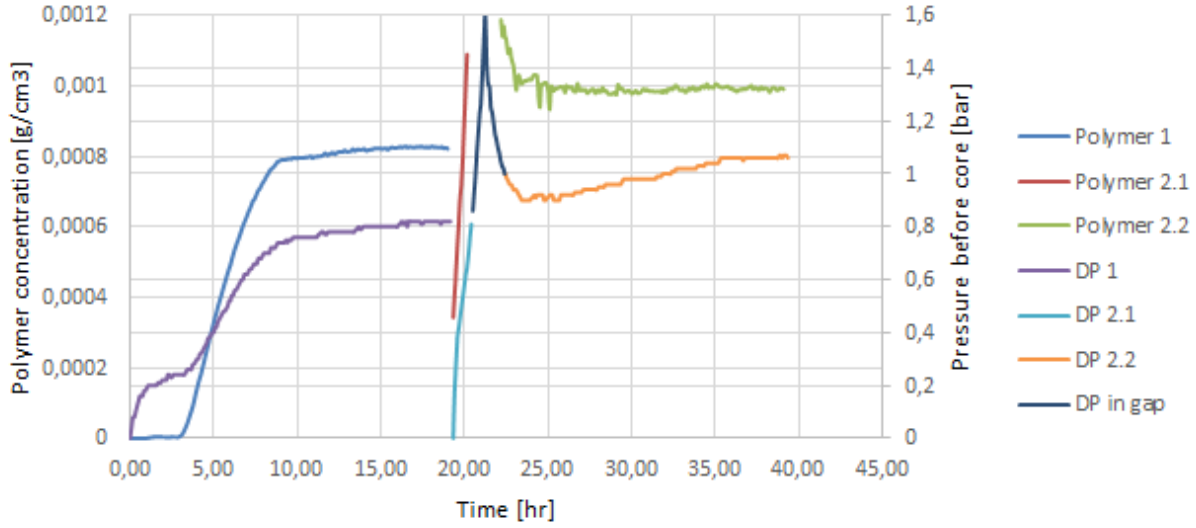

Figure 5.28 Polymer concentration compared to pressure manometer data (including data in gap) for core A.

5.5.2 Core B

The production curves from flooding core B with polymer and tracer for two rounds, described in 5.4.1 and 5.4.2, can be seen in Figure 5.29.

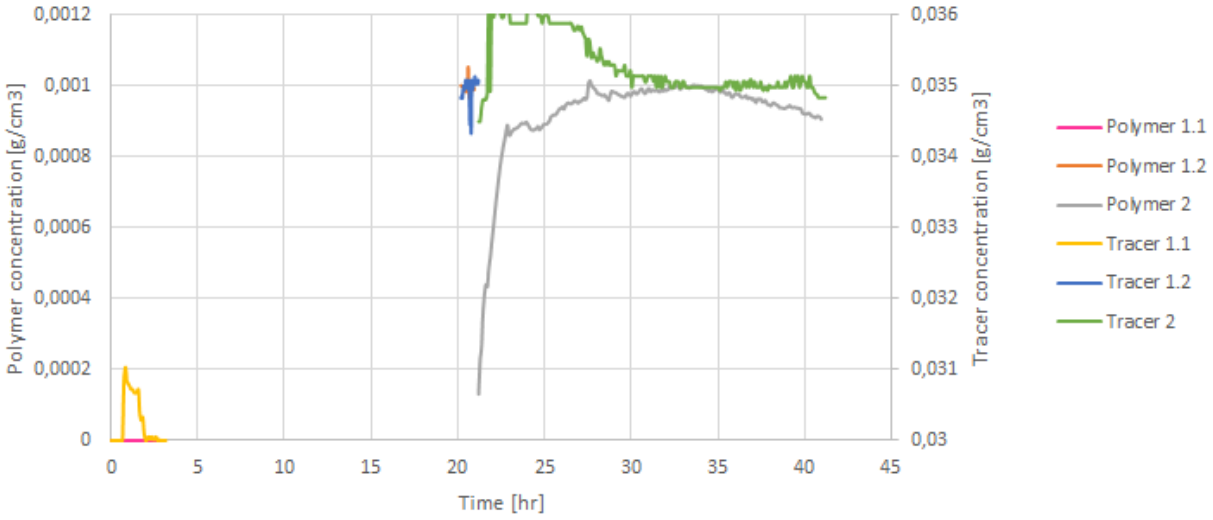

Figure 5.29 Production curves for core B.

.

6 Numerical simulation and sensitivities

A numerical simulation of the flooding of core A and core B was conducted in order to be able to compare and understand the experimental results better. In this Master thesis two base cases were made to represent the core floodings to be done in the lab. After the experiments were conducted, the new information of viscosities, permeabilities, porosity, adsorption, and IPV was implemented into the two base cases to make them as realistic as possible. These are the base cases that will be described in sub section 6.1.

6.1 Base cases

For the numerical simulation of the base cases, the commercially available reservoir simulator Eclipse has been used. The programs FloViz and Office were used to visualize the numerical results and plotting of production curves. As the buildup of the two data files is not the main purpose of this thesis, but rather the results they produced, an explanation of each key word that has been used will not be a part of this sub section. Those interested in the data files may study them in Appendix C.

The base cases have the same physical dimensions as the cores, which is 30 cm in the x-direction, 4.5 cm in the y-direction, and 4.5 cm in the z-direction. The models have been made 2-dimensional in order to reduce the running time for each simulation. A 3D run of the first version was also tested, and this did not give different results compared to the 2D run. There are 120 grid blocks in the x-direction, one in the y-direction, and 10 in the z-direction. This makes the size of the grid blocks 0.25 cm, 4.5 cm, and 0.45 cm in the x-, y-, and z-direction respectively.

Many of the input values were known after the experiments were done. The porosity was then put to 23.4 % in the low permeability layer for case A, and 29.3 % in the high permeability layer. For case B the average porosities were put to 27.9 % and 27.7 % for the low permeability layer and the high permeability layer respectively. The permeabilities of case A were set to 110 mD and 2001 mD, and for case B they were set to 171 mD and 609 mD. As there was no oil in the system, the relative permeability and capillary pressure curves are not relevant. The reservoir simulator still needs these as input. Some generic relative permeability curves were used, while the capillary pressures were set equal zero.

The polymer viscosity at a full concentration of 1000 ppm was put to 4.7 cP for case A, and 3.8 cP for case B, based on the experimental results. The IPV of the low permeability layer of case A was 0.73, and 0.21 for the high permeability layer. For case B they were 0.61 and 0.50

for the low permeability layer and the high permeability layer respectively. The maximum adsorption for the low permeability layer and high permeability layer for case A were $2.1*10^{-4}$ g/g and $9.1*10^{-5}$ g/g. The case B adsorptions were $2.5*10^{-4}$ g/g for the low permeability layer, and $1.6*10^{-4}$ for the high permeability layer. The rock densities of each of the four layers were found by dividing the weight of the dry rock by the rock volume of the core plugs. The densities were then 2.3 g/cm^3 for all layers except the high permeability layer of case A, which was 2.4 g/cm^3.

The brine salinity was modeled as a tracer. The injected brine had a concentration of 3.5 wt%, while the brine originally in place had a concentration of 3 wt%. The alternative of diffusion of tracer (TRDIF) was used, and the tracer diffusion coefficient was set to 0.0072 cm^2/hr (Schlumberger, 2011). This is a normal diffusion coefficient of Sodium Chloride in water, multiplied with 0.1 to adjust for the diffusion being in a porous media, ref. sub section 2.3.

An injection well was put into the first grid block in the z-direction, and the production well was put into the last grid block in the z-direction. The wells were perforated along the entire axis as the injection and production covered the whole cross-sectional area of the cores during the experiments. The injection rate was set to 19.8 ml/hr, and water was injected for half an hour until a polymer flood of 39 hours followed.

6.2 Results for base cases

6.2.1 Base case A

The resulting production curves of running case A, described in 6.1, compared to the experimental curves, are seen in Figure 6.1.

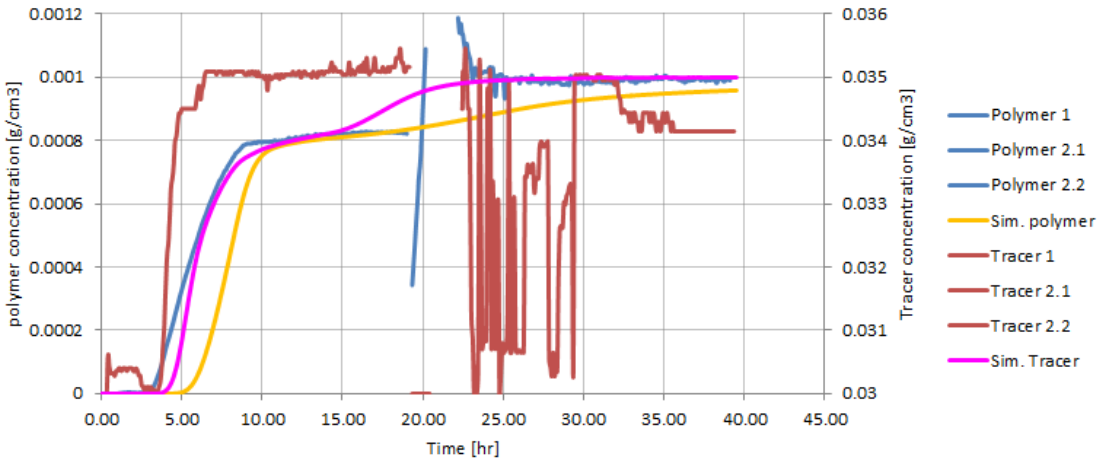

Figure 6.1 Production curves for base case A compared to production curves of core A in lab.

The polymer distribution for case A at the end of the simulation is shown in Figure 6.2.

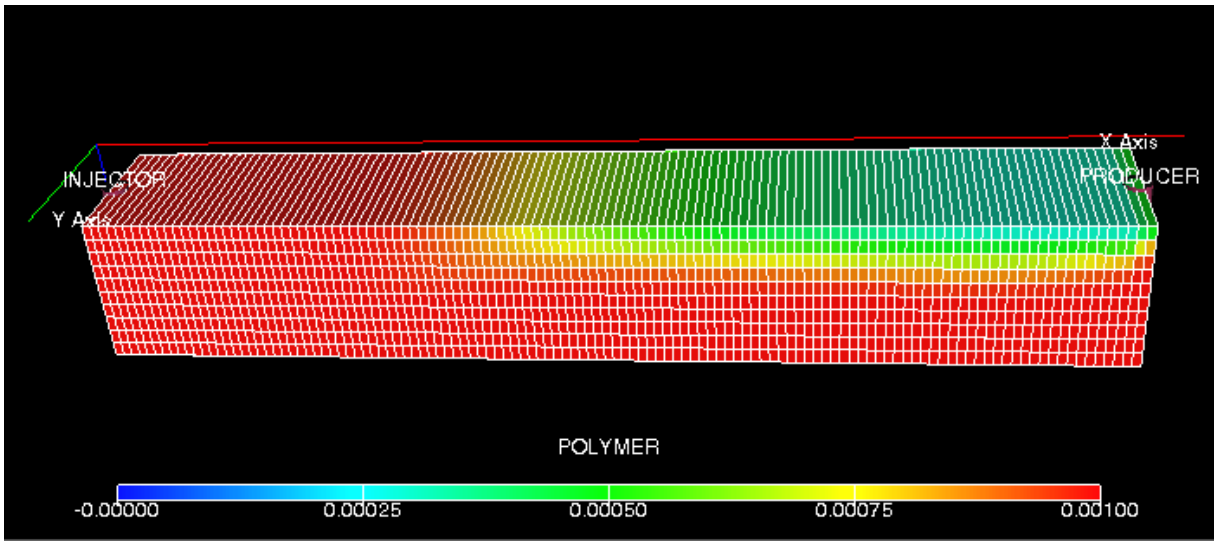

Figure 6.2 Polymer distribution at end of simulation for base case A.

6.2.2 Base case B

The resulting production curves of running case B, described in 6.1, compared to the experimental curves, are seen in Figure 6.3.

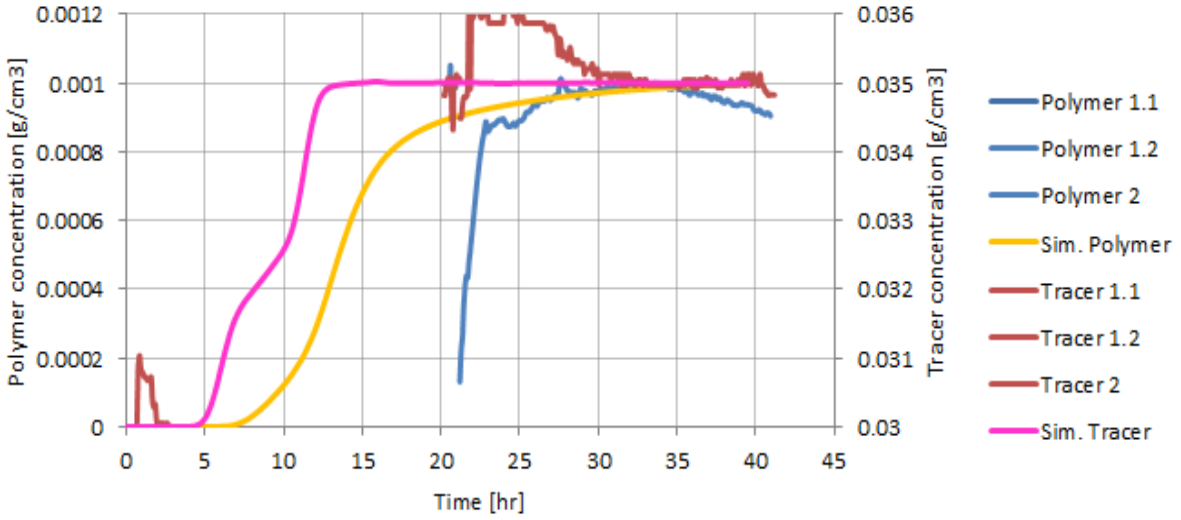

Figure 6.3 Production curves for base case B compared to production curves of core B in lab.

The polymer distribution for case B at the end of the simulation is shown in Figure 6.4.

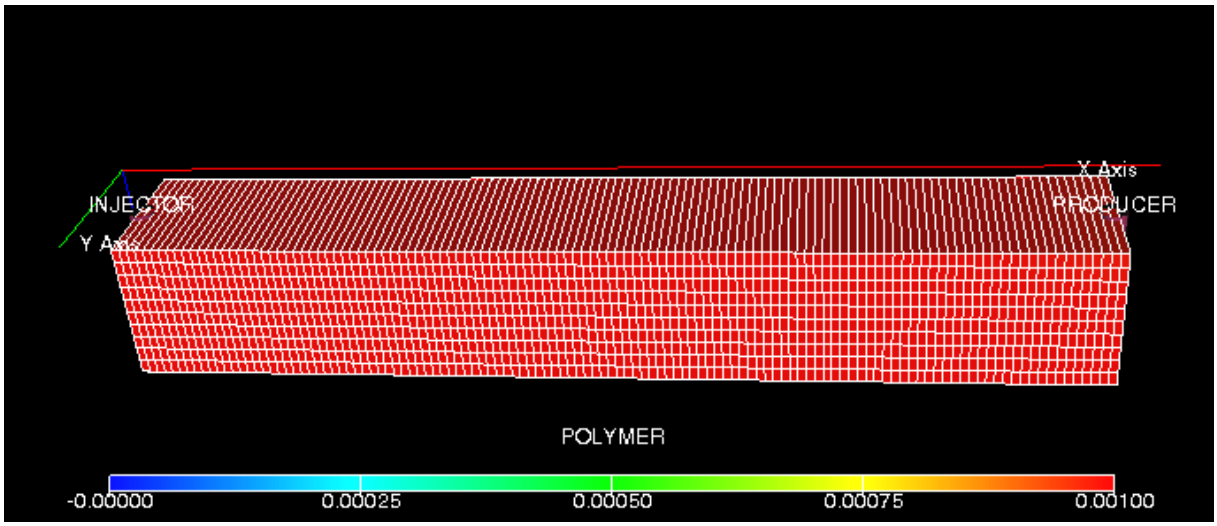

Figure 6.4 Polymer distribution at end of simulation for base case B.

6.3 Comparing experimental results for core A to the numerical results

Comparing the production curves from the numerical simulation of base case A to the experimental production curves of core A, see Figure 6.1, there are both similarities and differences between the different areas of the curves.

6.3.1 Comparing the polymer curves

The simulated polymer production curve has its breakthrough around 1.5 hours later than the experimental polymer curve. There is a relatively quick increase in polymer concentration until both polymer curves stabilizes at their first plateau. This plateau is at a concentration of 0.0008 g/cm^3 for the experimental curve, and 0.00078 g/cm^3 for the simulated curve. Both curves use about 6 hours to reach these concentrations. After the first plateau both curves have a small, but steady, increase in the polymer concentration. The next section of the experimental polymer curve is missing, but in the simulated polymer curve the concentration starts increasing at a higher rate again, until it seems to stabilize at a second plateau close to the maximum polymer concentration of 0.001 g/cm^3. The experimental curve also stabilizes at a second plateau after the measurements resumes again. This plateau has previously been assumed to be at 0.001 g/cm^3. The high degree of similarities between the two polymer curves indicates that there is a big possibility of the missing area of the experimental curve following the same shape as for the simulated curve, which is increasing at a higher rate until stabilizing again. The slow increasing area of the experimental curve lasts for approximately 9 hours, but this area of the simulated curve only endures for about 5 hours. The second plateau of the

experimental curve is reached 15 hours after the first one, but for the simulated curve this last plateau is not reached until 28 hours after the first plateau.

The first plateau of the two polymer production curves probably represents the time where the high permeability layer is filled up with polymer, and no polymer is being produced from the low permeability layer yet. The following small, but steady increase in concentration seem to originate from continuing adsorption, until an increasing amount of polymer also is produced from the lower permeability layer, causing the polymer curve to increase at a higher rate again. The end concentration will then be composed by the amount of polymer being produced as the high permeability layer is full, and the low permeability layer only is partly filled with polymer. The low permeability layer at the end of the simulation has the maximum polymer concentration in approximately the first half of the layer, but is only partly filled with polymer in the second half. See Figure 6.2. The polymer in the last half of this layer was transported by cross-flow from the high permeability layer, according to the simulation. The prolonged adsorption area for the experimental curve is probably caused by a slower adsorption rate than for the simulated case. It is believed that the polymer is adsorbed abruptly at the front of the polymer slug in the numerical simulator, causing this difference in adsorption time interval. The experimental polymer curve stabilizes at the end plateau earlier than for the simulated case, indicating that the low permeability layer is filled up quicker than in the numerical version of the core flooding.

6.3.2 Comparing the tracer curves

The simulated and experimental tracer curves have fewer similarities to each other than the two polymer curves. The simulated tracer curve has its breakthrough time almost one hour later than the experimental tracer curve. The experimental curve then increases steeply in tracer concentration over 1.5 hours until it reaches a plateau at a concentration of 0.0345 g/cm^3. The tracer concentration stays at this value for almost an hour before increasing quickly until it reaches a second plateau of the maximum tracer concentration of 0.035 g/cm^3. The curve is stable at this concentration until the second polymer flood is initiated. Then the experimental tracer curve seems highly unstable. It only stabilizes at the maximum tracer concentration for 2.5 hours in total, while the simulation predicts that it should have been at this concentration the entire time of the second flood. We do not have a good explanation for what causes the unstable curve during this flood. It might be caused by the resistivity apparatus being of poor quality.

The simulated tracer curve did not increase in tracer concentration as quickly as the experimental tracer cure, causing a softer buildup of the tracer curve over approximately 12 hours until it reaches the first plateau. It then continues to increase in concentration until it reaches a second plateau at the maximum tracer concentration of 0.035 g/cm^3 after another 14 hours.

As for the polymer curves, the first plateau probably indicates the time when the high permeability layer is completely filled with tracer. The constant concentration of the experimental tracer curve at the first plateau also implies that the slight increase in the polymer curve at the first plateau is caused by adsorption, as the tracer is not adsorbed. The sudden increase in tracer concentration until it reaches the second plateau, is then probably the increasing production from the low permeability layer that is being filled up with tracer. The tracer will fill up this layer quicker than it fills up with polymer, and according to the simulation both layers are completely filled with the maximum tracer concentration at the end of the flood.

The simulated tracer curve goes through the same stages as the experimental tracer curve, but uses longer time to do so. Since the match of the two tracer curves were not as good as the two polymer curves, it was tried to change certain parameters of the numerical base case in order to understand what might cause these differences. This is presented in the next sub section, 6.4.

6.4 Sensitivity studies on base case A

Some sensitivity studies were done on base case A in order to test what changing certain parameters caused of alterations in the production curves. By doing this, one might get a better understanding of the experimental production curves in sub section 5.5.1.

6.4.1 The low permeability layer holding a permeability of 50 mD

As the low permeability layer of core A originally was stated to hold a permeability of 50 mD, a version of base case A was run where the permeability in this layer was reduced from 110 mD to 50 mD. The resulting production curves compared to the experimental curves can be seen in Figure 6.5. The tracer curve had a steeper buildup of concentration, but did not have two plateaus, as in the experimental results. The polymer curve also changed shape to only having one plateau, making a poorer match to the experimental polymer curve than the base case. Both the production curves thereby imply that the low permeability layer has a

permeability closer to 110 mD than 50 mD, in accordance with the experimental measurements presented in 4.2.5.

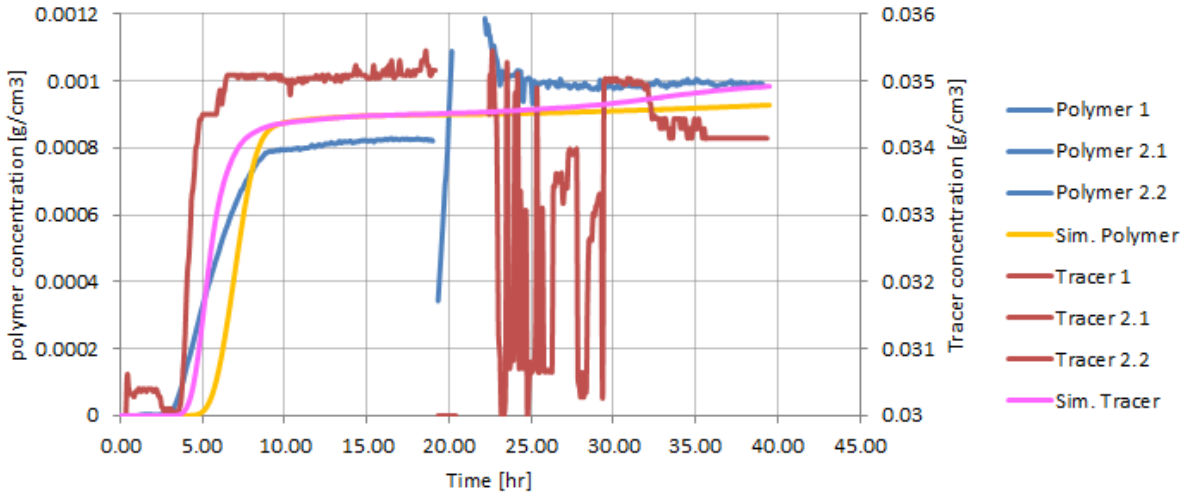

Figure 6.5 Production curves for base case A compared to experimental curves for core A when low permeability layer is holding a permeability of 50 mD.

6.4.2 Changing the adsorption values

To investigate the sensitivity of the adsorption values calculated based on the flooding of the homogeneous core plugs, two new versions of base case A was tested. In the first version the adsorption value in the high permeability layer was increased to $1.5*10^{-4}$ g/g and in the low permeability layer it was decreased to $1.8*10^{-4}$ g/g, making the adsorption values closer to each other. This version was named _HADSH_LADSL. In the second version the adsorption value in the high permeability layer was decreased to $1.0*10^{-6}$ g/g and in the low permeability layer it was increased to $5.0*10^{-4}$ g/g, making the differences in adsorption bigger. This version was named _LADSH_HADSL. See Figure 6.6 to see the production curves of both versions compared to base case A. FCPC represents the polymer production concentration and FTPCTR1 represents the tracer production concentration.

For the _HADSH_LADSL version the polymer curve got an even later break through time, and the tracer curve had the first plateau at a lower concentration than the base case, as well as the wrong shape after the plateau. Therefore this version did not give a better match to the experimental curves than the base case. For the _LADSH_HADSL version the tracer curve had a steeper buildup of tracer concentration than the base case, but the polymer curve had only one plateau. Therefore this version did not give a better match to the experimental curves than the base case either.

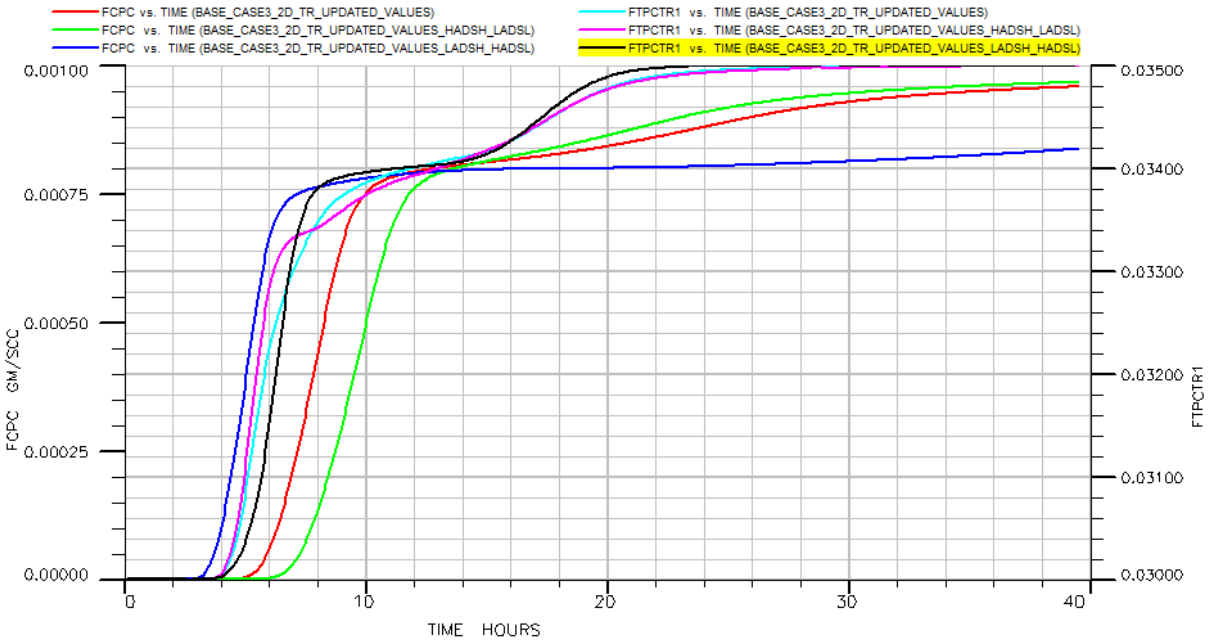

Figure 6.6 Production curves of base case A compared to two cases of new adsorption values.

6.4.3 Increasing the tracer diffusion

To check if there might be more diffusion of the tracer (salt) within core A than what was defined in the data file, the tracer diffusion coefficient was increased from 0.0072 cm^2/hr to 0.072 cm^2/hr. The resulting production curves of this scenario can be seen in Figure 6.7. The base case A tracer curve has also been added to the plot.

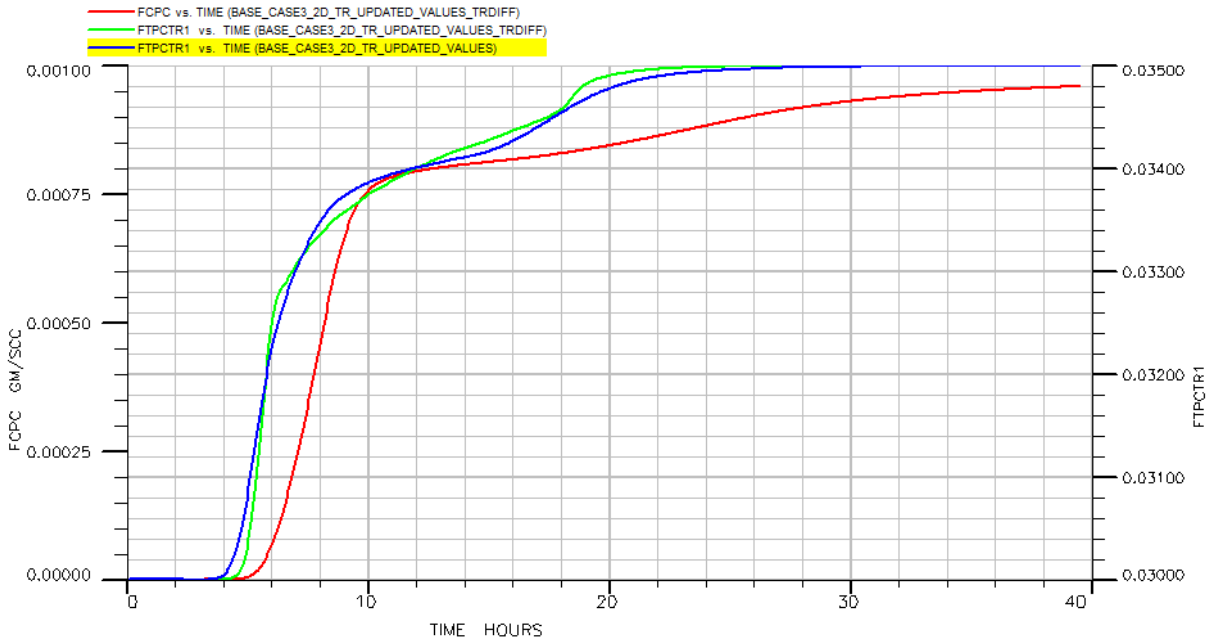

Figure 6.7 Production curves for base case A when the tracer diffusion coefficient has been increased.

The polymer curve will not be affected by the change in tracer diffusion coefficient, and will therefore stay the same. For the tracer the increased diffusion made the curve less smooth without a clear first plateau. The area that might represent the first plateau is at a lower concentration (0.0328 g/cm^3) than for the base case (0.034 g/cm^3). These observations make also this scenario a lesser match for the experimental curves than the base case.

6.4.4 Inserting poorer transmissibility between the two layers

As we do not have full overview of the manufacturing process, it is possible that the surface between the two layers consists of a low permeability zone. A version of the base case was therefore tested where the transmissibility between the high permeability layer to the low permeability layer was reduced. A transmissibility of 0.01 cP.rcm^3/hr/atm was put in for layer 5. The resulting production curves of this case, compared to the experimental curves for core A, can be seen in Figure 6.8.

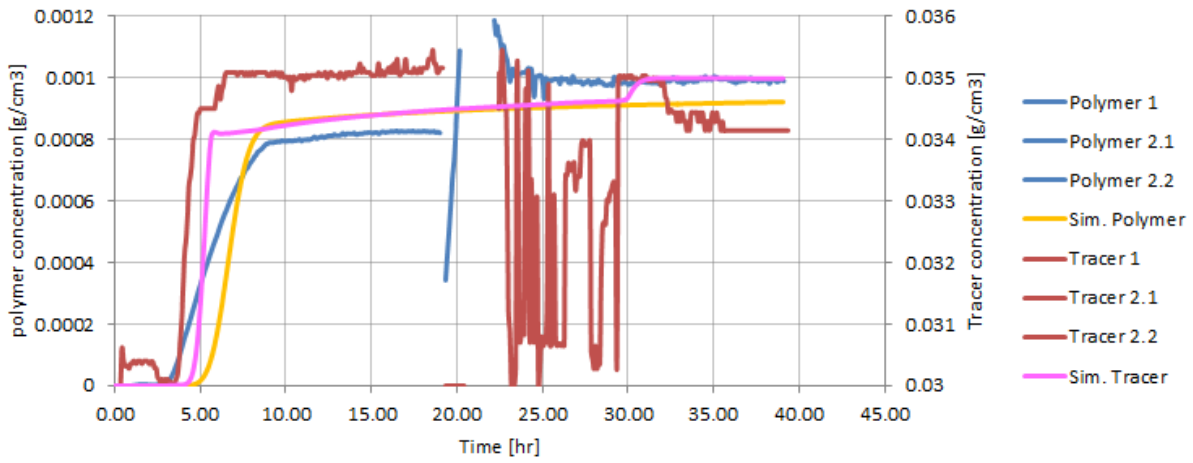

Figure 6.8 Production curves for base case A compared to experimental curves for core A when transmissibility between the layers are poorer.

The tracer curve gets a steeper increase in tracer concentration similar to the experimental tracer curve. Still, the area after the first plateau is very long and slightly increasing until it increases rapidly to a second plateau in the end, which is not similar to the experimental results. The polymer curve only has one plateau and is therefore quite different from the experimental polymer curve, which has two. This suggests that the surface area between the two layers has good connectivity.

6.4.5 Removing the tracer diffusion

By removing the alternative for tracer diffusion, which is the same as having no diffusion of salt, all the crossflow will be due to viscous flow, as discussed in sub section 2.3. The

resulting production curves of this scenario, compared to the base case, can be seen in Figure 6.9.

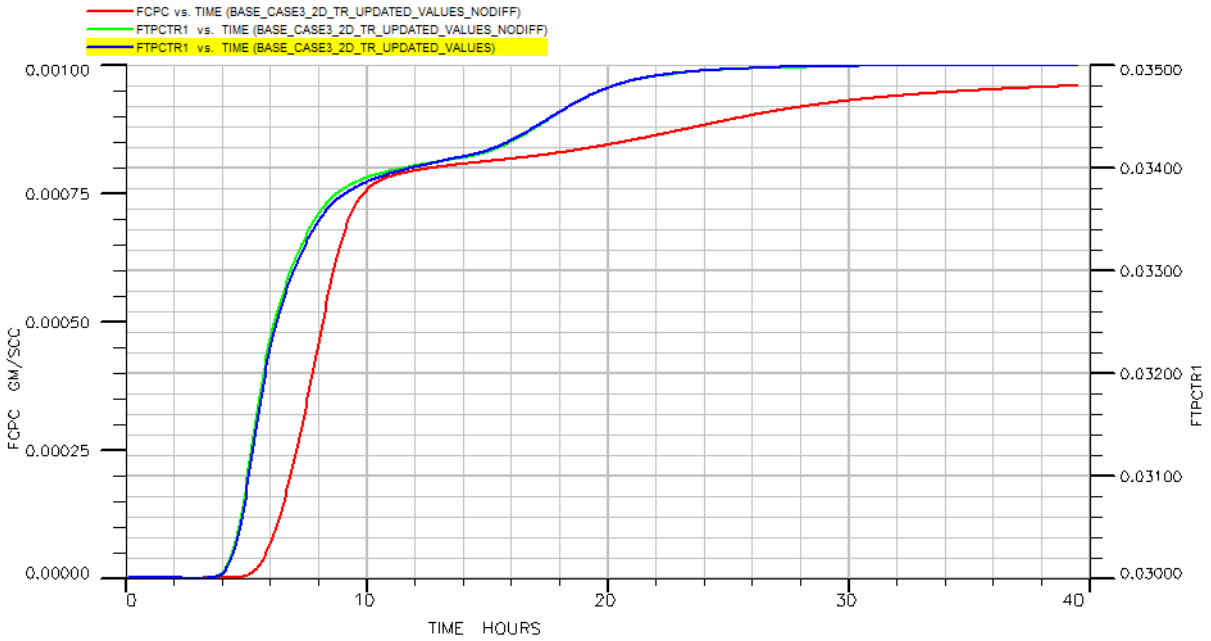

Figure 6.9 Production curves for base case A without tracer diffusion.

The polymer curve is not affected by the tracer diffusion, and stays the same as the base case, which is a good match for the experimental polymer curve. For the tracer curve it is a marginal difference for this scenario of no diffusion to the base case A with diffusion. The production curves of the scenario without diffusion together with the base case provide the closest match to the experimental tracer curve of what has been tested. This suggests that the crossflow of tracer from the high permeability layer to the low permeability layer is mainly due to viscous crossflow, and not significantly affected by tracer diffusion.

6.4.6 Break through times for polymer and tracer curves

Both the simulated polymer and tracer curve had a delayed break through time of respectively 1.5 hours and 1.0 hour, compared to the experimental curves. The breakthrough in the simulations corresponds to the time when the entire high permeability layer is filled with tracer/polymer. An explanation for an early tracer breakthrough is that the high-permeable layer has a smaller pore volume. As the high permeability layers fills up first, the earlier breakthrough time for the experimental curves have to be due to a reduced volume in this layer, as the production of the low permeability layer has not started yet. For polymer, IPV and adsorption values will also affect the breakthrough times. This causes the tracer and polymer curve to not have their breakthrough at the same time, as they approximately do for

the homogeneous core plugs. One of the possibilities of what might cause the reduced volume of the layered core, is that the epoxy surrounding the core has seeped into the outer pores before it set. This would mostly happen in the high permeability layer of 2000 mD, as the liquid epoxy will more easily flow in here. To test this theory, a version of the base case was run, and the high permeability layer was reduced by 2 rows (0.9 cm) in the z-direction. The resulting production curves of this scenario can be seen in Figure 6.10. The breakthroughs of the polymer and tracer curve are moved 1.5 hours back in time, making them close to the breakthrough time that took place in the lab. The simulated tracer curve now has its breakthrough at a somewhat earlier time than the experimental tracer curve due to the experimental production curves being closer together in breakthrough time than the simulated curves. The polymer curve has the first plateau at a concentration lower than the base case and the experimental case, and the adsorption period is even shorter. This makes this scenario a poorer match when it comes to the polymer curve than the base case. The simulated tracer curve also has the first plateau at a concentration lower than the base case and the experimental case. So, this case of less volume was a good match for the breakthrough times, but not for the rest of the changes of the production curve.

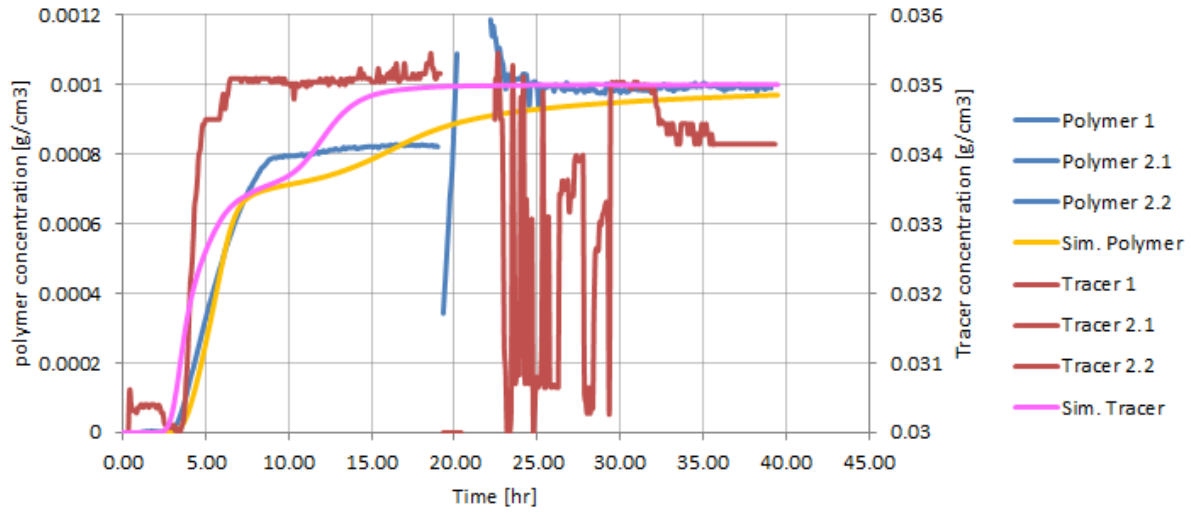

Figure 6.10 Production curves for base case A compared to experimental curves for core A with reduced volume in high permeability layer.

6.5 Comparing experimental results for core B to the numerical results

It is more difficult to compare the production curves for core B, as the entire build up section of the first polymer flood is missing in the experimental results. According to the simulated base case for core B, the polymer curve has just one plateau at the end. This is probably due

to the permeability differences being one to three, instead of one to 20. When the high permeability layer is filled with tracer or polymer, the low permeability layer is also quite full, making the transition of the increased production from this layer smoother. For the tracer curve there are two curvatures on the buildup section making it a bit clearer where the low permeability layer starts contributing to the production flow. Still, on this curve the buildup section is smoother than for base case A, and reaches maximum tracer concentration a lot earlier. The time it takes to reach maximum polymer concentration is on the other side 38 hours according to the simulation. Then both layers have obtained a full polymer concentration. See Figure 6.4. According to the experimental results the polymer curve reaches its maximum concentration after 20 hours. After 35 hours it starts declining again. This steady decrease of polymer concentration might be caused by the beginning desorption of polymer from the rock surface.

7 Discussion

7.1 The small core plugs

The polymer production curve for the low permeability core plug type A, which is the layer of lowest permeability of the four, never reaches the full polymer concentration of 1000 ppm. This is most likely due to this being the core plug of lowest permeability which has not yet fully reached the plateau of maximum concentration. It would probably take many extra hours of flooding to reach this stage. As it happens slowly it is difficult to see the tiny increase of polymer concentration at the top. Had the flooding of this core plug gotten the opportunity to continue until reaching the maximum concentration of 1000 ppm, the adsorption value would be higher.

For most core plugs, neither the production curves for tracer nor polymer went down to a concentration of zero during the water flood following the polymer flood. For the polymer curve this might be because of polymer starting to desorb from the rock. As for the reason why the tracer curve does not reach a zero concentration the most probable explanation is the resistivity apparatus giving bad measurements. Another possible explanation is salt being dissolved from the rock's surface, which is possible if any salt has precipitated during the time the core plugs have been saturated in brine.

The results of the IPV calculations were high for all the core plugs; 21 % for the high permeability core plug A, 50 % for the high permeability core plug B, 61 % for the low permeability core plug B, and 73 % for the low permeability core plug A. An IPV of 21 % is not unusual, but for a core plug with a permeability of 2000 mD it could have been a lot lower. Even though the IPVs seems high, they correlate to the permeability of each layer, where the layer with the lowest permeability of 100 mD has the highest IPV, and the layer with the highest permeability of 2000 mD has the lowest IPV.

The porosities of all cores are good, ranging from 22 % to 30 %. Usually cores of lower permeability also have lower porosities than cores of higher permeability, causing more difficulties for fluids to flow through the core. This is not the case for the B type core plugs, where the porosities of the 200 mD layer vary in the same range as the porosities of the 600 mD layer. For the A type cores the high permeability core of 2000 mD has higher porosities than the low permeability core of 100 mD, but the biggest porosity difference between these two layers is only 8 %. One theory of what is causing the high IPV for the cores, is that the

manufacturer have increased the use of clay in order to reduce the permeabilities for the different layers. This could cause a high IPV for the polymer.

Supporting the theory of increased clay content with decreasing permeability, are the adsorption values. They range from $9.1*10^{-5}$ g/g in the high permeability layer of core type A to $2.1*10^{-4}$ g/g for the low permeability layer of core type A. For the B type core the adsorption range from $1.6*10^{-4}$ g/g for the high permeability layer to $2.5*10^{-4}$ g/g for the low permeability layer. The reason why the layer of 200 mD in core B can have a higher adsorption than the layer of 100 mD in core A, is that they come from different cores and probably contain different amounts of clay. The porosity of the low permeability layer of core B is higher than for the low permeability layer of core A, and would therefore need more clay to reduce the permeability. Adsorption increases with the clay content within a rock.

The theory of increased clay content with decreasing permeability support the fact that the high IPV and adsorption values could be the correct ones, but to be able to say this for certain, it would be necessary to repeat the experiments to verify the results. This was not possible in the time frame given for this Master thesis, as it took a lot of time to build the flooding setup and get all the parts of the equipment, as well as the student lab being cleared the 15th of May, due to renovations. After this time it was not possible to do any more experiments.

7.2 The layered core plugs

7.2.1 Understanding the differences in flow between experimental and numerical cases for core A

In an attempt to understand how the flow propagates through the core for the experimental case, one can look at the differences in the production curves compared to the simulated case. Looking at the tracer curve the first plateau is at a tracer concentration of 0.0345 g/cm^3 for the experimental case, but in the simulated case without tracer diffusion the first plateau is seen at 0.034 g/cm^3. This can mean that there is a higher concentration of tracer flowing in the high permeability layer in the experiment than in the simulation. This implies that there is a smaller ratio of the injected fluid that enters the low permeability layer in the experiment. To prove this statement the fraction of the tracer that flows in the high permeability layer can be calculated. It is assumed that the production only comes from the high permeability layer until the tracer curve reaches the first plateau at the concentration of 0.0345 g/cm^3. With the maximum tracer concentration being 0.035 g/cm^3 and the minimum 0.03 g/cm^3, the fraction of the total flow of tracer flowing through the high permeability layer will be given by

$$Fraction\ of\ tracer\ in\ high\ perm.\ layer\ exp. = \frac{0.0345 - 0.03}{0.035 - 0.03} = 0.9. \quad \textbf{Eq. 7.1}$$

So in the experimental case 90 % of the tracer flows in the high permeability layer, and 10 % flows in the low permeability layer. Doing the same calculation for the simulated tracer curve the fraction of the total flow of tracer flowing through the high permeability layer becomes

$$Fraction\ of\ tracer\ in\ high\ perm.\ layer\ sim. = \frac{0.034 - 0.03}{0.035 - 0.03} = 0.8. \quad \textbf{Eq. 7.2}$$

So for the simulated case 80 % of the tracer flows in the high permeability layer, while 20 % flows in the low permeability layer.

This same method can be used to calculate the fraction of polymer flowing in the two layers in both the experimental and simulated case. The first plateau for the experimental case is at the concentration of 0.0008 g/cm^3, and for the simulated case it is 0.00078 g/cm^3. With the maximum polymer concentration being 0.001 g/cm^3 and the minimum concentration being 0.0 g/cm^3, the fraction of the polymer flowing in the high permeability layer becomes

$$Fraction\ of\ polymer\ in\ high\ perm.\ layer\ exp. = \frac{0.0008}{0.001} = 0.8. \quad \textbf{Eq. 7.3}$$

For the simulated case the fraction of the polymer flowing in the high permeability layer will be

$$Fraction\ of\ polymer\ in\ high\ perm.\ layer\ sim. = \frac{0.00078}{0.001} = 0.78. \quad \textbf{Eq. 7.4}$$

According to these calculations 80 % of the polymer flows in the high permeability layer in the experimental case, against 78 % in the simulated case. 20 % and 22 % of the polymer then flows in the low permeability layers.

Had the numbers calculated for flow of polymer given the real fraction of flow in the two layers, they would have been the same as the fraction of flow of tracer calculated in Eq. 7.1 and Eq. 7.2. The reason why it seems like the fraction of polymer flow in the high permeability layer for the experimental case is 0.8 instead of 0.9, is due to the adsorption causing the produced polymer concentration to be lower than when it went in. For the simulated case, the calculated fraction of flow of polymer in the high permeability layer is 0.78 instead of 0.8. The reason why the simulated case is closer to the real value calculated for the flow of tracer, is that the numerical simulator assumes abrupt and full adsorption of the polymer at the flood front. The adsorption then happens quicker than for the experimental

case, making the flow fraction of polymer closer in value to the fraction of polymer flow that actually flows in each layer.

The experimental tracer curve has its buildup a lot faster than the simulated tracer curve. This might be partly caused by the front of the polymer slug that is injected with the tracer. The numerical simulator assumes piston displacement of the brine within the core. It also assumes abrupt and full adsorption of the polymer at the flood front. In the experiment this adsorption takes longer and will then not only happen at the front of the polymer slug. This would make the flood front smeared out. As the smeared out flood front is propagating through the core, the viscosity of the front will decrease, causing the flow velocity to increase and the tracer reaching maximum concentrations faster.

7.2.2 Final remarks on comparison of the numerical results to the experimental results for core A

It has not been possible to replicate a perfect match of the experimental production curves by numerical simulation. The base case and the case where the alternative of tracer diffusion was switched off gave the best match for the experimental tracer and polymer curve. The theory of reduced volume within the high permeability layer gave a good match for the breakthrough times of the curves, but was a worse match for the rest of the experimental production curves if one compares with the base case. All the aspects of what has happened within the core during the experiment cannot be explained based on these simulations alone. In order to find out more, it would be necessary to do extra experiments as well as trying more complex alterations of the numerical simulation model.

7.3 Diffusion of polymer in layered cores

One of the main goals of this Master thesis was to find out if there had been any polymer diffusion from the high permeability layer to the low permeability layer. Both the cores were shut in for two days before flooding with polymer a second time, allowing time for diffusion. At the beginning of the second polymer flood it should have been possible to see a change in the response of the production curve, if there had been a significant diffusion of polymer into the low permeable layer during the two days the core was shut in.

In the experimental production curves for both core A and core B there were no clear sign of any change in the response, but as the curves of core A was missing data in the relevant area and the curve of core B was dominated by the pressure build up after being shut in, it is difficult to be certain of this. Therefore no final conclusion about the diffusion of polymer can

be made. Still, as there was little to no diffusion of salt according to the numerical sensitivity studies for base case A, the probability of polymer diffusion, at least in core A, is slim. Polymer will have an even smaller effect of diffusion than salt due to being larger molecules. The simulated polymer curve also gave reasonable curves compared to the experimental curve, and in the simulation there is no polymer diffusion. It is therefore possible to say that within these two-layered synthetic cores polymer diffusion is negligible.

8 Conclusions

- Based on numerical simulations it can be concluded that it is possible to find adsorption and IPV within a core sample by utilizing the method presented in chapter 3.
- To do experimental tests on synthetic two-layered cores can give interesting results for evaluation of polymer flooding.
- For the two layered cores used in this Master thesis the high permeability layer fills up with the injected fluid faster than the low permeability layer.
- In the numerical simulator utilized in this Master thesis, the adsorption of polymer happens abruptly at the front of the polymer slug, but during the flooding of the cores in the lab it was obvious that the polymer adsorption happened over time and not only at the flood front.
- Based on the numerical simulations and the experimental work it can be concluded that there were crossflow of the injected fluid from the high permeability layer to the low permeability layer.
- The crossflow between the layers of different permeabilities is most likely caused by viscous crossflow alone, where both salt and polymer diffusion is negligible.
- Based on the sensitivity studies utilizing numerical simulation it can be concluded that there is good fluid conductivity in the area between the two layers within the synthetic cores.

8.1 Further work

- Do more experiments on core plugs and the layered cores to verify production curves and results.
- Get more information about how the cores are made, the rock composition, clay content and so on. This could help to fully understand what is happening during the polymer flood within the cores.
- Build a more complex simulation model to for example incorporate a prolonged time of adsorption of polymer, as well as testing more intricate combinations of events in order to get a better match with the experimental curves.
- Further work that would require a bigger time frame than what is given for the Master thesis is testing different types of polymer, adding oil to the system, and doing the experiments at reservoir conditions of higher pressures and temperatures.

Nomenclature

A = cross-sectional area

C_{pol} = polymer concentration

$C_{pol,max}$ = maximum polymer concentration

$C_{pol,min}$ = minimum polymer concentration

$C_{pol,norm}$ = normalized polymer concentration

C_{tra} = tracer concentration

$C_{tra,max}$ = maximum tracer concentration

$C_{tra,min}$ = minimum tracer concentration

$C_{tra,norm}$ = normalized tracer concentration

DI water = purified water

EOR = enhanced oil recovery

FCPC = polymer production concentration

FTCPTR1 = tracer production concentration

f_w = water fraction

HPAM = hydrolyzed polyacrylamide

IPV = inaccessible pore volume

k_a = permeability measured after polymer flooding

k_{abs} = absolute permeability

k_b = permeability measured before polymer flooding

k_o = permeability to oil

k_w = permeability to water

K_1 = calibration constant 1

K_2 = calibration constant 2

L = length

m = mass

M = mobility ratio

NaCl = sodium chloride

p = pressure read from gauge

PAM = polyacrylamides

PV = pore volume

p_1 = pressure in reference cell

p_2 = initial pressure in sample chamber

Q = flow rate

r = radius

Rrf = residual resistance factor

S_w = water saturation

$TRDIF$ = tracer diffusion data

t_1 = flow time one

t_2 = flow time two

V = volume

V_B = bulk volume

V_K = volume of core plug minus the pore volume

V_p = pore volume

V_1 = reference volume

V_2 = volume of sample chamber (with core)

W_{rock} = weight of rock

ΔP = pressure drop

ΔPV = incremental change in pore volume

φ = porosity

ρ = density

ρ_r = resistivity

σ = conductivity

v = kinematic viscosity

ϑ = Hagenbach correction factor

μ = dynamic viscosity

μ_o = oil phase viscosity

μ_w = water phase viscosity

References

Berg, C.F. 2012. Re-examining Archie's law: Conductance description by tortuosity and constriction. *Phys. Rev*. E, 86:046314, Oct 2012.

Buchgraber, M., Clemens, T., Castanier, L.M. et al. 2011. A Microvisual Study of the Displacement of Viscous Oil by Polymer Solutions. *SPE Reservoir Evaluation & Engineering* **14** (03): 269-280. SPE-122400-PA.
http://dx.doi.org/10.2118/122400-PA.

Carter, W. H., Payton, J.T. and Pindell, R.G. 1980. Biopolymer Injection Into A Low Permeability Reservoir. Presented at the SPE/DOE Enhanced Oil Recovery Symposium, Tulsa, Oklahoma, 20-23 April. SPE-8836-MS.
http://dx.doi.org/10.2118/8836-MS.

Clifford, P.J. 1988. Simulation of Small Chemical Slug Behavior in Heterogeneous Reservoirs. Presented in the SPE Enhanced Oil Recovery Symposium, Tulsa, Oklahoma**,** 16-21 April. SPE-17399-MS.
http://dx.doi.org/10.2118/17399-MS.

Dahle, G.S. 2014. Master thesis: Investigation of how Hydrophilic Silica Nanoparticles Affect Oil Recovery in Berea Sandstone - An Experimental Study. Trondheim: Department of Petroleum engineering and Applied Geophysics at Norwegian University of Science and Technology.

Dawson, R. and Lantz, R.B. 1972. Inaccessible Pore Volume in Polymer Flooding. *Society of Petroleum Engineers Journal* **12** (05): 448-452. SPE-3522-PA.
http://dx.doi.org/10.2118/3522-PA.

Holt, T., 2015. Personal communication.

Lake, L.W. 1989. Polymer Methods. In *Enhanced Oil Recovery*, Chap. 8. Englewood Cliffs, New Jersey: Prentice Hall.

Levitt, D. B., Slaughter, W., Pope, G.A. et al. 2011. The Effect of Redox Potential and Metal Solubility on Oxidative Polymer Degradation. *SPE Reservoir Evaluation & Engineering* **14** (03): 287-298. SPE-129890-PA.
http://dx.doi.org/10.2118/129890-PA.

Lötsch, T., Müller, T. and Pusch, G. 1985. The Effect of Inaccessible Pore Volume on Polymer Coreflood Experiments. Presented at the SPE Oilfield and Geothermal Chemistry Symposium, Phoenix, Arizona, 9-11 March. SPE-13590-MS.
http://dx.doi.org/10.2118/13590-MS.

Moe, E.S., 2014. Literature survey of waterflooding theory and practical and theoretical aspects of polymer flooding. Trondheim: Department of Petroleum engineering and Applied Geophysics at Norwegian University of Science and Technology.

Moradi-Aragi, A. and Doe, P.H. 1987. Hydrolysis and Precipitation of Polyacrylamides in Hard Brines at Elevated Temperatures. *SPE Reservoir Engineering* **2** (02): 189-198. SPE-13033-PA.
http://dx.doi.org/10.2118/13033-PA.

Needham, R.B. and Doe, P.H. 1987. Polymer Flooding Review. *Journal of Petroleum Technology* **39** (12): 1503-1507. SPE-17140-PA.
http://dx.doi.org/10.2118/17140-PA.

Perkins, T.K. and Johnston, O.C. 1963. A Review of Diffusion and Dispersion in Porous Media. *Society of Petroleum Engineers Journal* **3** (01): 70-84. SPE-480-PA.
http://dx.doi.org/10.2118/480-PA.

Petrowiki #1, 2013. PEH:Polymers, Gels, Foams, and Resins (13 September 2013 revision), http://petrowiki.org/PEH%3APolymers,_Gels,_Foams,_and_Resins#Polymers (accessed 19.11.2014).

Petrowiki #2, 2013. Polymer impact on permeability (17 August 2013 revision), http://petrowiki.org/Polymer_impact_on_permeability (accessed 20.11.2014).

Petrowiki #3, 2014. Polymer waterflooding (28 October revision), http://petrowiki.org/Polymer_waterflooding#Permeability_reduction (accessed 21.11.2014).

Petrowiki #4, 2013. Polymers for conformance improvement (17 September 2013 revision), http://petrowiki.org/Polymers_for_conformance_improvement?_ga=1.119346827.387894894.1389957036 (accessed 03.12.2014).

Pope, G.A. 1980. The Application of Fractional Flow Theory to Enhanced Oil Recovery. *Society of Petroleum Engineers Journal* **20** (03): 191-205. SPE-7660-PA. http://dx.doi.org/10.2118/7660-PA.

Rivenq, R.C., Donche, A. and Nolk, C. 1992. Improved Scleroglucan for Polymer Flooding Under Harsh Reservoir Conditions. *SPE Reservoir Engineering* **7** (01): 15-20. SPE-19635-PA.
http://dx.doi.org/10.2118/19635-PA.

Schlumberger, 2011.1. *Eclipse Reference Manual*. Schlumberger.

Sheng, J.J. 2013. Polymer Flooding - Fundamentals and Field Cases. In *Enhanced Oil Recovery Field Case Studies*, Chap. 3, p. 63-82. Waltham, Massachusetts: Elsevier Inc.

Sohn, W.O., Maitin, B.K. and Volz, H. 1990. Preconditioning Concepts in Polymer Flooding in High-Salinity Reservoirs: Laboratory Investigations and Case Histories. *SPE Reservoir Engineering* **5** (04): 503-507. SPE-17675-PA.
http://dx.doi.org/10.2118/17675-PA.

Stosur, G.J., Hite, R.J., Carnahan, N.F. et al. 2003. The Alphabet Soup of IOR, EOR and AOR: Effective Communication Requires a definition of Terms. Presented at the SPE International Improved Oil Recovery Conference in Asia Pacific, Kuala Lumpur, Malaysia, 20-21 October. SPE-84908-MS.

http://dx.doi.org/10.2118/84908-MS.

Torsæter, O. and Abtahi, M. 2000. *Experimental Reservoir Engineering Laboratory Work Book*. Trondheim: Department of Petroleum engineering and Applied Geophysics at Norwegian University of Science and Technology.

Wellington, S.L. 1983. Biopolymer Solution Viscosity Stabilization-Polymer Degradation and Antioxidant Use. *Society of Petroleum Engineers Journal* **23** (06): 901-912. SPE-9296-PA.
http://dx.doi.org/10.2118/9296-PA.

Zaitoun, A. and Kohler, N. 1988. Two-Phase Flow Through Porous Media: Effect of an Adsorbed Polymer Layer. Presented at the 63rd Annual Technical Conference and Exhibition of the Society of Petroleum Engineers, Houston, Texas, 2-5 October. SPE-18085-MS. http://dx.doi.org/10.2118/18085-MS.

Zapata, V.J. and Lake, L.W., 1981. A Theoretical Analysis of Viscous Crossflow. Presented at the 56th Annual Fall Technical Conference and Exhibition of the Society of Petroleum Engineers of AIME, San Antonio, Texas, 5-7 October. SPE-10111-MS.
http://dx.doi.org/10.2118/10111-MS.

Appendix

A. Correlation curves and conductivity plots for core plugs

The correlation curve of tracer concentration versus conductivity for the low permeability core plug type A, is seen in Figure A. 1.

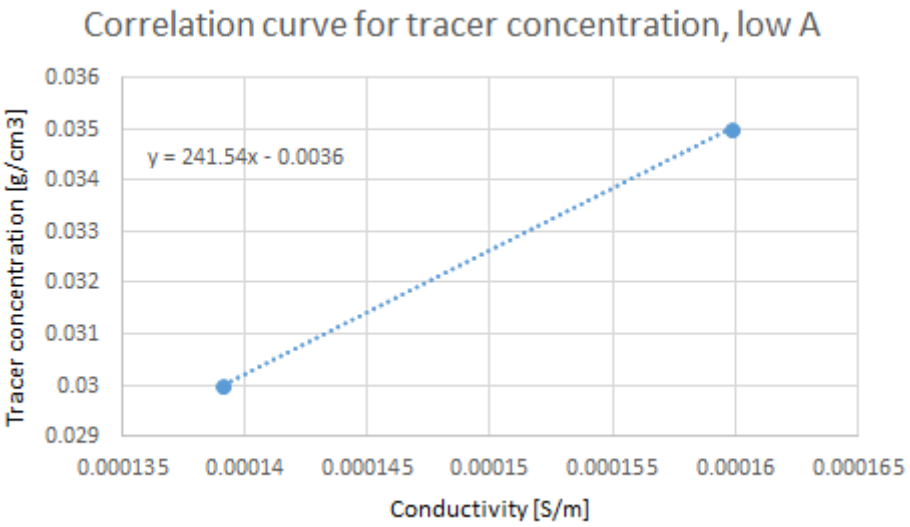

Figure A. 1 Correlation curve for tracer concentration for low permeability layer, type A core.

The conductivity plot for the core plug of the low permeability layer in core type A, is seen in Figure A. 2.

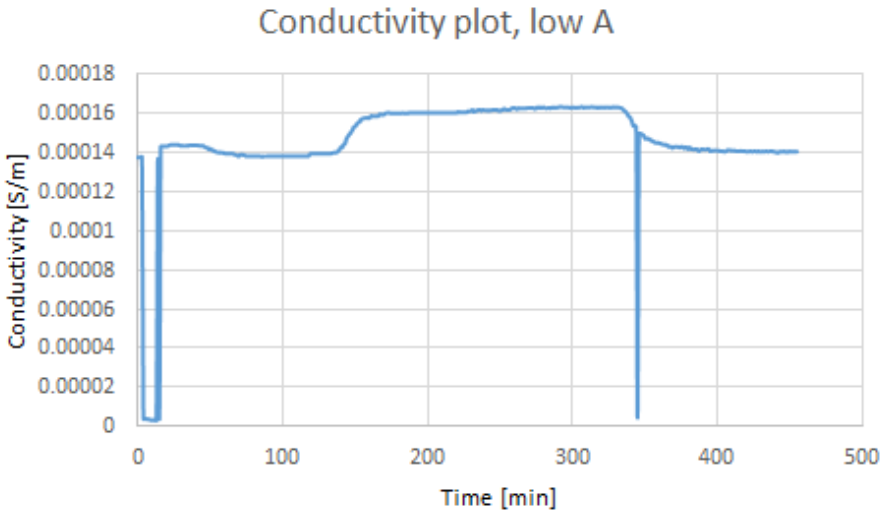

Figure A. 2 Conductivity plot for low permeability layer, type A core.

The correlation curve of tracer concentration versus conductivity for the high permeability core plug type B, is seen in Figure A. 3.

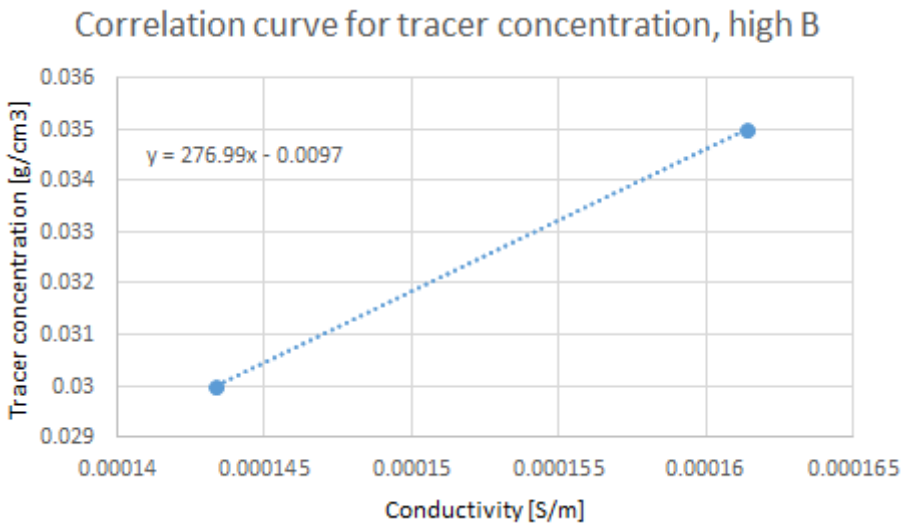

Figure A. 3 Correlation curve for tracer concentration for high permeability layer, type B core.

The conductivity plot for the core plug of the high permeability layer in core type B, is seen in Figure A. 4.

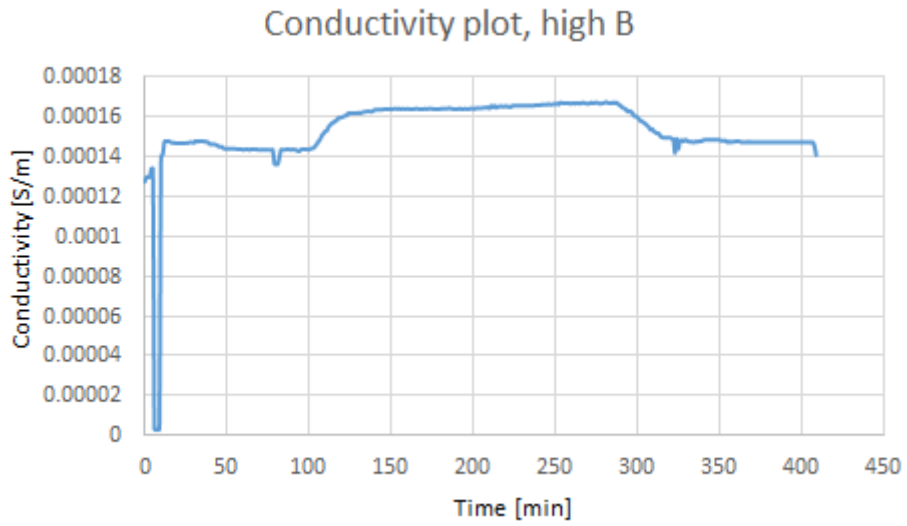

Figure A. 4 Conductivity plot for high permeability layer, type B core.

The correlation curve of tracer concentration versus conductivity for the low permeability core plug type B, is seen in Figure A. 5.

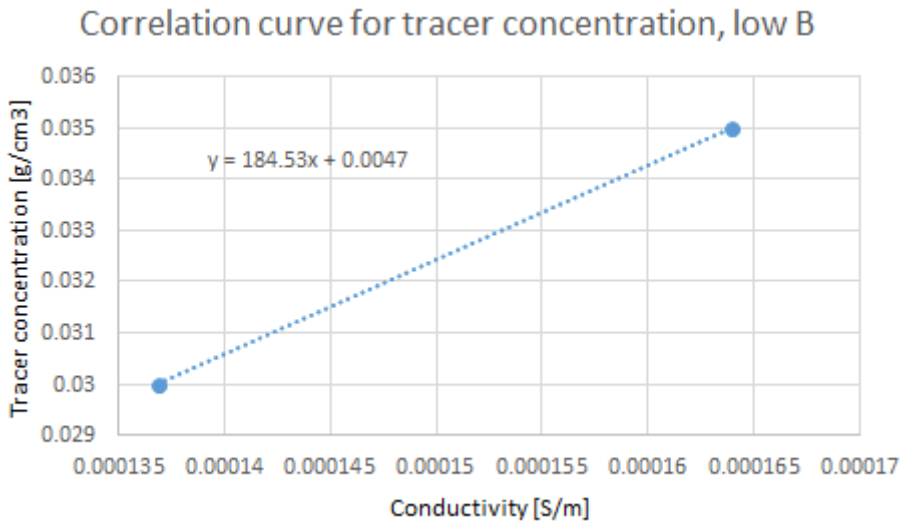

Figure A. 5 Correlation curve for tracer concentration for low permeability layer, type B core.

The conductivity plot for the core plug of the low permeability layer in core type B, is seen in Figure A. 6.

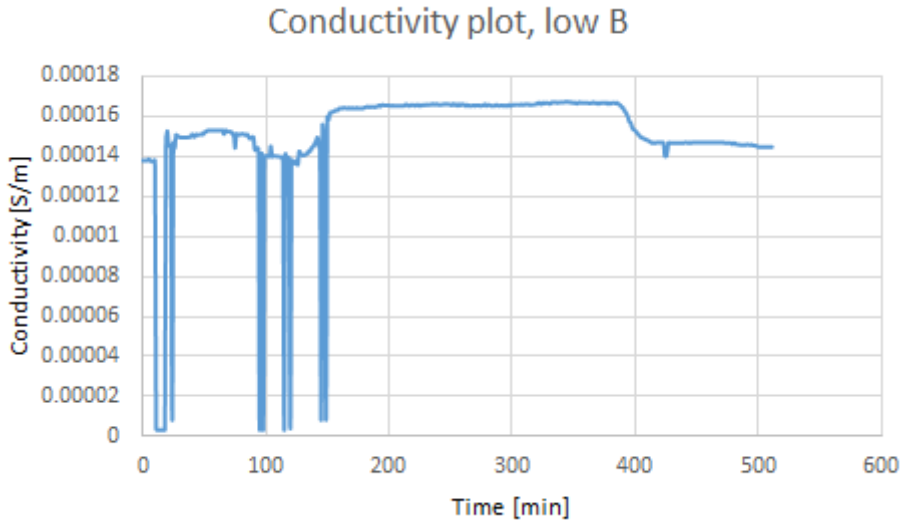

Figure A. 6 Conductivity plot for low permeability layer, type B core.

B. Trend lines for the adjusted production curves for the core plugs

The trend line for the polymer pressure drop area for the core plug of the high permeability layer in core type A, is seen in Figure B. 1.

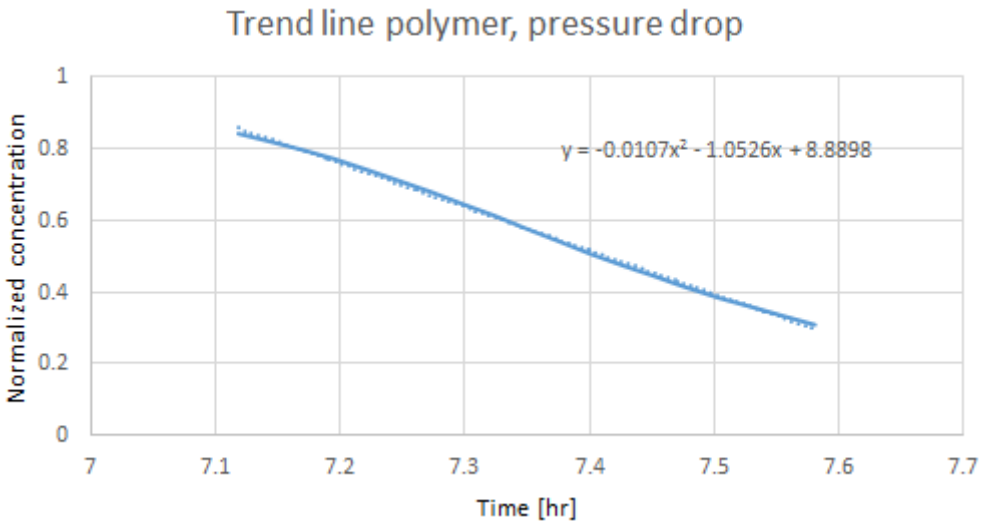

Figure B. 1 Trend line for polymer curve during pressure drop for high permeability layer, type A core.

The trend line for the polymer curve at the start area for the core plug of the high permeability layer in core type A, is seen in Figure B. 2.

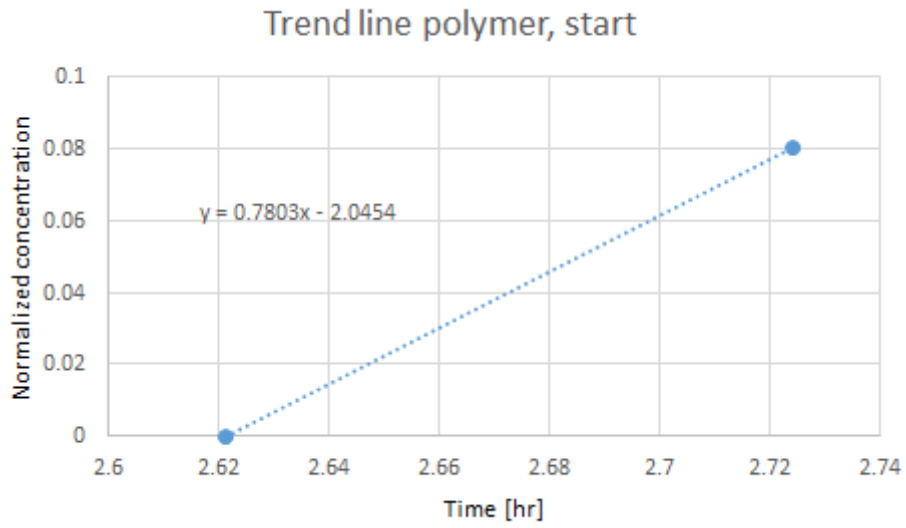

Figure B. 2 Trend line for polymer curve at start area for high permeability layer, type A core.

The trend line for the polymer curve at the end area for the core plug of the high permeability layer in core type A, is seen in Figure B. 3.

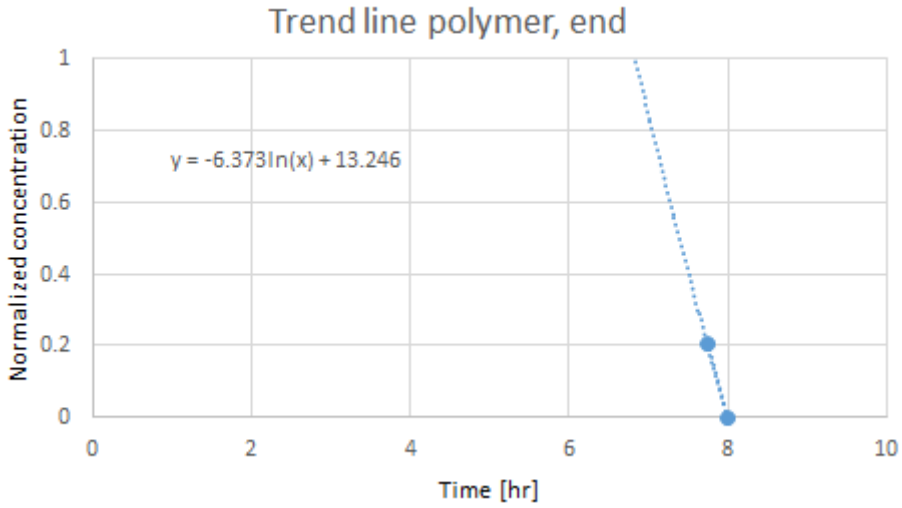

Figure B. 3 Trend line for polymer curve at end area for high permeability layer, type A core.

The trend line for the tracer curve at the end area for the core plug of the high permeability layer in core type A, is seen in Figure B. 4.

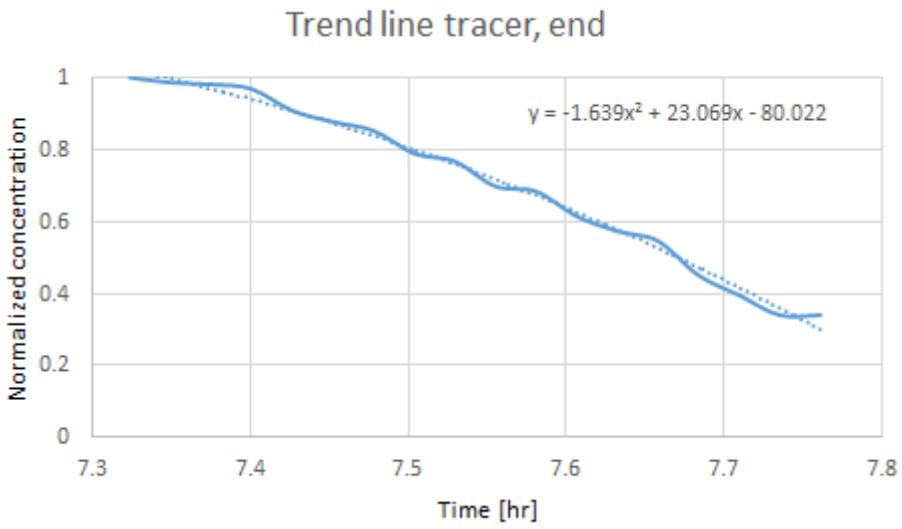

Figure B. 4 Trend line for tracer curve at end area for high permeability layer, type A core.

The trend line for the polymer pressure drop area for the core plug of the low permeability layer in core type A, is seen in Figure B. 5.

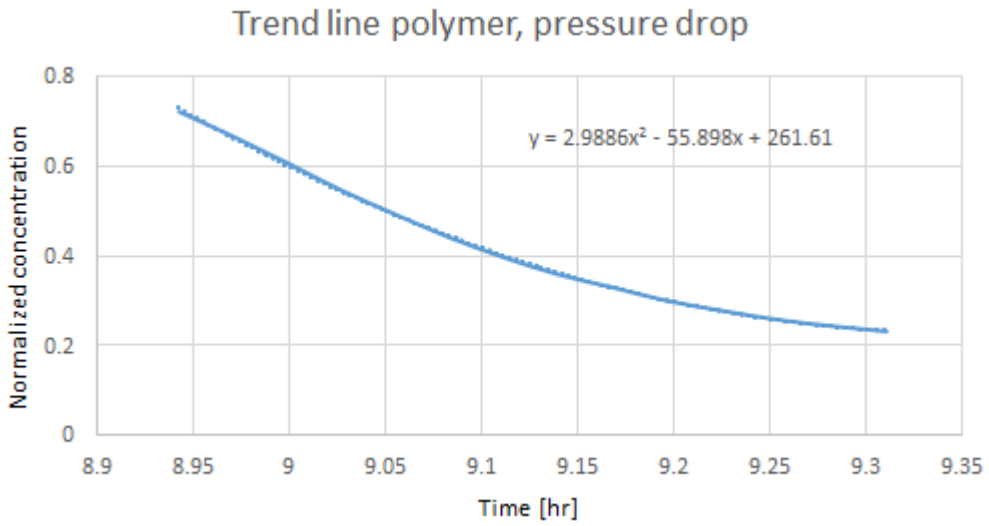

Figure B. 5 Trend line for polymer curve during pressure drop for low permeability layer, type A core.

The trend line for the polymer curve at the end area for the core plug of the low permeability layer in core type A, is seen in Figure B. 6.

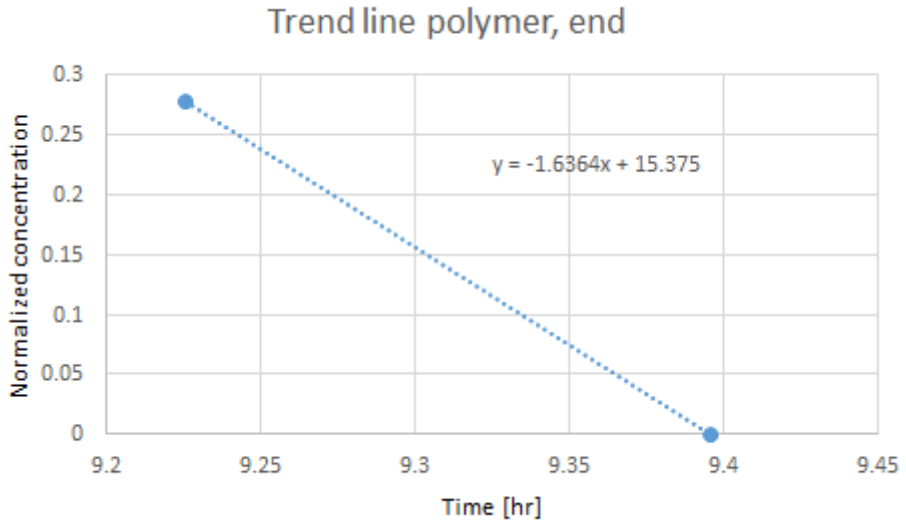

Figure B. 6 Trend line for polymer curve at end area for low permeability layer, type A core.

The trend line for the tracer curve at the end area for the core plug of the low permeability layer in core type A, is seen in Figure B. 7.

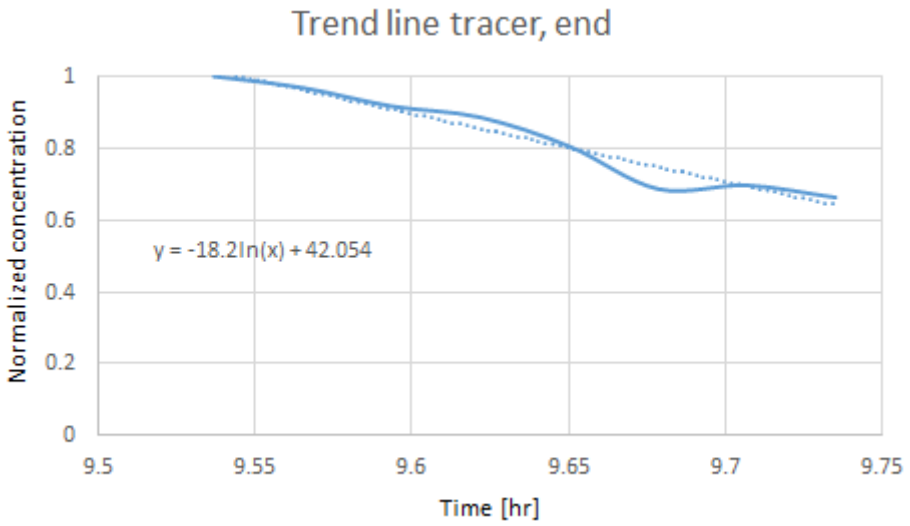

Figure B. 7 Trend line for tracer curve at end area for low permeability layer, type A core.

The trend line for the polymer pressure drop area for the core plug of the high permeability layer in core type B, is seen in Figure B. 8.

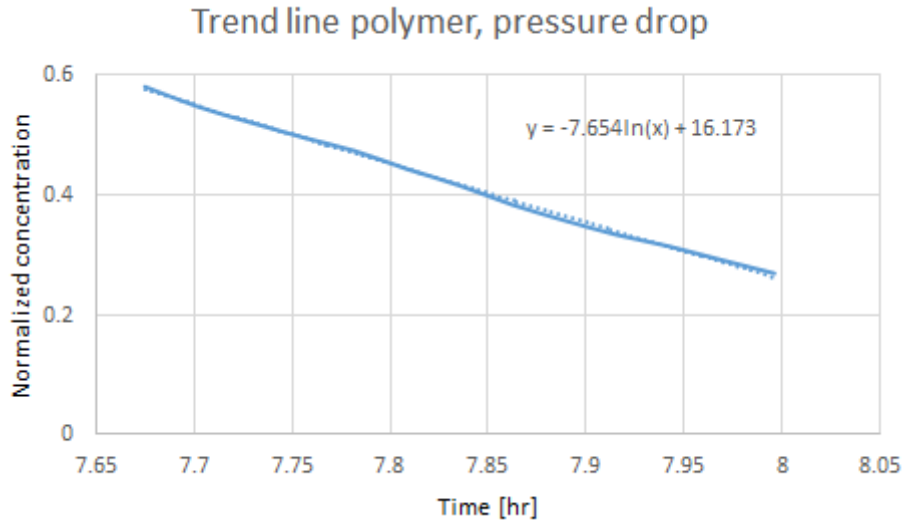

Figure B. 8 Trend line for polymer curve during pressure drop for high permeability layer, type B core.

The trend line of the extrapolation of the upward going polymer curve for the core plug of the high permeability layer in core type B, is seen in Figure B. 9.

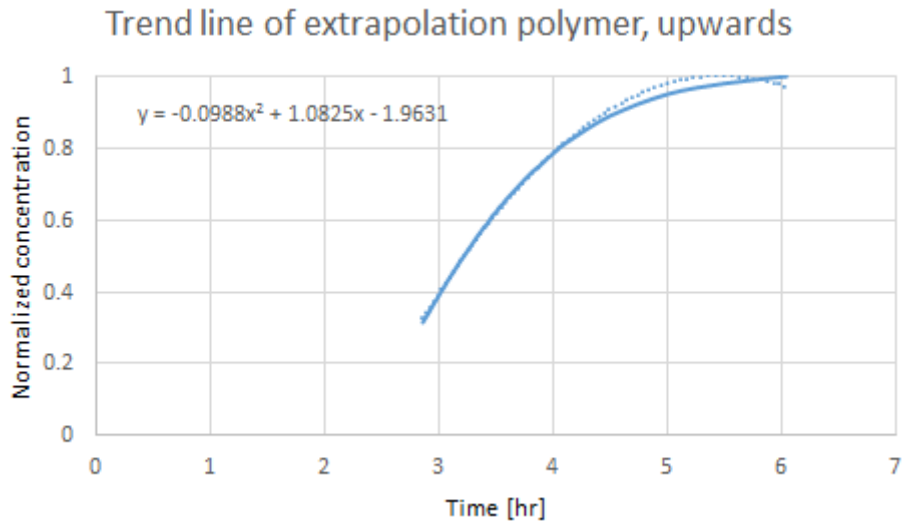

Figure B. 9 Trend line for extrapolation of upward going polymer curve for high permeability layer, type B core.

The trend line for the tracer curve at the end area for the core plug of the high permeability layer in core type B, is seen in Figure B. 10.

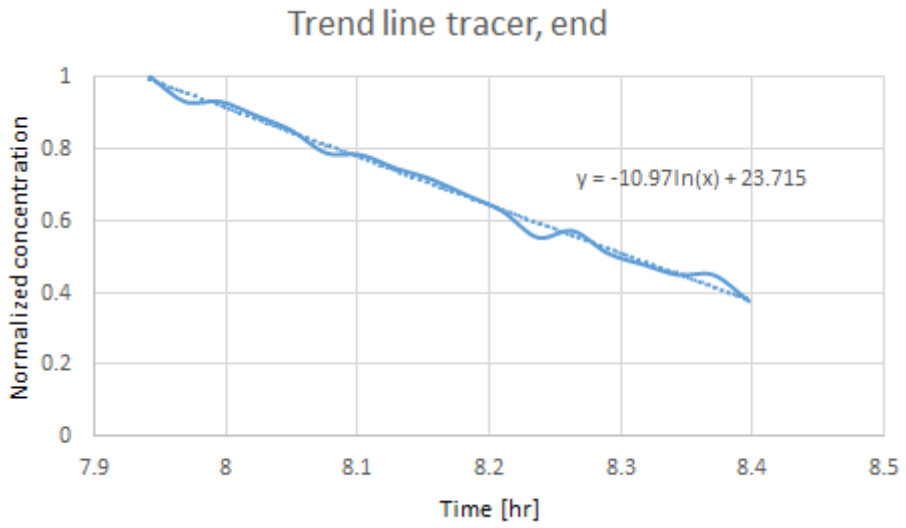

Figure B. 10 Trend line for tracer curve at end area for high permeability layer, type B core.

The trend line for the polymer pressure drop area for the core plug of the low permeability layer in core type B, is seen in Figure B. 11.

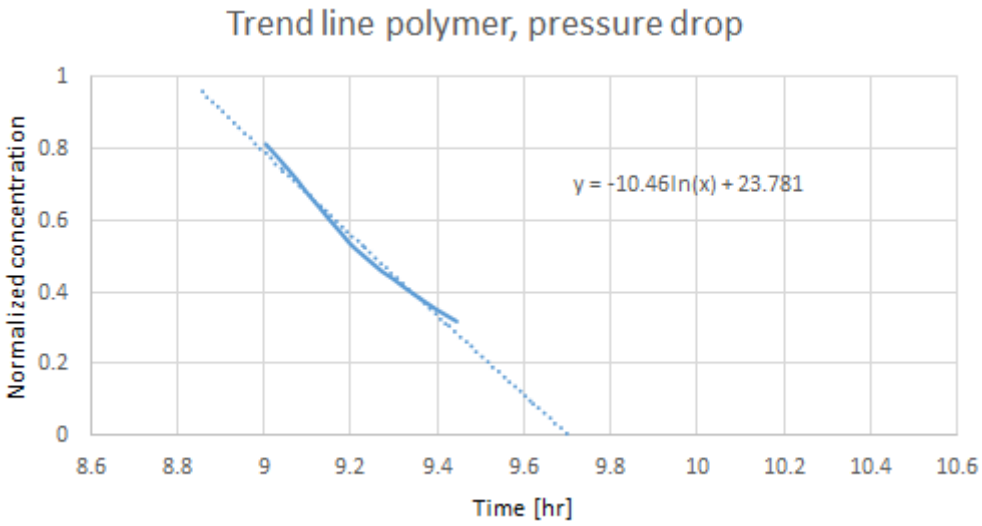

Figure B. 11 Trend line for polymer curve during pressure drop for low permeability layer, type B core.

The trend line for the upward going part of the tracer curve for the core plug of the low permeability layer in core type B, is seen in Figure B. 12.

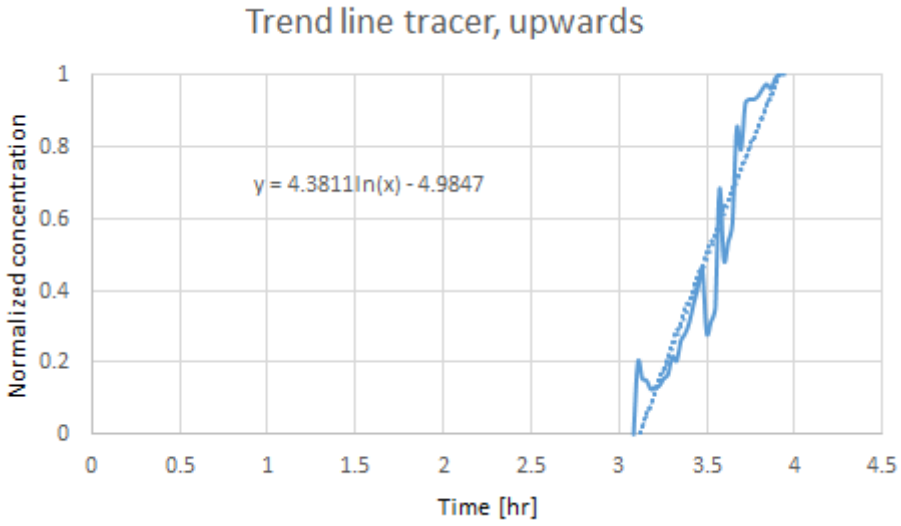

Figure B. 12 Trend line for upward going part of tracer curve for low permeability layer, type B core.

The trend line for the tracer curve at the end area for the core plug of the low permeability layer in core type B, is seen in Figure B. 13.

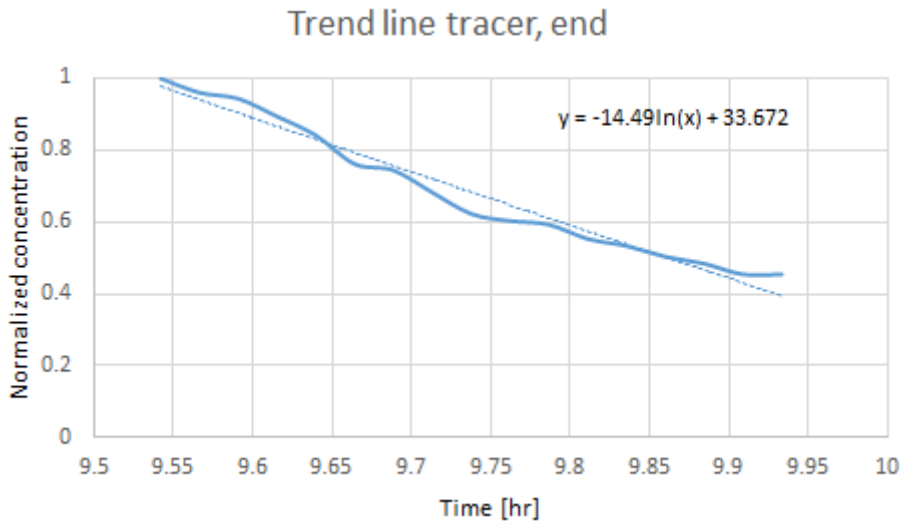

Figure B. 13 Trend line for tracer curve at end area for low permeability layer, type B core.

C. Data files

The data file used for the test case to prove the method used to find adsorption and IPV is as followed:

```
RUNSPEC
TITLE
   2D SQUARE PLUG MODEL

LAB

DIMENS
   40   1    5  /

OIL
WATER
POLYMER

EQLDIMS
    1   100   10    1    1 /

TRACERS
-- MAXOIL  MAXWAT  MAXGAS MAXENV
     0       2       0      0   /

TABDIMS
-- NTSFUN  NTPVT   NSSFUN   NPPVT   NTFIP   NRPVT
      1       1       50      2       1      12 /

WELLDIMS
-- max#wells  #conn   max#groups   max#ingroup
       2       10         1             2      /

START
  1 'JAN' 2015  /

NSTACK
  80  /

UNIFIN
UNIFOUT

GRID    ================================================================
INIT

GRIDFILE
1 /

--      ARRAY  VALUE      ------- BOX ------
EQUALS
        DX       0.25      /
        DY       4.5       /
        DZ       0.45      /
        PORO    0.25       /
        TOPS    1       1 40   1  1   1  1  /
        PERMX   50        1  40  1  1   1  5 /   -- Given in milli darcy
--      PERMX   2000        1  120  1  1   6  10 /   -- Given in milli darcy
--      PERMX   2000        1  2  1  1   1  5 /   -- Given in milli darcy
--      PERMX   2000        39  40  1  1   1  5 /   -- Given in milli darcy
/

COPY
      'PERMX'    'PERMY'   /
      'PERMX'    'PERMZ'   /
/


-- EQUALS
--      'MULTX'  0     2 2 1 1 1 5 /
-- /
```

```
PROPS    ================================================================

SWOF
--     Sw       Krw      Krow       Pcow
--                                  (bar)
     0.1000   0.0000   1.0000    1.198e-01
     0.1421   0.0092   0.9172    3.754e-02
     0.1842   0.0273   0.8370    2.547e-02
     0.2263   0.0522   0.7596    1.845e-02
     0.2684   0.0827   0.6851    1.331e-02
     0.3105   0.1182   0.6135    9.054e-03
     0.3526   0.1582   0.5449    5.384e-03
     0.3947   0.2024   0.4794    2.058e-03
     0.4368   0.2506   0.4171   -1.079e-03
     0.4789   0.3026   0.3581   -4.027e-03
     0.5211   0.3581   0.3026   -7.074e-03
     0.5632   0.4171   0.2506   -1.018e-02
     0.6053   0.4794   0.2024   -1.336e-02
     0.6474   0.5449   0.1582   -1.687e-02
     0.6895   0.6135   0.1182   -2.087e-02
     0.7316   0.6851   0.0827   -2.546e-02
     0.7737   0.7596   0.0522   -3.122e-02
     0.8158   0.8370   0.0273   -3.922e-02
     0.8579   0.9172   0.0092   -5.311e-02
     0.9000   1.0000   0.0000   -3.328e-01 / rock 1
--     0.1000   0.0000   1.0000    1.198e-01
--     0.1421   0.0092   0.9172    3.754e-02
--     0.1842   0.0273   0.8370    2.547e-02
--     0.2263   0.0522   0.7596    1.845e-02
--     0.2684   0.0827   0.6851    1.331e-02
--     0.3105   0.1182   0.6135    9.054e-03
--     0.3526   0.1582   0.5449    5.384e-03
--     0.3947   0.2024   0.4794    2.058e-03
--     0.4368   0.2506   0.4171   -1.079e-03
--     0.4789   0.3026   0.3581   -4.027e-03
--     0.5211   0.3581   0.3026   -7.074e-03
--     0.5632   0.4171   0.2506   -1.018e-02
--     0.6053   0.4794   0.2024   -1.336e-02
--     0.6474   0.5449   0.1582   -1.687e-02
--     0.6895   0.6135   0.1182   -2.087e-02
--     0.7316   0.6851   0.0827   -2.546e-02
--     0.7737   0.7596   0.0522   -3.122e-02
--     0.8158   0.8370   0.0273   -3.922e-02
--     0.8579   0.9172   0.0092   -5.311e-02
--     0.9000   1.0000   0.0000   -3.328e-01 / rock 2
--     0.1 0 1 0
--     0.9 1 0 0 / rock 3


DENSITY
--   O        W      G
     0.850    1.014    0.00082    /


PVTW
-- REF.PRES.   REF. FVF   COMPRESSIBILITY   REF.VISC.   VISCOSIBILITY
--                                            (cP)
     1         1.0         4.28e-5          0.5        0.00E+00 /

PVCDO
-- REF.PRES.   REF. FVF   COMPRESSIBILITY   REF.VISC.   VISCOSIBILITY
--                                            (cP)
     1         1.0         6.65e-5         1.5         0.0e+0    /

ROCK
-- REF.PRES    COMPRESSIBILITY
--   (atma)        (1/atm)
     1              4.0e-6        /
```

```
-- Polymer properties (keywords starting with PLY) -----------------------

-- PLYVISC: Viscosity multiplier (salt option).
-- Defined as PLYVISC=u/uw, where uw is water viscosity.
PLYVISC
0        1.0
0.001    40.0  /


PLYROCK
-- Note: AI=1 is desorption, AI=2 gives no desorption.
-- IPV   RRF  dens   AI   max ads
   0.2   1.0  2.000   2    70.0e-6 / rock 1
--   0.2   1.0  2.000   2    20.0e-6 / rock 2
--   0.2   1.0  2.000   2    1.0e-7 / rock 3

--PLYADS: Adsorption isotherm
PLYADS
--   conc      adsorb-conc
-- (gm/scc)     (gm/gm)
     0.0       0.0e-6
     0.001     70.0e-6 / rock 1
--     0.0       0.0e-6
--     0.001     20.0e-6 / rock 2
--     0.0       0.0e-6
--     0.001     0.0e-6  / rock 3


--Polymer: Todd-Longstaff mixing parameter. 1 = full mixing
PLMIXPAR
 1.0  /


PLYMAX
 0.001  0.0  /

TRACER
 'TR1'    WAT /
/

TRDIFTR1
 0.072 /


REGIONS    ====================================================================

EQUALS
--                  VAL         ------- BOX ------
       SATNUM   1       1  40  1  1   1  5 /
--       SATNUM   2       1  120  1  1   6  10 /
--       SATNUM   2       1  2  1  1   1  5 /
--       SATNUM   2       39  40  1  1   1  5 /
/


SOLUTION ===================================================================

SWAT
 200*1.0 /

PRESSURE
 200*1.1 /

SPOLY
 200*0.0 /

TBLKFTR1
 200*0.03 /
```

```
SUMMARY  =====================================================================

RUNSUM
EXCEL
SEPARATE


ALL
FLPR
FGPR
FRPV
FVIT

-- TRACER
FTPRTR1
FTPTTR1
FTIRTR1
FTITTR1
FTPCTR1
FTICTR1

-- POLYMER
FCPC
FCPR
FCIR
FCIC
FCPT
FCIT


SCHEDULE =====================================================================


RPTRST
  'BASIC=6' 'FREQ=1' /


WELSPECS
--      WELL    GROUP    LOCATION    BHP    PI
--      NAME    NAME       I    J    DEPTH DEFN
    'PRODUCER' 'G'      40   1    1     'OIL'   /
    'INJECTOR' 'G'      1    1    1     'WATER'  /
/

COMPDAT
--      WELL      -LOCATION- OPEN/ SAT CONN  WELL
--      NAME       I     J  K1 K2 SHUT  TAB FACT  DIAM
    'PRODUCER'    40    1  1  5  'OPEN' 2*       0.1/
    'INJECTOR'    1     1  1  5  'OPEN' 2*       0.1/
/


-- Short time-steps to (try to) avoid numerical problems
TUNING
  0.0001 0.05 0.000001  /
  /
  500 1 500 1 100 1* 1* 0.2 /


------------------------------------------------------------------------------
-- CONTROL: WATER AND POLYMER INJECTION
------------------------------------------------------------------------------

WCONPROD
--       WELL      OPEN/  CNTL   OIL  WATER   GAS  LIQU   RES   BHP
--       NAME      SHUT   MODE  RATE   RATE  RATE  RATE  RATE
     'PRODUCER' 'OPEN'   'BHP'   4*                      1*     1      /
/


WCONINJE
--       WELL       INJ      OPEN/   CNTL        FLOW
--       NAME      TYPE      SHUT    MODE        RATE
--                                              (rcc/hr)
     'INJECTOR'  'WATER'   'OPEN'   'RESV'  1*  15  /
/
```

```
WPOLYMER
  'INJECTOR'  0.0  0.0 /
/

WTRACER
  'INJECTOR' 'TR1' 0.03 /
/

TSTEP
5*0.1
/


WCONINJE
--      WELL        INJ     OPEN/   CNTL        FLOW
--      NAME       TYPE     SHUT    MODE        RATE
--                                              (rcc/hr)
     'INJECTOR'   'WATER'   'OPEN'   'RESV'  1*  15  /
/


WPOLYMER
  'INJECTOR'  0.001 0.0 /
/

WTRACER
  'INJECTOR' 'TR1' 0.035 /
/

TSTEP
80*0.05
/

-------------------------------------------------------------------------------
-- CONTROL: PURE WATER INJECTION
-------------------------------------------------------------------------------

TUNING
  0.0001 0.05 0.000001  /
  /
  500 1 500 1 100 1* 1* 0.2 /

WPOLYMER
 'INJECTOR'  0.0  0.0 /
/

WTRACER
  'INJECTOR' 'TR1' 0.03 /
/

TSTEP
  1*5
/

WPOLYMER
  'INJECTOR'  0.001 0.0 /
/

WTRACER
  'INJECTOR' 'TR1' 0.035 /
/

TSTEP
80*0.05
/

WPOLYMER
 'INJECTOR'  0.0  0.0 /
/

WTRACER
  'INJECTOR' 'TR1' 0.03 /
/

TSTEP
  1*5
/

END     ============================================================
```

The data file for base case A is as followed:

```
RUNSPEC
TITLE
   2D SQUARE PLUG MODEL

LAB

DIMENS
   120   1    10  /

OIL
WATER
POLYMER

EQLDIMS
    1   100   10    1    1 /

TRACERS
-- MAXOIL  MAXWAT  MAXGAS MAXENV
     0       2       0      0   /

TABDIMS
-- NTSFUN  NTPVT   NSSFUN   NPPVT   NTFIP   NRPVT
      3       1       50      2       1      12 /

WELLDIMS
-- max#wells  #conn   max#groups   max#ingroup
       2       10         1             2      /

START
  1 'JAN' 2015  /

NSTACK
  80  /

UNIFIN
UNIFOUT

GRID    ================================================================
INIT

GRIDFILE
1 /

--      ARRAY  VALUE      ------- BOX ------
EQUALS
       DX       0.25       /
       DY       4.5       /
       DZ       0.45       /
       PORO   0.234        1  120  1  1   1  5 /
       PORO   0.293        1  120  1  1   6  10 /
       TOPS    1       1 120   1  1   1  1  /
       PERMX   110        1  120  1  1   1  5 /   -- Given in milli darcy
       PERMX   2001        1  120  1  1   6  10 /   -- Given in milli darcy
       PERMX   2001        1  2  1  1   1  10 /   -- Given in milli darcy
       PERMX   2001        119  120  1  1   1  10 /   -- Given in milli darcy
/

COPY
      'PERMX'    'PERMY'   /
      'PERMX'    'PERMZ'   /
/
```

```
PROPS    ================================================================

SWOF
--     Sw       Krw     Krow      Pcow
--                                (bar)
0.1      0        1        0.00E+000
0.1421   0.0092   0.9172   0.00E+000
0.1842   0.0273   0.837    0.00E+000
0.2263   0.0522   0.7596   0.00E+000
0.2684   0.0827   0.6851   0.00E+000
0.3105   0.1182   0.6135   0.00E+000
0.3526   0.1582   0.5449   0.00E+000
0.3947   0.2024   0.4794   0.00E+000
0.4368   0.2506   0.4171   0.00E+000
0.4789   0.3026   0.3581   0.00E+000
0.5211   0.3581   0.3026   0.00E+000
0.5632   0.4171   0.2506   0.00E+000
0.6053   0.4794   0.2024   0.00E+000
0.6474   0.5449   0.1582   0.00E+000
0.6895   0.6135   0.1182   0.00E+000
0.7316   0.6851   0.0827   0.00E+000
0.7737   0.7596   0.0522   0.00E+000
0.8158   0.837    0.0273   0.00E+000
0.8579   0.9172   0.0092   0.00E+000
0.9      1        0        0.00E+000        /       rock    1
0.1      0        1        0.00E+000
0.1421   0.0092   0.9172   0.00E+000
0.1842   0.0273   0.837    0.00E+000
0.2263   0.0522   0.7596   0.00E+000
0.2684   0.0827   0.6851   0.00E+000
0.3105   0.1182   0.6135   0.00E+000
0.3526   0.1582   0.5449   0.00E+000
0.3947   0.2024   0.4794   0.00E+000
0.4368   0.2506   0.4171   0.00E+000
0.4789   0.3026   0.3581   0.00E+000
0.5211   0.3581   0.3026   0.00E+000
0.5632   0.4171   0.2506   0.00E+000
0.6053   0.4794   0.2024   0.00E+000
0.6474   0.5449   0.1582   0.00E+000
0.6895   0.6135   0.1182   0.00E+000
0.7316   0.6851   0.0827   0.00E+000
0.7737   0.7596   0.0522   0.00E+000
0.8158   0.837    0.0273   0.00E+000
0.8579   0.9172   0.0092   0.00E+000
0.9      1        0        0.00E+000        /       rock    2
0.1      0        1        0
0.9      1        0        0        /       rock    3


DENSITY
--   O        W      G
    0.850    1.014   0.00082   /


PVTW
-- REF.PRES.   REF. FVF  COMPRESSIBILITY  REF.VISC.   VISCOSIBILITY
--                                          (cP)
     1         1.0         4.28e-5         1.0        0.00E+00 /

PVCDO
-- REF.PRES.   REF. FVF  COMPRESSIBILITY  REF.VISC.   VISCOSIBILITY
--                                          (cP)
     1         1.0         6.65e-5        1.5         0.0e+0   /

ROCK
-- REF.PRES   COMPRESSIBILITY
--   (atma)       (1/atm)
     1             4.0e-6       /
```

```
-- Polymer properties (keywords starting with PLY) ------------------------

-- PLYVISC: Viscosity multiplier (salt option).
-- Defined as PLYVISC=u/uw, where uw is water viscosity.
PLYVISC
0        1.0
0.001    4.7  /


PLYROCK
-- Note: AI=1 is desorption, AI=2 gives no desorption.
-- IPV   RRF  dens   AI   max ads
   0.73   1.0  2.300   2    0.00021 / rock 1
   0.21   1.0  2.400   2    0.000091 / rock 2
   0.2   1.0  2.000   2    1.0e-7 / rock 3

--PLYADS: Adsorption isotherm
PLYADS
--   conc      adsorb-conc
-- (gm/scc)     (gm/gm)
     0.0       0.0e-6
     0.001     0.00021 / rock 1
     0.0       0.0e-6
     0.001     0.000091 / rock 2
     0.0       0.0e-6
     0.001     0.0e-6  / rock 3


--Polymer: Todd-Longstaff mixing parameter. 1 = full mixing
PLMIXPAR
 1.0  /

PLYMAX
 0.001  0.0  /

TRACER
 'TR1'   WAT /
/

TRDIFTR1
 0.0072 /


REGIONS    ====================================================================

EQUALS
--                  VAL         ------- BOX ------
       SATNUM   1       1  120  1  1   1  5 /
       SATNUM   2       1  120  1  1   6  10 /
       SATNUM   3       1  2  1  1   1  10 /
       SATNUM   3       119  120  1  1   1  10 /
/


SOLUTION ===================================================================

SWAT
 1200*1.0 /

PRESSURE
 1200*1.1 /

SPOLY
 1200*0.0 /

TBLKFTR1
 1200*0.03 /
```

```
SUMMARY  ====================================================================
RUNSUM
EXCEL
SEPARATE
ALL
FLPR
FGPR

-- TRACER
FTPRTR1
FTPTTR1
FTIRTR1
FTITTR1
FTPCTR1
FTICTR1

-- POLYMER
FCPC
FCPR
FCIR
FCIC
FCPT
FCIT


SCHEDULE ====================================================================


RPTRST
  'BASIC=6' 'FREQ=1' /


WELSPECS
--     WELL    GROUP    LOCATION    BHP    PI
--     NAME    NAME      I    J    DEPTH DEFN
    'PRODUCER' 'G'      120  1     1     'OIL'   /
    'INJECTOR' 'G'      1    1     1     'WATER'  /
/

COMPDAT
--     WELL      -LOCATION- OPEN/ SAT CONN  WELL
--     NAME       I     J  K1 K2 SHUT  TAB FACT  DIAM
    'PRODUCER'   120   1  1  10 'OPEN' 2*       0.1/
    'INJECTOR'   1     1  1  10 'OPEN' 2*       0.1/
/


-- Short time-steps to (try to) avoid numerical problems
TUNING
  0.0001 0.05 0.000001  /
  /
  500 1 500 1 100 1* 1* 0.2 /


-------------------------------------------------------------------------------
-- CONTROL: WATER AND POLYMER INJECTION
-------------------------------------------------------------------------------

WCONPROD
--      WELL      OPEN/  CNTL   OIL  WATER   GAS  LIQU   RES   BHP
--      NAME      SHUT   MODE  RATE   RATE  RATE  RATE  RATE
     'PRODUCER' 'OPEN'  'BHP'   4*                      1*     1      /
/


WCONINJE
--      WELL       INJ     OPEN/   CNTL       FLOW
--      NAME      TYPE     SHUT    MODE       RATE
--                                           (rcc/hr)
     'INJECTOR'  'WATER'  'OPEN'  'RESV'  1*  19.8  /
/
```

```
WPOLYMER
  'INJECTOR'  0.0  0.0 /
/

WTRACER
  'INJECTOR' 'TR1' 0.03 /
/

TSTEP
5*0.1
/


WCONINJE
--      WELL        INJ      OPEN/   CNTL        FLOW
--      NAME       TYPE      SHUT    MODE        RATE
--                                                (rcc/hr)
     'INJECTOR'   'WATER'   'OPEN'   'RESV'  1*  19.8  /
/



WPOLYMER
  'INJECTOR'  0.001 0.0 /
/

WTRACER
  'INJECTOR' 'TR1' 0.035 /
/

TSTEP
380*0.05
/

TSTEP
400*0.05
/

END     ================================================================
```

The data file for base case B is as followed:

```
RUNSPEC
TITLE
   2D SQUARE PLUG MODEL

LAB

DIMENS
   120   1    10  /

OIL
WATER
POLYMER

EQLDIMS
    1   100   10    1    1 /

TRACERS
-- MAXOIL  MAXWAT  MAXGAS MAXENV
     0       2       0      0   /

TABDIMS
-- NTSFUN  NTPVT   NSSFUN   NPPVT   NTFIP   NRPVT
      3      1       50      2       1      12 /

WELLDIMS
-- max#wells  #conn   max#groups   max#ingroup
       2       10         1             2      /

START
  1 'JAN' 2015  /

NSTACK
  80  /

UNIFIN
UNIFOUT

GRID    ================================================================
INIT

GRIDFILE
1 /

--      ARRAY  VALUE      ------- BOX ------
EQUALS
       DX       0.25      /
       DY       4.5       /
       DZ       0.45      /
       PORO   0.279        1  120  1  1   1  5 /
       PORO   0.277        1  120  1  1   6  10 /
       TOPS    1       1 120   1  1   1  1  /
       PERMX   171         1  120  1  1   1  5 /   -- Given in milli darcy
       PERMX   609         1  120  1  1   6  10 /   -- Given in milli darcy
       PERMX   609         1  2  1  1   1  10 /   -- Given in milli darcy
       PERMX   609         119  120  1  1   1  10 /   -- Given in milli darcy
/

COPY
      'PERMX'    'PERMY'   /
      'PERMX'    'PERMZ'   /
/
```

```
PROPS    ================================================================

SWOF
--     Sw       Krw     Krow      Pcow
--                                (bar)
0.1      0        1        0.00E+000
0.1421   0.0092   0.9172   0.00E+000
0.1842   0.0273   0.837    0.00E+000
0.2263   0.0522   0.7596   0.00E+000
0.2684   0.0827   0.6851   0.00E+000
0.3105   0.1182   0.6135   0.00E+000
0.3526   0.1582   0.5449   0.00E+000
0.3947   0.2024   0.4794   0.00E+000
0.4368   0.2506   0.4171   0.00E+000
0.4789   0.3026   0.3581   0.00E+000
0.5211   0.3581   0.3026   0.00E+000
0.5632   0.4171   0.2506   0.00E+000
0.6053   0.4794   0.2024   0.00E+000
0.6474   0.5449   0.1582   0.00E+000
0.6895   0.6135   0.1182   0.00E+000
0.7316   0.6851   0.0827   0.00E+000
0.7737   0.7596   0.0522   0.00E+000
0.8158   0.837    0.0273   0.00E+000
0.8579   0.9172   0.0092   0.00E+000
0.9      1        0        0.00E+000        /       rock    1
0.1      0        1        0.00E+000
0.1421   0.0092   0.9172   0.00E+000
0.1842   0.0273   0.837    0.00E+000
0.2263   0.0522   0.7596   0.00E+000
0.2684   0.0827   0.6851   0.00E+000
0.3105   0.1182   0.6135   0.00E+000
0.3526   0.1582   0.5449   0.00E+000
0.3947   0.2024   0.4794   0.00E+000
0.4368   0.2506   0.4171   0.00E+000
0.4789   0.3026   0.3581   0.00E+000
0.5211   0.3581   0.3026   0.00E+000
0.5632   0.4171   0.2506   0.00E+000
0.6053   0.4794   0.2024   0.00E+000
0.6474   0.5449   0.1582   0.00E+000
0.6895   0.6135   0.1182   0.00E+000
0.7316   0.6851   0.0827   0.00E+000
0.7737   0.7596   0.0522   0.00E+000
0.8158   0.837    0.0273   0.00E+000
0.8579   0.9172   0.0092   0.00E+000
0.9      1        0        0.00E+000        /       rock    2
0.1      0        1        0
0.9      1        0        0        /       rock    3


DENSITY
--   O        W      G
    0.850    1.014   0.00082   /


PVTW
-- REF.PRES.  REF. FVF  COMPRESSIBILITY  REF.VISC.  VISCOSIBILITY
--                                          (cp)
     1         1.0        4.28e-5         1.0       0.00E+00 /

PVCDO
-- REF.PRES.  REF. FVF  COMPRESSIBILITY  REF.VISC.  VISCOSIBILITY
--                                          (cp)
     1         1.0        6.65e-5        1.5        0.0e+0   /

ROCK
-- REF.PRES   COMPRESSIBILITY
--   (atma)       (1/atm)
     1             4.0e-6       /
```

```
-- Polymer properties (keywords starting with PLY) ------------------------

-- PLYVISC: Viscosity multiplier (salt option).
-- Defined as PLYVISC=u/uw, where uw is water viscosity.
PLYVISC
0        1.0
0.001    3.8  /


PLYROCK
-- Note: AI=1 is desorption, AI=2 gives no desorption.
-- IPV   RRF  dens   AI   max ads
   0.61   1.0  2.330   2    0.00025 / rock 1
   0.50   1.0  2.340   2    0.00016 / rock 2
   0.2   1.0  2.000   2    1.0e-7 / rock 3

--PLYADS: Adsorption isotherm
PLYADS
--   conc      adsorb-conc
-- (gm/scc)     (gm/gm)
     0.0       0.0e-6
     0.001     0.00025 / rock 1
     0.0       0.0e-6
     0.001     0.00016 / rock 2
     0.0       0.0e-6
     0.001     0.0e-6  / rock 3


--Polymer: Todd-Longstaff mixing parameter. 1 = full mixing
PLMIXPAR
 1.0  /

PLYMAX
 0.001  0.0  /

TRACER
 'TR1'   WAT /
/

TRDIFTR1
 0.0072 /


REGIONS    ====================================================================

EQUALS
--                  VAL         ------- BOX ------
       SATNUM   1        1  120  1  1   1  5 /
       SATNUM   2        1  120  1  1   6  10 /
       SATNUM   3        1  2  1  1   1  10 /
       SATNUM   3        119  120  1  1   1  10 /
/


SOLUTION ===================================================================

SWAT
 1200*1.0 /

PRESSURE
 1200*1.1 /

SPOLY
 1200*0.0 /

TBLKFTR1
 1200*0.03 /
```

```
SUMMARY  ============================================================
RUNSUM
EXCEL
SEPARATE
ALL
FLPR
FGPR

-- TRACER
FTPRTR1
FTPTTR1
FTIRTR1
FTITTR1
FTPCTR1
FTICTR1

-- POLYMER
FCPC
FCPR
FCIR
FCIC
FCPT
FCIT


SCHEDULE ============================================================


RPTRST
  'BASIC=6' 'FREQ=1' /


WELSPECS
--     WELL    GROUP    LOCATION    BHP    PI
--     NAME    NAME      I     J    DEPTH DEFN
    'PRODUCER' 'G'      120   1     1     'OIL'   /
    'INJECTOR' 'G'      1     1     1     'WATER'  /
/

COMPDAT
--     WELL      -LOCATION- OPEN/ SAT CONN  WELL
--     NAME       I     J  K1 K2 SHUT  TAB FACT  DIAM
    'PRODUCER'   120   1  1  10 'OPEN' 2*       0.1/
    'INJECTOR'   1     1  1  10 'OPEN' 2*       0.1/
/


-- Short time-steps to (try to) avoid numerical problems
TUNING
  0.0001 0.05 0.000001  /
  /
  500 1 500 1 100 1* 1* 0.2 /


-------------------------------------------------------------------------
-- CONTROL: WATER AND POLYMER INJECTION
-------------------------------------------------------------------------

WCONPROD
--      WELL     OPEN/  CNTL   OIL  WATER   GAS  LIQU   RES   BHP
--      NAME     SHUT   MODE  RATE   RATE  RATE  RATE  RATE
     'PRODUCER' 'OPEN'  'BHP'   4*                      1*     1      /
/


WCONINJE
--      WELL       INJ     OPEN/   CNTL       FLOW
--      NAME      TYPE     SHUT    MODE       RATE
--                                          (rcc/hr)
     'INJECTOR'  'WATER'  'OPEN'  'RESV'  1*  19.8  /
/
```

```
WPOLYMER
  'INJECTOR'  0.0  0.0 /
/

WTRACER
  'INJECTOR' 'TR1' 0.03 /
/

TSTEP
5*0.1
/


WCONINJE
--      WELL        INJ     OPEN/   CNTL        FLOW
--      NAME       TYPE     SHUT    MODE        RATE
--                                              (rcc/hr)
     'INJECTOR'  'WATER'  'OPEN'  'RESV'  1*  19.8  /
/


WPOLYMER
  'INJECTOR'  0.001 0.0 /
/

WTRACER
  'INJECTOR' 'TR1' 0.035 /
/

TSTEP
380*0.05
/

TSTEP
400*0.05
/

END     ================================================================
```

D. Risk analysis

Detaljert Risikorapport

ID	149	**Status**	**Dato**
Risikoområde	Risikovurdering: Helse, miljø og sikkerhet (HMS)	Opprettet	02.02.2015
Opprettet av	Eline Skurtveit Moe	Vurdering startet	03.02.2015
Ansvarlig	Eline Skurtveit Moe	Tiltak besluttet	
		Avsluttet	11.02.2015

Experimental and numerical study of polymer flooding in heterogeneous porous media

Gyldig i perioden:

2/2/2015 - 6/10/2018

Sted:

NTNU

Mål / hensikt

Målet er å undersøke effekten av polymer som økt utvinningsmetode i heterogene reservoarer.

Bakgrunn

Er en del av min masteroppgave og denne risikovurderingen må gjennomføres for å kunne få tilgang til lab.

Beskrivelse og avgrensninger

Forutsetninger, antakelser og forenklinger

Denne risikovurderingen er forbeholdt arbeidet som skal utføres i lab, og ikke det resterende arbeidet en masteroppgave inneholder.

Vedlegg

[Ingen registreringer]

Referanser

[Ingen registreringer]

Oppsummering, resultat og endelig vurdering

I oppsummeringen presenteres en oversikt over farer og uønskede hendelser, samt resultat for det enkete konsekvensområdet.

Farekilde: **løsningsmidler**

Uønsket hendelse: **søle utover labbenken**

Konsekvensområde:		
	Helse	Risiko før tiltak: Risiko etter tiltak:
	Ytre miljø	Risiko før tiltak: Risiko etter tiltak:
	Materielle verdier	Risiko før tiltak: Risiko etter tiltak:

Farekilde: **høyt trykk**

Uønsket hendelse: **blir for høyt trykk for deler av utstyret**

Konsekvensområde:		
	Helse	Risiko før tiltak: Risiko etter tiltak:
	Ytre miljø	Risiko før tiltak: Risiko etter tiltak:
	Materielle verdier	Risiko før tiltak: Risiko etter tiltak:

Farekilde: **høy temperatur**

Uønsket hendelse: **lekkasje av væske med høy temperatur**

Konsekvensområde:		
	Helse	Risiko før tiltak: Risiko etter tiltak:
	Ytre miljø	Risiko før tiltak: Risiko etter tiltak:
	Materielle verdier	Risiko før tiltak: Risiko etter tiltak:

Farekilde: **polymer**

Uønsket hendelse: **komme i kontakt med polymer under bruk**

Konsekvensområde:		
	Helse	Risiko før tiltak: Risiko etter tiltak:

Endelig vurdering

Sannsynligheten for at man kan søle utover labbenken mens man håndterer løsemidler er gjerne stor, men hvilken konsekvens dette vil ha er avhengig av blant annet hvor mye løsemiddel en bruker om gangen. Bruker man små mengder om gangen vil det være lite som blir sølt og skadene på helse, ytre miljø og materielle verdier vil være svært små, om noen i det hele tatt.

Oversikt involverte enheter og personell

En risikovurdering kan gjelde for en, eller flere enheter i organisasjonen. Denne oversikten presenterer involverte enheter og personell for gjeldende risikovurdering.

Enhet /-er risikovurderingen omfatter

- NTNU

Deltakere

Ole Torsæter

Georg Voss

Lesere

[Ingen registreringer]

Andre involverte/interessenter

[Ingen registreringer]

Følgende akseptkriterier er besluttet for risikoområdet Risikovurdering: Helse, miljø og sikkerhet (HMS):

Helse	Materielle verdier	Omdømme	Ytre miljø
			

Oversikt over eksisterende, relevante tiltak som er hensyntatt i risikovurderingen

I tabellen under presenteres eksisterende tiltak som er hensyntatt ved vurdering av sannsynlighet og konsekvens for aktuelle uønskede hendelser.

Farekilde	Uønsket hendelse	Tiltak hensyntatt ved vurdering
løsningsmidler	søle utover labbenken	verneutstyr
	søle utover labbenken	avtrekksskap
	søle utover labbenken	opplæring i bruk av utstyr
høyt trykk	blir for høyt trykk for deler av utstyret	verneutstyr
	blir for høyt trykk for deler av utstyret	opplæring i bruk av utstyr
høy temperatur	lekkasje av væske med høy temperatur	verneutstyr
	lekkasje av væske med høy temperatur	opplæring i bruk av utstyr
polymer	komme i kontakt med polymer under bruk	verneutstyr
	komme i kontakt med polymer under bruk	opplæring i bruk av utstyr

Eksisterende og relevante tiltak med beskrivelse:

verneutstyr
For å beskytte mot høyt trykk og temperatur og kjemikalier

avtrekksskap
ved jobb med løsningsmidler

opplæring i bruk av utstyr
Vil gi det bakgrunnsstoffet og erfaringen jeg trenger til å utføre forsøket på en trygg måte

Risikoanalyse med vurdering av sannsynlighet og konsekvens

I denne delen av rapporten presenteres detaljer dokumentasjon av de farer, uønskede hendelser og årsaker som er vurdert. Innledningsvis oppsummeres farer med tilhørende uønskede hendelser som er tatt med i vurderingen.

Følgende farer og uønskede hendelser er vurdert i denne risikovurderingen:

- **løsningsmidler**
  - søle utover labbenken
- **høyt trykk**
  - blir for høyt trykk for deler av utstyret
- **høy temperatur**
  - lekkasje av væske med høy temperatur
- **polymer**
  - komme i kontakt med polymer under bruk

Oversikt over besluttede risikoreduserende tiltak med beskrivelse:

løsningsmidler (farekilde)

kan være farlig ved innåndning eller ved kontakt med hud. Kan også være brannfarlige

løsningsmidler/søle utover labbenken (uønsket hendelse)

Identifiserte årsaker til hendelsen

bommer på enheten en skal fylle på

Samlet sannsynlighet vurdert for hendelsen: Ganske sannsynlig (4)

Kommentar til vurdering av sannsynlighet:

Er sannsynlig, men vil være avhengig av mengde sølt hvor mye skade det vil føre til

Vurdering av risiko for følgende konsekvensområde: Helse

Vurdert sannsynlighet (felles for hendelsen): Ganske sannsynlig (4)

Vurdert konsekvens: Liten (1)

Kommentar til vurdering av konsekvens:

[Ingen registreringer]

høyt trykk (farekilde)

kan føre til ødeleggelse av utstyr

høyt trykk/blir for høyt trykk for deler av utstyret (uønsket hendelse)

kan føre til lekkasje og ødeleggelse av laboppsettet

Identifiserte årsaker til hendelsen

for dårlig forberedelse angående hva utstyret tåler

Samlet sannsynlighet vurdert for hendelsen: Svært lite sannsynlig (1)

Kommentar til vurdering av sannsynlighet:

Er lite sannsynlig hvis man forbereder seg godt på forhånd

Vurdering av risiko for følgende konsekvensområde: Helse

Vurdert sannsynlighet (felles for hendelsen): Svært lite sannsynlig (1)

Vurdert konsekvens: Liten (1)

Kommentar til vurdering av konsekvens:

[Ingen registreringer]

høy temperatur (farekilde)

kan føre til skade på hud

høy temperatur/lekkasje av væske med høy temperatur (uønsket hendelse)

kan lekke noe væske med høy temperatur som kan treffe den som utfører eksperimentet

Identifiserte årsaker til hendelsen

ikke tett system, får en lekkasje

Samlet sannsynlighet vurdert for hendelsen: Svært lite sannsynlig (1)

Kommentar til vurdering av sannsynlighet:

Er ikke særlig sannsynlig hvis en er godt forberedt og opplært i bruk av utstyr. Vil heller ikke bli brukt høye rater, så hvis en lekkasje skulle skje ville det ikke vært snakk om mye væske som kom ut før det kan stoppes.

Vurdering av risiko for følgende konsekvensområde: Helse

Vurdert sannsynlighet (felles for hendelsen): Svært lite sannsynlig (1)

Vurdert konsekvens: Liten (1)

Kommentar til vurdering av konsekvens:

[Ingen registreringer]

polymer (farekilde)

kan være giftig og allergifremkallende avhengig av type polymer som vil bli brukt

polymer/komme i kontakt med polymer under bruk (uønsket hendelse)

Identifiserte årsaker til hendelsen

uforsiktighet ved håndtering av polymer

Samlet sannsynlighet vurdert for hendelsen: Svært lite sannsynlig (1)

Kommentar til vurdering av sannsynlighet:

Er lite sannsynlig hvis man bruker verneutstyr og har opplæring i hvordan man skal håndtere dette kjemikaliet.

Vurdering av risiko for følgende konsekvensområde: Helse

Vurdert sannsynlighet (felles for hendelsen): Svært lite sannsynlig (1)

Vurdert konsekvens: Liten (1)

Kommentar til vurdering av konsekvens:

[Ingen registreringer]